Genetic tools derived from *Staphylococcus aureus* for biotechnological applications in Gram-positive bacteria

Memoria presentada por

Pedro Luis Dorado Morales

para optar al grado de Doctor por la Universidad Pública de Navarra

Director: Dr. Iñigo Lasa Uzcudun

Directora: Dra. Cristina Solano Goñi

Pamplona - Iruña, 2020

https://doi.org/10.48035/Tesis/2454/41085

Dr. Iñigo Lasa Uzcudun, Catedrático del área de Microbiología del Departamento de Ciencias de la Salud de la Universidad Pública de Navarra,

Dra. Cristina Solano Goñi, Profesora Titular del área de Microbiología del Departamento de Ciencias de la Salud de la Universidad Pública de Navarra,

INFORMAN:

Que la presente memoria de Tesis Doctoral **"Genetic tools derived from *Staphylococcus aureus* for biotechnological applications in Gram-positive bacteria"** elaborada por Don **Pedro Luis Dorado Morales** ha sido realizada bajo su dirección y que cumple las condiciones exigidas por la legislación vigente para optar al grado de Doctor.

Y para que así conste, firman la presente en Pamplona, a 30 de septiembre de 2020

Fdo. Iñigo Lasa Uzcudun

Fdo. Cristina Solano Goñi

Forzando su espaciada ejecución -2015/2020- reúno hoy estas historias un poco por ver si ilustran, con sus frágiles estructuras, el apólogo del haz de mimbres. Toda vez que las hallé en cuadernos sueltos tuve la certeza de que se necesitaban entre sí, que su soledad las perdía. Acaso merezcan estar juntas porque el desencanto de cada una creció la voluntad de la siguiente.

Las doy en un libro a fin de cerrar un ciclo y quedarme solo frente a otro. Un libro más es un libro menos; un acercarse al último que espera en el ápice, ya perfecto.

Julio Cortázar (modificado)

A M, A y P.

Otra vez, y nunca serán bastantes

Acknowledgements

En primer lugar, me gustaría dar las gracias a todas las instituciones que han hecho posible esta tesis: a la Universidad Pública de Navarra, al centro de investigación Navarrabiomed y al Ministerio de Economía y Competitividad.

A mis directores, Iñigo y Cristina, les debo el más sincero agradecimiento, por abrirme las puertas de su laboratorio, aguantar los miles de millones de preguntas y, sobre todo, por enseñarme a escribir y pensar.

A mis compañeros, y en muchos casos amigos, de geles y matraces: Maite, Carmen G., Pablo, Maribel, Jaio, Ale, Saio, Marta, Tana, Margarita…, a todos, gracias.

A José R. Penadés no podré nunca agradecerle lo suficiente el que me acogiese e hiciera sentir como uno más desde el primer momento en que pisé su laboratorio. Gracias una y mil veces.

A Mapi, a la cual espero conocer algún día en persona, le agradezco la ayuda que me prestó en mi paso por el universo de los plásmidos, gracias por estar siempre disponible y hacerlo todo más fácil. Un verdadero placer y una ayuda inestimable. A Eduardo e Igor, que han sufrido a mi lado las aventuras y desventuras con nuestro amigo *Rhodococcus*, gracias.

A Manel, tengo que agradecerle la apuesta que hizo por alguien cuya primera entrevista no pudo ser más desastrosa, el acompañarme en mis primeros pasos en el mundo científico y, por encima de todo, su amistad. A Daniel Ramón, que me permitió explorar el mundo de la empresa, muchas gracias.

A todos aquellos con los que he tenido la gran suerte de hacer equipo de cervezas, zumos, paseos y juegos: al club de Trolls más dicharachero que se ha visto por el

laboratorio, y fuera de él, (Bego, Gabo, el Grinch, Arrebola y la juiciosa Lili); a la gente del almuercico (Sara, Pedro I, Lara, Leticia, Javi y Marta[2]); y a mi cuadrilla: Santi, Tania, Judith y Xabi; gracias por hacer de Navarra mi casa.

A los Glasgowian: Nuria, Alfred, Andreas, Jorge, Rodrigo, Dion y Martge; gracias por todas las cervezas trasnochadas y por hacer de mi tiempo en Escocia un recuerdo que atesorar.

A todos los que llegaron para quedarse: a Sara, Zafri y Ouafae por encarnar la definición más precisa de la amistad; a Bea, por la melomanía compartida; a Toki, por ser mi villana favorita, ahora y siempre; a Charo, Paula, Xavi, Lucas, Vicente y Dani, por los infinitos reencuentros; a Vic, por las cervezas, los arroces al horno y las risas compartidas; a Protozoo, por los kilómetros andados, las rutas cicleadas, su amistad y cariño; las palabras no pueden alcanzar la magnitud de lo que os debo, gracias.

Y por último, me gustaría dar las gracias a mi familia. A esas dos personas que, pese a que se fueron demasiado pronto de mi lado, están, y estarán, siempre presentes. A mis padres y mi hermana, gracias por ser siempre mi pensamiento feliz, por quererme incondicionalmente y, porque sé que, como diría Vicente Andrés Estellés, aunque llegue un día en que solos no podamos más, juntos lo podremos todo.

INDEX

SUMMARY

Staphylococcus aureus is a versatile human pathogen that has emerged as one of the most successful infectious agents of recent times, able to cause a range of diseases including skin and soft tissue infections, endocarditis, sepsis, pneumonia, osteomyelitis, bacteremia, and abscesses in organ tissues. Besides its clinical relevance, *S. aureus* has served as a model to study fundamental cellular processes, such as biofilm formation, the regulatory functions of small RNAs or growth and division of spherical cocci. Based on the accumulated knowledge of *S. aureus* biology, the availability of database resources and the advances in high-throughput genome sequencing, in this work we have aimed at developing new genetic tools derived from *S. aureus* for biotechnological applications in Gram-positive bacteria.

Staphylococcus aureus together with *Staphylococcus epidermidis* are the most frequent causes of biofilm-associated infections on indwelling medical devices. Inside biofilms, bacteria exhibit a high cell density and superior tolerance to physicochemical insults and harsh reaction conditions, when compared to their planktonic counterparts. These properties that usually have deleterious consequences in clinical settings, can be of great appeal in the field of environmental biotechnology. In Chapter I, we investigated whether promoting bacterial biofilm formation capability results in a higher ability to degrade recalcitrant compounds. As a proof of principle, we selected the environmental Gram-positive bacteria *Rhodococcus erythropolis*, which presents diverse metabolic activities and serves as a model organism for biodesulfurization, a process that intends for the removal of the recalcitrant sulfur of aromatic heterocycles present in fuels. To promote biofilm formation in this bacterium, we implemented three approaches based on the

molecular traits that *S. aureus* uses to build a biofilm. The selected strategy that consisted in the overexpression of a heterologous diguanylate cyclase that drove the synthesis of high levels of the secondary messenger cyclic-di-GMP, resulted in a strong biofilm forming phenotype both under batch and flow conditions. Importantly, *Rhodococcus* cells inside the biofilm showed a significantly improved desulfurization activity when compared to their planktonic counterparts. Results of Chapter I indicate that our approach might be promising to enhance the biodegradation potential of not only *Rhodococcus* but also many other environmentally relevant bacterial species.

Plasmids are main agents in the spread of antibiotic resistance genes. These genetic elements usually produce physiological alterations in their host that provoke a reduction in fitness. However, despite this fitness cost, plasmids are generally maintained over time in the absence of selection for plasmid encoded traits. Most studies intended to understand this paradox have been carried out in Gram-negative bacteria, mostly in the *Pseudomonas* genus, and little is known about the mechanisms that Gram-positive bacteria use to compensate plasmid cost. Taking all the above into account, in Chapter II, we aimed at analysing the initial fitness cost that plasmids confer on clinical staphylococcal isolates and also the co-evolutionary dynamics that determine plasmid maintenance in *S. aureus*. The first part of this study focused on the development of a tool that allows plasmid curing in *S. aureus* strains without altering any other genetic feature. This tool consisted in a plasmid that encodes essential modules for CRISPR-Cas9 targeting of conserved sequences in *S. aureus* plasmids. Our curing system resulted in very high plasmid curing efficiencies both

in laboratory and clinical *S. aureus* strains. One of the clinical cured isolates was then transformed with other plasmids coming from clinical strains of different origins, thus generating new bacterium-plasmid associations. Fitness cost comparisons showed that one of the plasmids produced a significant cost in both its original strain and also the new host. The second part of the study then focused on analysing the co-evolution of this new host-costly plasmid association by subjecting bacteria to experimental evolution during thirty five days of growth in liquid medium without selective pressure. During the evolution process, most bacteria lost the costly plasmid. Notably, at the end of evolution, some clones were selected with an alleviated fitness cost that contained a plasmid harbouring a deletion comprising several antimicrobial resistance genes. Sequencing results indicated that plasmid rearrangement occurs via plasmid-borne IS*Sau*10 insertion sequences. Overall, results of Chapter II underscore the importance of insertion sequences mediated rearrangements for plasmid maintenance and also highlight the probable benefits of reducing the use of antibiotics for the loss of clinical multidrug resistance plasmids in *S. aureus*. It is important to note that the plasmid curing tool developed here might be manipulated to target plasmids of other staphylococcal species.

In the past few decades, extensive, and often indiscriminate use of antimicrobial agents has led to a dramatic increase in the incidence of nosocomial infections caused by *S. aureus* that are resistant to multiple antibiotics. With the aim of developing alternative approaches to the sole use of antibiotics for the treatment of *S. aureus* related infections, in Chapter III, we modified a native *S. aureus* pathogenicity island in order to carry a CRISPR-Cas9 system targeting conserved sequences of the *S. aureus*

chromosome. Generation of the recombinant pathogenicity island was achieved via the use of a previously described yeast-mediated recombineering strategy that proved to be simple and efficient. Combinations of these modified islands with currently used antibiotics showed an *in vitro* synergistic killing effect on *S. aureus*, proving their potential use as versatile and effective anti-staphylococcal therapeutic agents. Although our results are still preliminary and efficacy of the combination of synthetic pathogenicity islands with antibiotics needs to be confirmed in animal models, we can foresee that, as long as characterized islands of other bacterial species are available, this strategy could be extrapolated to the treatment of infections caused by different antimicrobial resistance pathogens that place a significant burden on healthcare systems.

OBJECTIVES

The specific objectives of this thesis are:

1. Implementation of genetic engineering strategies to promote *Rhodococcus erythropolis* biofilm formation and evaluation of the efficacy of biofilm cells as biocatalysts.

2. Investigation of plasmid cost carriage in clinical isolates of *Staphylococcus aureus* in the absence of antibiotics using a new tool for plasmid removal.

3. Construction of engineered staphylococcal pathogenicity islands and analysis of their combined use with antibiotics for the treatment of *Staphylococcus aureus* infections.

INTRODUCTION

1. The genus *Staphylococcus*

Staphylococcus is a non-motile, Gram-positive, ubiquitous bacterial group of the Firmicutes phylum. Members of the genus *Staphylococcus* form a coherent and well-defined cluster of related species. Morphologically, they are spherical with a diameter ranging from 0.5 to 1.8 µm. *Staphylococcus* species are facultative anaerobic organisms. The genome-GC content is low with an average of approximately 33-40%. Although widely known as causative agents of a broad spectrum of diseases with varying degrees of severity in humans and other animals, not all staphylococci are pathogens and some are exploited in food industry and biotechnology (Götz, 1990; Place *et al.*, 2003; Corbiere Morot-Bizot *et al.*, 2007).

Some representatives of the genus (such as *S. aureus*, *S. epidermidis*, *S. saprophyticus*, *S. capitis*, *S. pseudointermedius*, *S. haemolyticus* and *S. simulans*) have been extensively studied and, as a consequence, widespread mechanisms, important to understand fundamental biological processes such as biofilm formation, were initially described and characterized within this phylogenetic group. That is the case of the polysaccharide intercellular adhesin (PIA) (Tojo *et al.*, 1988), the family of biofilm-associated proteins (BAP) (Cucarella *et al.*, 2001), and the regulatory small RNA (sRNA) RNAIII (Novick *et al.*, 1993).

2. *Staphylococcus aureus*

Staphylococcus aureus is the most clinically relevant species inside the *Staphylococcus* genus. It is routinely isolated as a commensal organism in more than

a third of the human population, being the anterior nares of the nose the most frequent carriage site of this bacterium (Kluytmans *et al.*, 1997). When the epithelial barrier is disrupted, *S. aureus* can gain access to the underlying tissues or the bloodstream causing a plethora of infections including abscesses, pneumonia, septicaemia, endocarditis, osteomyelitis and toxic shock syndrome (Arvidson and Tegmark, 2001).

The success of *S. aureus* as a pathogen stems from its strong biofilm formation capacity, the combined action of extensive virulence factors, the presence of specific and global regulatory networks that orchestrate the expression of the aforementioned virulence factors at specific growth phases and in response to environmental signals and, the acquired resistance to commonly used antibiotics (Archer, 1998).

2.1. *Staphylococcus aureus* and the biofilm formation process

Biofilm formation and the subsequent irreversible attachment to biotic and abiotic surfaces is one of the main pathogenicity factors of *S. aureus* and, therefore, the molecular mechanisms underlying its regulation and synthesis have been studied in great detail (Gotz, 2002; O'Gara, 2007).

2.1.1. General principles of the biofilm formation process

In general, biofilms are multilayered communities of bacteria that grow embedded in a self-produced extracellular matrix. The matrix, which holds bacterial biofilms together, is a complex mixture of macromolecules including

exopolysaccharides, proteins and extracellular DNA (eDNA) (Whitchurch *et al.*, 2002). The biofilm lifestyle confers upon bacteria many advantages over their planktonic counterparts (e.g. easier access to nutrients, increased genetic exchange, protection against predation, higher tolerance to antimicrobial agents and harsh environments, etc.) by mechanisms that, in some cases, are still somewhat unclear (Høiby *et al.*, 2010).

The transition from a planktonic to a biofilm lifestyle occurs in response to environmental changes and involves multiple regulatory networks, necessary to translate environmental cues to the cellular machinery. The biofilm formation process is believed to occur as sequential steps where cells attach to a surface, proliferate, accumulate in clusters and, eventually, detach from the biofilm and disseminate to other distant locations where a new biofilm might be formed (Hall-Stoodley and Stoodley, 2005).

Biofilm formation is usually associated with detrimental effects on industrial processes (Galié *et al.*, 2018), the medical practice and the agriculture sector (Donlan and Costerton, 2002; Walker *et al.*, 2004). Biofilms are an especially concerning issue in industrial settings involving water distribution systems and food processing equipment (Donlan and Costerton, 2002; Shi and Zhu, 2009). In the medical sector, chronic infections have been linked to biofilm development on the surface of medical devices, implants and host tissues (Donlan and Costerton, 2002). Current treatment guidelines recommend the removal of infected devices, given their persistence and recalcitrance using conventional antibiotic therapy (Donlan, 2011).

This bacterial way of life may be also exploited to our benefit as bacterial biofilms are the most common way of microorganisms organization in nature (e.g. microbiomes) and they present a different metabolic activity if compared with their planktonic counterparts. Some interesting examples can be found in the scientific literature where bacterial biofilms have been proposed as a therapy to prevent the colonization of different tissues by pathogenic bacteria (Vuotto *et al.*, 2014), used to degrade xenobiotic compounds and in soil bioremediation (Nicolella *et al.*, 2005; Singh *et al.*, 2006), or as biocontrol agents (Chen *et al.*, 2013).

2.1.2. Signal transduction systems and biofilm formation: the c-di-GMP mediated signalling

Biofilm development, like many other bacterial processes, requires bacteria to sense changes in the intracellular and extracellular environment and respond accordingly. To establish this functional connectiveness, bacteria have evolved signal transduction systems that transmit external stimuli to the cellular machinery, leading to specific changes in gene expression patterns, metabolism, physiology and bacterial behaviour. Signalling pathways in bacteria comprise two-component systems (TCSs), methyl-accepting chemotaxis proteins (MCPs), signal transduction systems based on cyclic di-nucleotides levels (such as bis-(3′-5′)-cyclic dimeric guanosine monophosphate or c-di-GMP), serine/threonine/tyrosine protein kinases and one-component signal transduction proteins (Galperin, 2005; Ulrich *et al.*, 2005).

c-di-GMP is an ubiquitous secondary messenger that plays an essential role in regulating the transition from a planktonic to a sessile bacterial lifestyle. Several

studies have shown that high levels of c-di-GMP inhibit bacterial mobility and stimulate the biosynthesis of adhesins and polysaccharides, which are part of the extracellular matrix of biofilms (Simm *et al.*, 2004; Pérez-Mendoza and Sanjuán, 2016).

The levels of c-di-GMP in bacteria depend on proteins with diguanylate cyclase (DGC) and phosphodiesterase (PDE) activity, which respectively regulate its synthesis and degradation (Schirmer and Jenal, 2009). Using bioinformatic, biochemical and structural approaches, the catalytic domains of DGCs and PDEs proteins have been identified and characterized. DGCs have been associated with the presence of a GGDEF domain and PDEs with that of EAL or HD-GYP domains (Römling *et al.*, 2013). The GGDEF, EAL and HD-GYP nomenclature relates to conserved amino-acid motifs in these domains (Galperin *et al.*, 2001). DGCs facilitate the condensation of two guanosine triphosphate (GTP) molecules, which then cycle to c-di-GMP in the presence of Mg^{2+} ions (Römling *et al.*, 2013). PDEs with an EAL domain end c-di-GMP-mediated signalling by catalysing the conversion of c-di-GMP to linear 5′-phosphoguanylyl-(3′-5′)-guanosine (5'-pGpG) (Römling, 2009), which is subsequently hydrolysed into two molecules of GMP by the oligoribonuclease Orn (an exoribonuclease) (Cohen *et al.*, 2015; Orr *et al.*, 2015). On the other hand, PDEs that present an HD-GYP domain can directly hydrolyse c-di-GMP into two GMP molecules (Stelitano *et al.*, 2013).

The GGDEF and EAL-domains are very often located in the carboxy-terminal (C-terminal) region whereas the amino-terminal (N-terminal) part of the proteins usually contains the sensory domains (e.g. PAS, GAF, MASE, CHASE, REC y HTH).

The aforementioned sensory domains can respond to different internal and external signals, triggering activation or inhibition of these c-di-GMP turnover enzymes (Galperin, 2006; Cruz *et al.*, 2012). Once synthesized, c-di-GMP levels are sensed by c-di-GMP-binding effectors that generate a given output, either directly or by acting on downstream targets, allowing the bacteria to respond accordingly to the previously detected environmental variation. Some c-di-GMP effectors described in the scientific literature are messenger RNAs (mRNAs), riboswitches (elements commonly found in the 5′-untranslated region (5'-UTR) of mRNAs that exert a regulatory control over the transcript by directly binding a small molecule ligand (Winkler *et al.*, 2002)), transcriptional regulators, proteins with degenerated GGDEF and EAL domains (enzymatically inactive but still able to bind c-di-GMP), and proteins containing PilZ domains (Jenal *et al.*, 2017).

In *S. aureus*, the c-di-GMP-mediated signalling system is reduced to the GdpS protein that contains a GGDEF domain with an intact GGEEF motif (Holland *et al.*, 2008). However, *in vitro*, the purified GdpS protein does not show diguanylate cyclase activity in the presence of GTP. Furthermore, the role of GdpS in *S. aureus* biofilm development is subject of controversy, as a *gdpS* deletion in different genetic backgrounds has led to opposite results, that is an increase, decrease or even no effect in the production of a biofilm (Holland *et al.*, 2008; Shang *et al.*, 2009; Fischer *et al.*, 2014; Chou and Galperin, 2016; Zhu *et al.*, 2017). Overall, pieces of evidence suggest that GdpS might be the vestige of an ancient c-di-GMP signalling pathway in *S. aureus*.

2.1.3. Lessons from *S. aureus*: universal biofilm matrix components

The PIA exopolysaccharide and the BAP family are important components of the biofilm matrix that were initially described within the *Staphylococcus* genus and, afterwards, were proved widespread across different bacterial taxa.

2.1.3.1. The PIA/PNAG exopolysaccharide

Extracellular polysaccharides are usually very important components of biofilm matrices. Initially described in *S. epidermidis* and termed PIA (Tojo *et al.*, 1988; Heilmann *et al.*, 1996; Mack *et al.*, 1996; McKenney *et al.*, 1998) and later on in *S. aureus* as poly-N-acetylglucosamine (PNAG) according to its chemical composition (Cramton *et al.*, 1999; McKenney *et al.*, 1999), PIA/PNAG is one of the main components of the biofilm matrices of staphylococci. PIA/PNAG is composed of β-1-6 linked N-acetylglucosamine monomers and has a cationic character. PIA/PNAG synthesis depends on the action of four proteins (IcaA, IcaB, IcaC and IcaD) encoded in the *icaADBC* (intercellular adhesion) operon. IcaA is a N-acetylglucosamine transferase with low transferase-activity on its own but when it is co-expressed with IcaD, it reaches full transferase activity. IcaD appears to be a chaperone that directs the correct folding and membrane insertion of IcaA and, besides, it might act as a link between the IcaA and IcaC proteins. N-acetylglucosamine oligomers produced by IcaAD may reach a maximal length of only 20 residues and, for longer oligomers to be synthesized, the activity of the membrane-anchored IcaC is needed. IcaC is also involved in the translocation of the growing polysaccharide chain to the bacterial surface. IcaB is located on the bacterial surface and is the polysaccharide deacetylase.

The deacetylation process introduces positive charges to the polysaccharide molecule and is crucial for its biological role: biofilm formation, increased resistance to antimicrobial peptides, neutrophil phagocytosis, etc. Upstream of the *icaADBC* operon and transcribed in the opposite direction is the *icaR* gene whose product is a repressor of the *ica* operon (Lasa, 2006; O'Gara, 2007; Arciola *et al.*, 2015).

Although much progress has been made in elucidating the role of PIA/PNAG in biofilm development and the pathogenesis of staphylococcal device-related infections, many questions remain about how the *ica* operon expression and PIA/PNAG biosynthesis are regulated (Gotz, 2002; O'Gara, 2007).

2.1.3.2. The family of biofilm-associated proteins

Although exopolysaccharides are important and often essential compounds of the biofilm matrix, recent pieces of evidence suggest that a group of surface proteins plays a leading role during the development of microbial biofilms (Latasa *et al.*, 2006). The first member of this group of proteins (Bap, for biofilm-associated protein) was described in a *S. aureus* bovine mastitis isolate (Cucarella *et al.*, 2001). Bap is a large multidomain protein of 2276 amino acids structurally organized into four domains. Region A contains two short repeats of 32 amino acids. Region B contains two EF-hand motifs that regulate Bap functionality upon binding to calcium (Arrizubieta *et al.*, 2004). Region C consists of a series of identical repeats of 86 amino acids and is followed by a C-terminal region D containing a serine-aspartate-rich repeated sequence. Because Bap is covalently linked to the cell wall, it was believed that Bap mediates intercellular adhesion through homophilic interactions between opposing

proteins in neighbouring cells, as has been shown for the SasG protein (Geoghegan *et al.*, 2010). However, recent results indicate that Bap behaves in a completely different manner. After secretion, Bap is proteolytically processed, and the N-terminal region (amino acids 49 to 819) is released (Taglialegna *et al.*, 2016). The resulting N-terminal fragments self-assemble into amyloid-like aggregates when the pH becomes acidic and the calcium concentration is below 1 mM. At higher calcium concentrations, binding of the cation to the EF-hand domains of region B inhibits the self-assembly of the N-terminal region. These findings define a dual function for Bap, first as a sensor and then as a scaffold protein that promotes biofilm development under specific environmental conditions (Taglialegna *et al.*, 2016). More recently, it has been shown that Esp, a Bap-orthologous protein produced by *Enterococcus faecalis*, displays a similar amyloidogenic behaviour (Taglialegna *et al.*, 2020). At acidic pH, the N-terminal region of Esp (Esp_N) forms aggregates with an amyloid-like conformation. Furthermore, exogenous addition of purified recombinant Esp_N (rEsp_N) to liquid cultures of *E. faecalis* and *S. aureus* is able to promote bacterial aggregation. Biophysical characterization indicated that the N-terminal domain of Esp self-assembles in β-sheet rich aggregates with amyloidogenic properties in acidic conditions. Surface proteins homologous to Bap exist in many bacteria including *Salmonella enterica*, *Acinetobacter baumannii*, *Pseudomonas putida*, *Listeria monocytogenes*, *Burkholderia cepacia* and *Shewanella oneidensis*. All the BAP proteins share several structural and functional features: (i) are present on the bacterial surface; (ii) show a high molecular weight; (iii) contain a core domain of tandem repeats; (iv) confer upon bacteria the capacity to form a biofilm; (v) play a

relevant role in bacterial infectious processes; and (vi) very often are contained in mobile genetic elements (MGEs) (Lasa and Penadés, 2006).

2.2. Horizontal gene transfer, mobile genetic elements and the spread of antibiotic resistance in *S. aureus*

Bacterial genomes, although stable, are remarkably dynamic on an evolutionary timescale (Darmon and Leach, 2014). This genetic diversity can be achieved by chromosomal DNA mutations, genome rearrangements or by the acquisition of DNA sequences from distantly related organisms in a process designated horizontal gene transfer (HGT) (Spratt, 1994; Ochman *et al.*, 2000; Darmon and Leach, 2014).

The main drivers of HGT are the mobile genetic elements, DNA segments that catalyse their own movement within and between genomes. Once transferred, MGEs need to be stably maintained in the new host either by autonomous replication or integration in the host genome. MGEs have often acquired a wide variety of so-called accessory genes, which encode properties that provide the host bacterium with immediate selective advantages such as antibiotic-resistance genes (ARGs) (Frost *et al.*, 2005).

In *S. aureus*, around 15-20 % of the genome is composed of MGEs including plasmids, phages, *S. aureus* pathogenicity islands (SaPIs; a particular case of phage inducible chromosomal islands or PICIs), transposable elements, integrative conjugative elements (ICEs), integrons and staphylococcal cassette chromosomes (SCCs), where all but phages may carry ARGs (Haaber *et al.*, 2017).

2.2.1. *S. aureus* and antibiotic resistance

Infections caused by antibiotic-resistant strains of *S. aureus* have reached epidemic proportions (Grundmann *et al.*, 2006; Chambers and DeLeo, 2009). β-lactam antibiotics were the traditional treatment for staphylococcal associated infections. However, in the 1960s, the emergence and subsequent spread of methicillin-resistant strains forced the use of new antibiotics in the clinical practice (Haaber *et al.*, 2017). The term methicillin-resistant *S. aureus* (MRSA) refers to a group of *S. aureus* isolates resistant to a wide range of β-lactam antibiotics. The genetic determinant responsible for the resistance to β-lactam antibiotics, either *mecA* or *mecC*, is located in a MGE called the staphylococcal cassette chromosome *mec* (SCC*mec*) (Ballhausen *et al.*, 2014). Based on risk factors associated with exposure, MRSA strains are often classified as healthcare-associated MRSA (HA-MRSA), community-acquired MRSA (CA-MRSA) and livestock-associated MRSA (LA-MRSA) (Diekema *et al.*, 2001; Ballhausen *et al.*, 2014).

Given the impossibility of using β-lactam antibiotics, vancomycin has become the treatment of choice for MRSA-associated infections. Nevertheless, the increased used of this antibiotic has led to the emergence of vancomycin-intermediate *S. aureus* (VISA) and vancomycin-resistant *S. aureus* (VRSA) isolates (Hiramatsu, Aritaka *et al.*, 1997; Hiramatsu *et al.*, 1997; Chambers and DeLeo, 2009; Périchon and Courvalin, 2009; Howden *et al.*, 2010). The VISA phenotype is associated with a cell wall thickening and restricted vancomycin access to its site of activity in the division septum, although it may vary because the mutations leading to it can differ between isolates (Howden *et al.*, 2010). On the other hand, *S. aureus* clinical strains resistant

to methicillin and vancomycin have been described. Genetic characterization of this strains has shown the presence of a *vanA* gene located within the Tn1546 transposon. This transposon was verly likely transferred from an *E. faecalis* conjugative plasmid (Inc-18 like) to a resident plasmid in the original MRSA (Zhu *et al.*, 2008; Périchon and Courvalin, 2009; Rossi *et al.*, 2014).

Nowadays, other MRSA alternative treatments include daptomycin and linezolid but its effectivity in the long term seems to be compromised (Dortet *et al.*, 2013; Gu *et al.*, 2013). MRSA strains resistant to other antibiotic classes are referred to as multidrug-resistant *S. aureus* (MDRSA). The high prevalence of MRSA and MDRSA-associated infections is considered a serious challenge in the medical practice and consequently, the development of novel treatment methodologies and alternative therapies using new agents are urgently needed. In fact, the World Health Organization (WHO) recently categorized *S. aureus* among the organisms for which new antibiotics are urgently needed (Álvarez *et al.*, 2019).

2.2.2. Plasmids in the *Staphylococcus* genus

Plasmids are autonomously replicating DNA molecules that usually remain physically independent of the bacterial chromosome (Phillips and Funnell, 2004). Most *S. aureus* clinical isolates carry plasmids that may range from 1 to 60 kilo-base pairs (kbp) in size (Novick, 1989). Staphylococci plasmids typically contain one to multiple genes involved in antimicrobial, heavy metal and other toxic substances resistance (Novick, 1989; Yoon *et al.*, 1991; Chu *et al.*, 1992; Broer *et al.*, 1993; Bjorland *et al.*, 2001). In these MGEs, it is also relatively common to find toxin coding

genes (Yamaguchi *et al.*, 2001; Argudín *et al.*, 2010; Wladyka *et al.*, 2015), virulence modulators (Bukowski *et al.*, 2013) and host-specific virulence factors important for successful colonization of new hosts (Lowder *et al.*, 2009; McCarthy *et al.*, 2014).

Staphylococcal plasmids have been historically divided in three classes. Class I include small (1 to 8 kbp), high-copy number (15-50 copies per cell) plasmids that replicate via an asymmetric rolling-circle (RC) mechanism. Many of these plasmids are cryptic or encode a single resistance determinant, usually against agents that interfere with protein biosynthesis (erythromycin, chloramphenicol, tetracycline, neomycin, streptomycin, etc.) (Novick, 1989; Schwarz *et al.*, 2011, 2014; Haaber *et al.*, 2017). Plasmids within classes II and III are greater than 8 kbp in size and divide following a theta (Θ) replication model though they differ upon their conjugative proficiency (Sheehy and Novick, 1975; Novick, 1989; Firth *et al.*, 2000). Resistance to aminoglycosides, heavy metals, β-lactams and macrolides are commonly found in theta-replicating plasmids (Novick, 1989; Haaber *et al.*, 2017).

Plasmids, and therefore the ARGs and virulence factors they carry, spread within bacterial populations either by natural competence (Morikawa *et al.*, 2012), generalized transduction (Varga *et al.*, 2012, 2016), or conjugative mobilization (O'Brien *et al.*, 2015; Ramsay *et al.*, 2016; Ramsay and Firth, 2017).

Once in a new host, small plasmids usually replicate at high copy numbers. During division, plasmid copies randomly distributed across the cytoplasm guarantees the inheritance by both nascent cells. This strategy, however, is not feasible for larger plasmids as it would maximize their burden to their host. To encompass inherent stability and low copy number, large plasmids encode active

partitioning and post-segregational killing (e.g. toxin-antitoxin pairs) systems (Sengupta and Austin, 2011; Million-Weaver and Camps, 2014). Besides, when transferred to a distantly related bacterium, where the replication machinery may be compromised, plasmids can undergo recombination processes, form cointegrates with resident elements such as other plasmids or the bacterial chromosome (Schwarz *et al*., 2014, 2011; Zhu *et al*., 2008).

These persistence mechanisms do not comprise the full picture. In the absence of selection for plasmid-encoded traits, plasmid carriage imposes a multilevel cost that generates selection against plasmid-bearing bacterial clones (survival of the fittest). Besides, the possibility of plasmid-beneficial traits moving to the bacterial chromosome has the potential to render plasmids redundant, resulting in selection against plasmid carriage. This conundrum of how plasmids manage to persist in an evolutionary time scale is known as plasmid paradox. Although several hypotheses have been proposed, the mechanisms underlying plasmid maintenance in bacterial populations are still poorly understood (Bergstrom *et al.*, 2000; MacLean and San Millan, 2015; Carroll and Wong, 2018).

2.2.3. *Staphylococcus aureus* bacteriophages as vehicles for HGT

Bacteriophages are viruses that infect and replicate only in bacterial cells. Bacteriophages, according to their lifecycles, can be categorized as either lytic or temperate. Lytic phages are characterized by, upon entering in a new host, immediately sequestering the machinery of the bacterial cell, turning off the synthesis of bacterial components and redirecting the bacterial machinery to make

phage components (genome and proteins). The ultimate consequences of these processes are the inhibition of the host cellular processes and the release of mature phage particles when the bacterial cell wall breaks as a consequence of the damage caused by phage replication and assembly. A temperate phage, by contrast, can establish a long-term association with its host by integrating directly into the bacterial chromosome and passively replicating along with it. In this latter scenario, called lysogeny, the quiescent chromosome-integrated phage is known as prophage. Prophage activation can be triggered either spontaneously or via activation of the SOS response induced following DNA damage, elicited by exposure to environmental oxidative stressors (e.g. antibiotics or UV light). A phage particle (virion) consists of a nucleic acid genome encased in a shell of phage-encoded proteins (capsid) and, in most cases, a tail which is designed for host recognition, cell wall penetration, and genome ejection into the host (Ackermann, 2007). Bacteriophages are major vehicles for HGT and, after being integrated into bacterial genomes, contribute to the diversification, evolution and adaptation of their hosts either by affecting the genome architecture, protecting bacteria for lytic infections or contributing to the virulence and fitness of the bacteria that carry them (Canchaya *et al.*, 2003; Brüssow *et al.*, 2004).

Despite *S. aureus* phages rarely carry ARGs, they play a central role in their mobility when entering the lytic cycle by different mechanisms: (i) general transduction; plasmids, SCCs and random genome regions are erroneously encapsidated (Penadés *et al.*, 2015); (ii) specialized transduction; packaging of DNA regions adjacent to the prophage integration site by aberrant excision (Chiang *et al.*,

2019); (iii) lateral transduction; replication of the prophage while still integrated into the chromosome cause in-situ DNA amplification and efficient packaging of genome regions located downstream of the prophage insertion site (Chen *et al.*, 2018); and (iv) phage exploitation and machinery hijacking by other MGEs (e.g. SaPIs) (Penadés and Christie, 2015).

S. aureus strains usually harbour one to four functional prophages in their genomes (Goerke *et al.*, 2009). All *S. aureus* phages described up to date belong to the *Caudovirales* order and most of them are part of the *Siphoviridae* family (Deghorain and Van Melderen, 2012). *Caudovirales* phage particles present an icosahedral capsid filled with double-stranded DNA and a filamentous tail (Deghorain and Van Melderen, 2012; Xia and Wolz, 2014). The genomes of *Siphoviridae* phages are around 40 kbp and are usually structured in five functional modules arranged as follows: (i) lysogeny; (ii) replication and regulation; (iii) DNA packaging and capsid morphogenesis; (iv) tail morphogenesis; and (v) host cell lysis. Virulence factors, when present, are usually located downstream the lysis module or between the lysogeny and DNA metabolism modules (Canchaya *et al.*, 2003; Brüssow *et al.*, 2004; Kwan *et al.*, 2005; Bae *et al.*, 2006; Deghorain and Van Melderen, 2012).

Virions of all *Caudovirales* are assembled in a similar process. The portal protein (PP) initiates head assembly, nucleating the co-assembly of the major capsid protein and scaffold proteins to form an empty prohead (procapsid). In parallel, phage DNA replication yields concatemers (genome units linked head-to-tail). The terminase complex recognizes a packaging signal (*pac* or *cos*) on the concatemer and makes an endonucleolytic cut, generating a free end to which the terminase complex remains

bound. The DNA-bound terminase complex docks on the PP and initiates DNA translocation, utilizing energy from ATP hydrolysis. After encapsidating the viral genome, the terminase complex makes another cut, terminating packaging and dissociating from the head while remaining bound to the newly generated concatemer end (Oram and Black, 2011; Rao and Feiss, 2015). The terminase complex is composed of large and small subunits, with a clear division of labour. The large subunits, TerL, are responsible for the nuclease activity and the ATP-driven packaging process whereas the small terminase subunits, TerS, mediate the recognition of *pac* or *cos* sites within the phage genome (Oram and Black, 2011; Rao and Feiss, 2015).

2.2.4. *Staphylococcus aureus* Pathogenicity Islands

SaPIs are phage satellites of around 15 kbp that maintain an intimate relationship with certain (helper) phages, whose lifecycles they parasite (**Figure 1**). SaPI-like elements (PICIs) are not unique to staphylococci, actually, pathogenicity islands widely occur in other Gram-positive and negative bacteria (Fillol-Salom *et al*., 2018).

SaPI genes are usually clustered composing four functional modules, which parallels the genomic organization of bacteriophages: transcriptional regulation, integration-excision, replication and helper exploitation or packaging (Novick *et al.*, 2010; Penadés and Christie, 2015). They also frequently carry accessory genes (such as superantigens, virulence factor or genetic determinants for biofilm formation and

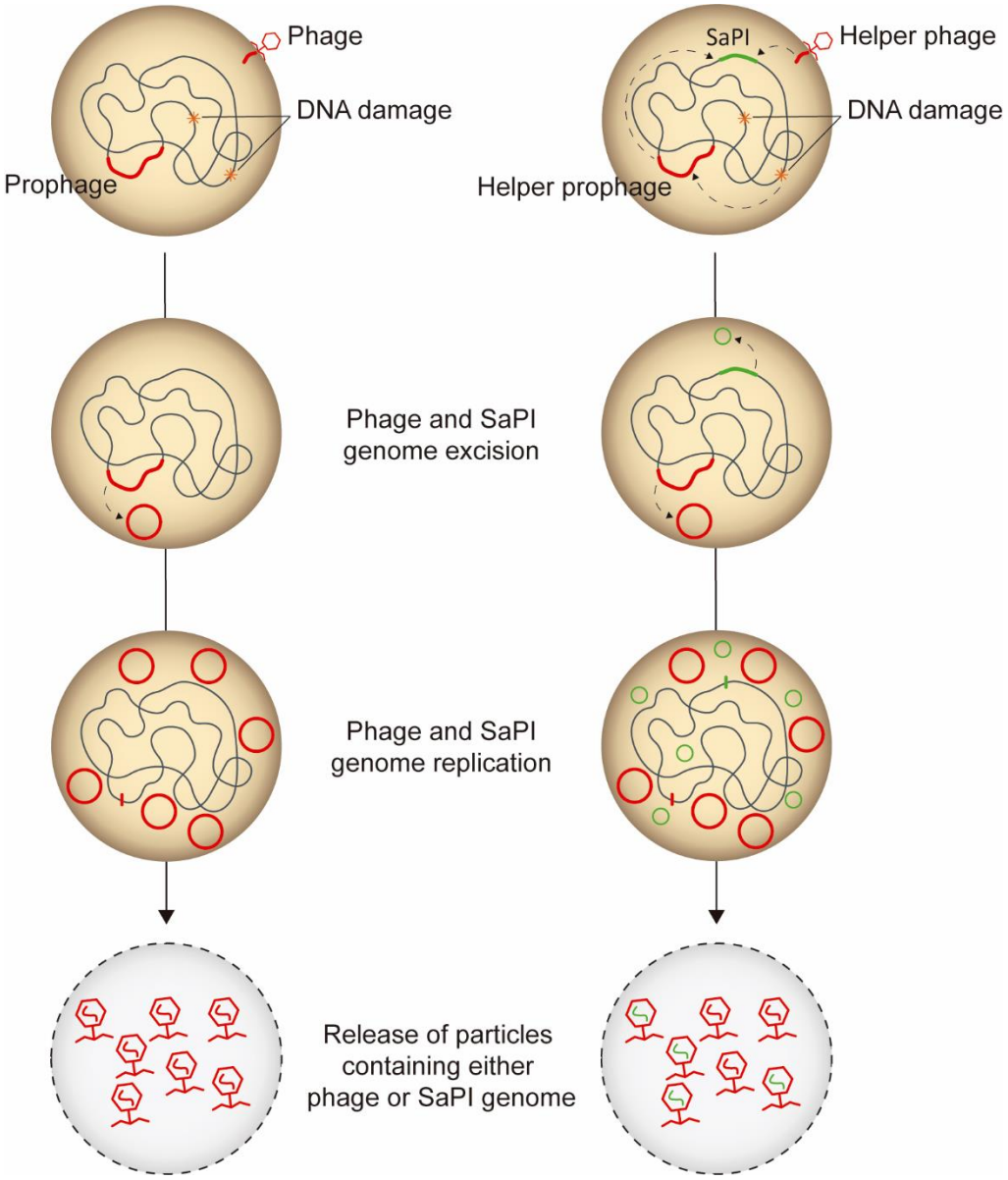

Figure 1. Phage packaging overview (left) **and SaPI element transduction** (right)**.** In red, phage genome and proteins; in green, SaPI DNA. Upon DNA damage or following entrance in a new host, the phage is induced: the lysogeny module is silenced and the transcription of genes involved in DNA replication starts. A specific phage protein interacts with Stl, the SaPI global repressor, and the SaPI cycle initiates. Phage and SaPI genomes excise from the chromosome and undergo theta replication, followed by rolling circle replication. Phage and SaPI genomes are packaged into phage procapsids through the action of the terminase complex. The mature phage and SaPI particles are released to the surroundings after phage-induced cell host lysis.

antibiotic resistance) in the former and latter modules (Úbeda *et al*., 2003; Kuroda *et al*., 2005; O'Neill *et al*., 2007; Malachowa and Deleo, 2010; Novick *et al*., 2010; Viana *et al*., 2010).

Because SaPIs require phage proteins to be packaged, they reside quiescently in the host chromosome until they are derepressed by a cognate helper phage (Úbeda *et al.*, 2005; Maiques *et al.*, 2006; Selva *et al.*, 2009; Penadés and Christie, 2015). Helper phages differ in their ability to mobilize different SaPIs (Novick *et al.*, 2010; Penadés and Christie, 2015). SaPIs always integrate in a certain chromosomal location with a concrete orientation and are flanked by direct repeats (*attL* and *attR*). The integration specificity depends on each SaPI-encoded integrase (Int) and the integration regions, core sequence of about 15-22 bp, are commonly known as chromosomal attachment sites (*attC* sites). Up to date, six different *attC* sites have been described within the *S. aureus* genome, each one of them able to virtually contain only one SaPI at a time (Novick *et al.*, 2010; Penadés and Christie, 2015).

SaPIs, like most MGEs, regulate their own excision and transfer. Briefly, following either the infection by a helper phage or the induction of an endogenous helper prophage, the orchestrated expression of the excisionase (*xis*) and integrase (*int*) ensures an efficient SaPI excision from the chromosome. The excised SaPI then circularizes by a head-to-tail *attL* and *attR*-mediated cross-over, replicates autonomously forming concatemers and starts its packaging by exploiting the helper phage morphogenetic functions (TerL and the virion structural proteins). Finally, phage-mediated lysis releases both phage and SaPI particles. On entry into a new host, SaPIs follow a replicative pathway in the presence of a helper phage or an

integrative pathway in their absence. The *attL* and *attR* sites are absolutely required for the excision and integration processes (Novick *et al.*, 2010; Penadés and Christie, 2015).

Three SaPI-mediated interference mechanisms have been identified so far (Novick and Ram, 2017): (i) diminishing the transcription levels of the phage late operon, which genes are involved in phage morphogenesis and lysis processes, by the SaPI-encoded Pti (phage transcription inhibitor) proteins (Ram *et al.*, 2014); (ii) inhibition of the phage TerS by the production of a SaPI-encoded protein termed Ppi (phage packaging interference) which once coupled with the expression of the SaPI homologue of the phage terminase small subunit modifies the DNA package specificity in favour of the island genome (Ubeda *et al.*, 2009; Ram *et al.*, 2012; Bento *et al.*, 2014); and (iii) a capsid size redirection process mediated by the gene products of *cpmA* and *cpmB*, which catalyse the formation of small capsids where the SaPI, but not the phage, genome is packaged (Damle *et al.*, 2012).

These strategies, alone or in combination, allow SaPIs to be packaged and transferred at very high frequencies, not only intra but also among genera (Maiques *et al.*, 2007; Chen and Novick, 2009; Winstel *et al.*, 2013; Chen *et al.*, 2015).

2.2.5. Insertion sequences

The insertion sequences (ISs), a group of transposable elements, are small (usually less than 2.5 kbp) segments of DNA that do not carry any genetic information except

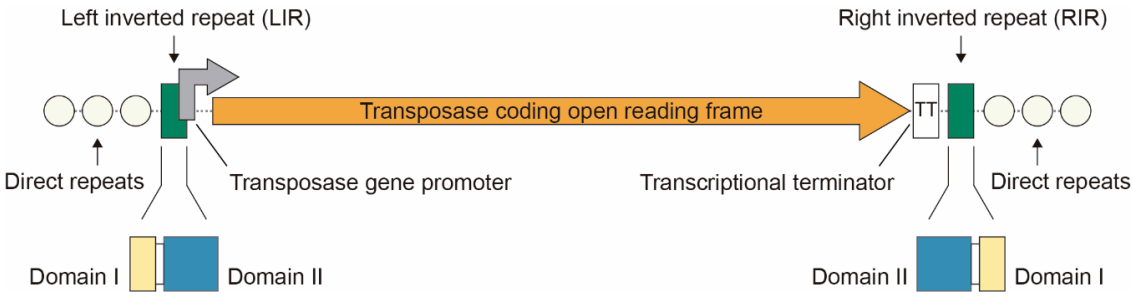

Figure 2. Typical organization of an insertion sequence. Inverted repeats are labelled as left inverted repeat (LIR) and right inverted repeat (RIR). A typical domain structure of the IRs is indicated beneath LIR and RIR. The transposase promoter, as shown in the diagram, is partially localized within the LIR. The transposase coding gene is represented as a single open reading frame along almost the entire length of the IS.

the one required for their own mobility. They are comprised of two inverted repeat (IRs) sequences (between 10 and 40 bp) at the ends of the element, and one open reading frame (ORF) that include almost the entire length of the element and codify an enzyme, the transposase, which recognizes and processes the repeated ends. IRs can be divided into two functional domains: the innermost or domain II, to which the transposase binds in a sequence-specific manner, and the terminal or domain I, 2 or 3 base pairs (bp) required for the cleavage and transfer reactions leading to the transposition of the element. Another general feature of IS elements is that on insertion, most generate short directly repeated sequences (DRs) of the target DNA flanking the IS. The length of the DR, between 2 and 14 bp, is characteristic for a given element that will normally generate a duplication of fixed length (Chandler and Siguier, 2013) (**Figure 2**).

ISs are widespread elements within the bacterial world and can be located either on the bacterial chromosome or plasmids (Młynarczyk *et al.*, 1998; Chandler and Siguier, 2013; Firth *et al.*, 2018)

In staphylococci, ISs play a central role in genome evolution and the emergence of antibiotic-resistant strains by modulating gene expression, via transcriptional promotion or insertional inactivation, and by facilitating the translocation of genes between IS replicons (Firth *et al.*, 2018).

2.3. Immunity against mobile genetic elements: CRISPR-Cas systems

The constant exposure to exogenous DNA via transduction, conjugation and transformation has forced prokaryotes to develop an array of defence mechanisms that allow them to recognize exogenous DNA and to survive from invasive MGEs. These systems maintain genetic integrity, yet occasionally allow uptake and conservation of genetic material advantageous for adaptation to the environment. Certain strategies are protective against specific types of MGEs (e.g. prevention of adsorption, blocking of injection and abortive infection are mechanisms devised to avoid phage infection), whereas other defence systems (e.g. restriction-modification systems (RM), the use of sugar-nonspecific nucleases and the clustered regularly interspaced short palindromic repeats (CRISPR)-*cas* (CRISPR associated genes) systems) are more general and target invading nucleic acid (Barrangou *et al.*, 2007; Horvath and Barrangou, 2010).

CRISPR-Cas systems are acquired immunity systems that are widespread in archaea and bacteria (Sorek *et al.*, 2008). It has recently been proposed that these systems may also have non-defensive roles, such as regulators of collective behaviour and pathogenicity (Louwen *et al.*, 2014; Sampson and Weiss, 2014; Westra *et al.*, 2014). CRISPR loci consist of several non-contiguous direct repeats separated by stretches of variable sequences called spacers, which mostly correspond to segments of captured foreign genetic elements such as viruses and plasmids (Horvath and Barrangou, 2010). Despite being highly divergent between species, within a given CRISPR locus, repeats are almost always identical with respect to size and sequence (Jansen *et al.*, 2002). In any CRISPR array, spacers are generally unique and frequently show high sequence identity to phages and other extrachromosomal elements (Mojica *et al.*, 2005; Makarova *et al.*, 2006). The size of CRISPR repeats and spacers varies between 23 to 47 bp and 21 to 72 bp, respectively (Jansen *et al.*, 2002; Grissa *et al.*, 2007). CRISPR loci are typically located in the chromosome, although some have been identified in plasmids (Mojica *et al.*, 2005; Godde and Bickerton, 2006; Lillestøl *et al.*, 2009). *cas* genes are strictly associated with CRISPR elements and always occur near a repeat cluster. Numerous, highly diverse Cas proteins are involved in the different stages of CRISPR activity (**Figure 3**). Specific functional domains identified in Cas proteins include endonuclease and exonuclease domains, helicases, RNA and DNA-binding domains, and domains that are involved in transcription regulation (Haft *et al.*, 2005). CRISPR, in combination with Cas proteins, forms the CRISPR-Cas systems.

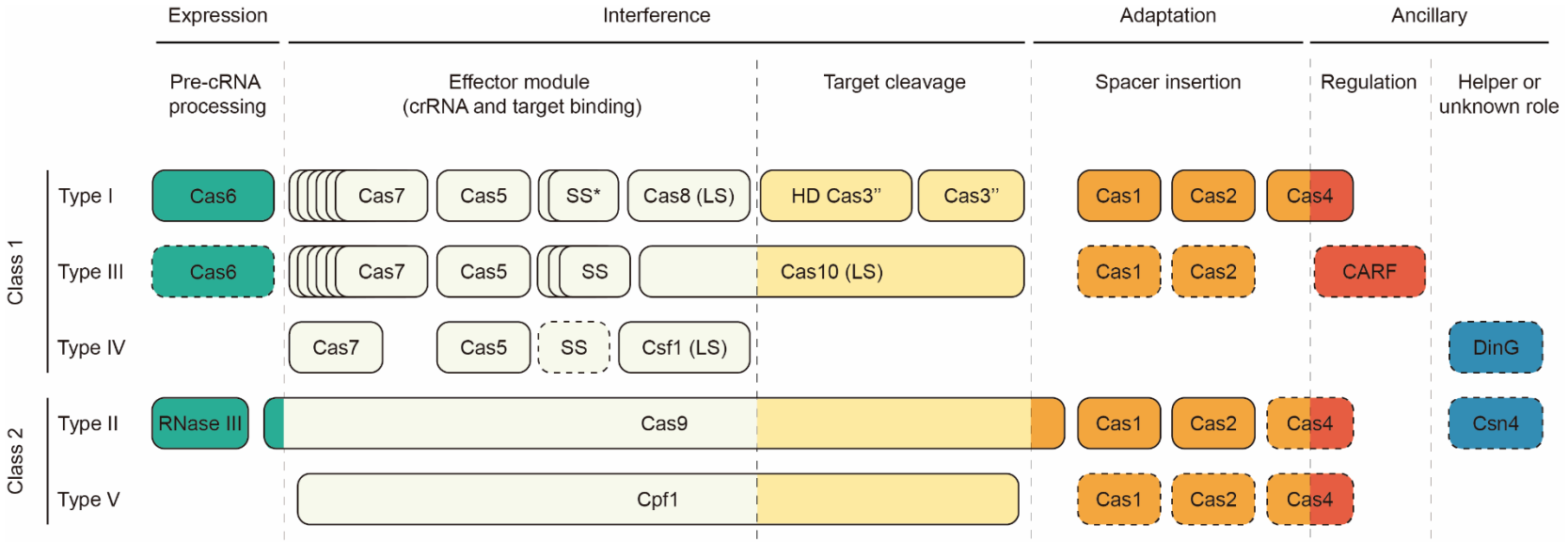

Figure 3. Functional classification of Cas proteins. Protein names follow the current nomenclature and classification. Dispensable components are indicated by dashed outlines. Colours reflect contribution to the different stages of the CRISPR–Cas response. Figure modified from Makarova *et al*., 2015.

CRISPR-Cas systems can be functionally divided in two classes based on the number of genes encoding the effector modules. Class 1 systems are characterized by the presence of multi-subunit effector complexes (the CRISPR-associated complex for antiviral defence or Cascade complex (Brouns *et al.*, 2008), the Csm complex (Marraffini and Sontheimer, 2008; Rouillon *et al.*, 2013) or the Cmr complex (Zhang *et al.*, 2012)), whereas in class 2 systems all functions of the effector complex are carried out by a single protein (Cas9, Cpf1). Classes 1 and 2 are subdivided into types I, III and IV and, II and V, respectively, each type with a distinctive composition of expression, interference and adaptation modules (Makarova *et al.*, 2015) (**Figure 3**).

CRISPR-Cas immunity involves three distinct mechanistic stages: adaptation, expression and interference (Garneau *et al.*, 2010; Westra *et al.*, 2012; Barrangou, 2013). The adaptation stage involves the incorporation of new spacers from fragments of foreign nucleic acids (protospacers) into the CRISPR array. Protospacer acquisition in many CRISPR-Cas systems requires recognition of a short protospacer adjacent motif (PAM) in the target molecule. It is important to note that the PAM sequence is not included when the protospacer is incorporated in the CRISPR locus, allowing the CRISPR-Cas system to distinguish between self and invader nucleic acid molecules. The PAM sequence varies depending on the effector. Cas1 and Cas2, which are present in most CRISPR-Cas systems (Chylinski *et al.*, 2014) (**Figure 3**), form a complex that represents the adaptation module and are required for the generation of this cellular memory (insertion of protospacers into CRISPR arrays) (Yosef *et al.*, 2012). During the expression stage, the CRISPR locus is transcribed generating a pre-mature CRISPR RNA (pre-crRNA) molecule that will be processed

into active CRISPR RNAs (crRNAs). In class 1 CRISPR-Cas systems, this processing is carried out by an endonuclease subunit of the multi-subunit effector complex (Wang *et al.*, 2011). In the case of class 2 CRISPR-Cas systems, the generation of mature crRNAs occurs via an alternative mechanism where an additional RNA, the transactivating CRISPR RNA (tracrRNA), binds to the pre-crRNA molecule, due to sequence complementarity with the repeat regions of the CRISPR-locus, generating a double-stranded RNA that is processed by RNase III; it results in crRNA:tracrRNA molecules (also known as guide-RNAs or gRNAs) containing just one spacer sequence (Deltcheva *et al.*, 2011). Finally, at the interference stage, the mature crRNA or crRNA:tracrRNA bound to either the multi-subunit effector complex or Cas9, screens and cleaves DNA or RNA upon recognition of its cognate and PAM sequences (Jinek *et al.*, 2012).

On account of their ability to direct sequence-specific DNA cleavage within complex genomes, CRISPR-Cas systems, especially type II, due to its simplicity and reduced number of components (it requires a single multi-domain protein, Cas9, and two RNA components: crRNA and the tracrRNA), have been widely used in genome editing and the development of versatile genetic tools (Hsu *et al.*, 2014; Pickar-Oliver and Gersbach, 2019). To make the system easy to engineer, the dual tracrRNA:crRNA can be artificially fused as a single RNA chimaera (single-guide RNA or sgRNA), which also directs sequence-specific Cas9 double-stranded DNA (dsDNA) cleavage but does not require a maturation process as the transcript emulates the active crRNA:tracrRNA molecules (Jinek *et al.*, 2012) (**Figure 4**).

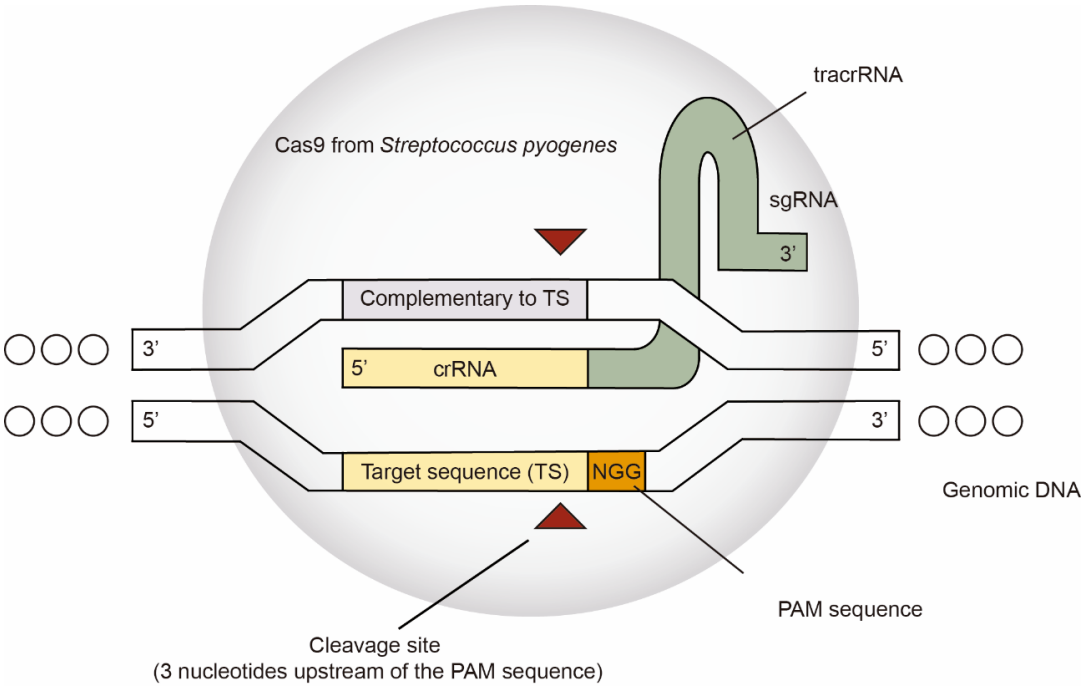

Figure 4. Schematic representation of the most common CRISPR-Cas system used in genome editing. A chimaeric RNA, generated by fusing the 3' end of crRNA to the 5' end of tracrRNA, directs Cas9-mediated site-specific cleavage upon recognition of a target sequence complementary to the crRNA. The target sequence must contain a PAM sequence, specific for each Cas protein, for the system to work. The endonucleolytic cut takes place 3 nucleotides upstream of the PAM sequence.

Up to date, *Steptococcus pyogenes* Cas9 (SpCas9), which recognizes a 5'-NGG-3' PAM, is, among the Cas9 proteins described, the most commonly used in genome editing platforms. However, there are other orthologues displaying similar efficiency yields and advantages over SpCas9. A main SpCas9 limitation, when basic research and therapeutic applications are considered, is its size and thus, the small Cas9 ortholog from *S. aureus* (*Staphylococcus aureus* Cas9 or SaCas9), that recognizes the 5'-NNGRRT-3' PAM sequence, is an attractive alternative to SpCas9 (Ran *et al.*, 2015; Tan *et al.*, 2019; Yourik *et al.*, 2019).

References

Ackermann, H.W. (2007) 5500 Phages examined in the electron microscope. *Arch Virol* **152**: 227–243.

Álvarez, A., Fernández, L., Gutiérrez, D., Iglesias, B., Rodríguez, A., and García, P. (2019) Methicillin-resistant *Staphylococcus aureus* in hospitals: latest trends and treatments based on bacteriophages. *J Clin Microbiol* **57**.

Archer, G.L. (1998) *Staphylococcus aureus* : a well–armed pathogen. *Clin Infect Dis* **26**: 1179–1181.

Arciola, C.R., Campoccia, D., Ravaioli, S., and Montanaro, L. (2015) Polysaccharide intercellular adhesin in biofilm: structural and regulatory aspects. *Front Cell Infect Microbiol* **5**.

Argudín, M.Á., Mendoza, M.C., and Rodicio, M.R. (2010) Food poisoning and *Staphylococcus aureus* enterotoxins. *Toxins (Basel)* **2**: 1751–1773.

Arrizubieta, M.J., Toledo-Arana, A., Amorena, B., Penadés, J.R., and Lasa, I. (2004) Calcium inhibits *bap*-dependent multicellular behavior in *Staphylococcus aureus*. *J Bacteriol* **186**: 7490–7498.

Arvidson, S. and Tegmark, K. (2001) Regulation of virulence determinants in *Staphylococcus aureus*. *Int J Med Microbiol* **291**: 159–170.

Bae, T., Baba, T., Hiramatsu, K., and Schneewind, O. (2006) Prophages of *Staphylococcus aureus* Newman and their contribution to virulence. *Mol Microbiol* **62**: 1035–1047.

Ballhausen, B., Kriegeskorte, A., Schleimer, N., Peters, G., and Becker, K. (2014) The *mecA* homolog *mecC* confers resistance against β-lactams in *Staphylococcus aureus* irrespective of the genetic strain background. *Antimicrob Agents Chemother* **58**: 3791–3798.

Barrangou, R. (2013) CRISPR-Cas systems and RNA-guided interference. *Wiley Interdiscip Rev RNA* **4**: 267–278.

Barrangou, R., Fremaux, C., Deveau, H., Richards, M., Boyaval, P., Moineau, S., *et al*. (2007) CRISPR provides acquired resistance against viruses in prokaryotes. *Science* **315**: 1709–1712.

Bento, J.C., Lane, K.D., Read, E.K., Cerca, N., and Christie, G.E. (2014) Sequence determinants for DNA packaging specificity in the *S. aureus* pathogenicity island SaPI1. *Plasmid* **71**: 8–15.

Bergstrom, C.T., Lipsitch, M., and Levin, B.R. (2000) Natural selection, infectious transfer and the existence conditions for bacterial plasmids. *Genetics* **155**: 1505–1519.

Bjorland, J., Sunde, M., and Waage, S. (2001) Plasmid-borne *smr* gene causes resistance to quaternary ammonium compounds in bovine *Staphylococcus aureus*. *J Clin Microbiol* **39**: 3999–4004.

Broer, S., Ji, G., Broer, A., and Silver, S. (1993) Arsenic efflux governed by the arsenic resistance determinant of *Staphylococcus aureus* plasmid pI258. *J Bacteriol* **175**: 3480–3485.

Brouns, S.J.J., Jore, M.M., Lundgren, M., Westra, E.R., Slijkhuis, R.J.H., Snijders, A.P.L., *et al*. (2008) Small CRISPR RNAs guide antiviral defense in prokaryotes. *Science* **321**: 960–964.

Brüssow, H., Canchaya, C., and Hardt, W.-D. (2004) Phages and the evolution of bacterial pathogens: from genomic rearrangements to lysogenic conversion. *Microbiol Mol Biol Rev* **68**: 560–602.

Bukowski, M., Lyzen, R., Helbin, W.M., Bonar, E., Szalewska-Palasz, A., Wegrzyn, G., *et al*. (2013) A regulatory role for *Staphylococcus aureus* toxin-antitoxin system PemIK Sa. *Nat Commun* **4**: 2012.

Canchaya, C., Proux, C., Fournous, G., Bruttin, A., and Brussow, H. (2003) Prophage genomics. *Microbiol Mol Biol Rev* **67**: 238–276.

Carroll, A.C. and Wong, A. (2018) Plasmid persistence: costs, benefits, and the plasmid paradox. *Can J Microbiol* **64**: 293–304.

Chambers, H.F. and DeLeo, F.R. (2009) Waves of resistance: *Staphylococcus aureus* in the antibiotic era. *Nat Rev Microbiol* **7**: 629–641.

Chandler, M. and Siguier, P. (2013) Insertion sequences. *Brenner's Encyclopedia of Genetics: Second Edition*. Elsevier Inc., 86–94.

Chen, J., Carpena, N., Quiles-Puchalt, N., Ram, G., Novick, R.P., and Penadés, J.R.

(2015) Intra- and inter-generic transfer of pathogenicity island-encoded virulence genes by *cos* phages. *ISME J* **9**: 1260–1263.

Chen, J. and Novick, R.P. (2009) Phage-mediated intergeneric transfer of toxin genes. *Science* **323**: 139–141.

Chen, J., Quiles-Puchalt, N., Chiang, Y.N., Bacigalupe, R., Fillol-Salom, A., Chee, M.S.J., *et al*. (2018) Genome hypermobility by lateral transduction. *Science* **362**: 207–212.

Chen, Y., Yan, F., Chai, Y., Liu, H., Kolter, R., Losick, R., and Guo, J.H. (2013) Biocontrol of tomato wilt disease by *Bacillus subtilis* isolates from natural environments depends on conserved genes mediating biofilm formation. *Environ Microbiol* **15**: 848–864.

Chiang, Y.N., Penadés, J.R., and Chen, J. (2019) Genetic transduction by phages and chromosomal islands: the new and noncanonical. *PLOS Pathog* **15**: e1007878.

Chou, S.H. and Galperin, M.Y. (2016) Diversity of cyclic di-GMP-binding proteins and mechanisms. *J Bacteriol* **198**: 32–46.

Chu, L., Mukhopadhyay, D., Yu, H., Kim, K.S., and Misra, T.K. (1992) Regulation of the *Staphylococcus aureus* plasmid p1258 mercury resistance operon. *J Bacteriol* **174**: 7044–7047.

Chylinski, K., Makarova, K.S., Charpentier, E., and Koonin, E.V. (2014) Classification and evolution of type II CRISPR-Cas systems. *Nucleic Acids Res* **42**: 6091–105.

Cohen, D., Mechold, U., Nevenzal, H., Yarmiyhu, Y., Randall, T.E., Bay, D.C., *et al*. (2015) Oligoribonuclease is a central feature of cyclic diguanylate signaling in *Pseudomonas aeruginosa*. *Proc Natl Acad Sci USA* **112**: 11359–11364.

Corbiere Morot-Bizot, S., Leroy, S., and Talon, R. (2007) Monitoring of staphylococcal starters in two French processing plants manufacturing dry fermented sausages. *J Appl Microbiol* **102**: 238–244.

Cramton, S.E., Gerke, C., Schnell, N.F., Nichols, W.W., and Götz, F. (1999) The intercellular adhesion (*ica*) locus is present in *Staphylococcus aureus* and is required for biofilm formation. *Infect Immun* **67**: 5427–5433.

Cruz, D.P., Huertas, M.G., Lozano, M., Zárate, L., and Zambrano, M.M. (2012) Comparative analysis of diguanylate cyclase and phosphodiesterase genes in *Klebsiella pneumoniae*. *BMC Microbiol* **12**: 139.

Cucarella, C., Solano, C., Valle, J., Amorena, B., Lasa, Í., and Penadés, J.R. (2001) Bap, a *Staphylococcus aureus* surface protein involved in biofilm formation. *J Bacteriol* **183**: 2888–2896.

Damle, P.K., Wall, E.A., Spilman, M.S., Dearborn, A.D., Ram, G., Novick, R.P., *et al*. (2012) The roles of SaPI1 proteins gp7 (CpmA) and gp6 (CpmB) in capsid size determination and helper phage interference. *Virology* **432**: 277–282.

Darmon, E. and Leach, D.R.F. (2014) Bacterial genome instability. *Microbiol Mol Biol Rev* **78**: 1–39.

Deghorain, M. and Van Melderen, L. (2012) The staphylococci phages family: an overview. *Viruses* **4**: 3316–3335.

Deltcheva, E., Chylinski, K., Sharma, C.M., Gonzales, K., Chao, Y., Pirzada, Z.A., *et al*. (2011) CRISPR RNA maturation by trans-encoded small RNA and host factor RNase III. *Nature* **471**: 602–607.

Diekema, D.J., Pfaller, M.A., Schmitz, F.J., Smayevsky, J., Bell, J., Jones, R.N., and Beach, M. (2001) Survey of infections due to *Staphylococcus* species: frequency of occurrence and antimicrobial susceptibility of isolates collected in the United States, Canada, Latin America, Europe, and the Western Pacific Region for the SENTRY antimicrobial surveillance program, 1997–1999. *Clin Infect Dis* **32**: S114–S132.

Donlan, R.M. (2011) Biofilm elimination on intravascular catheters: important considerations for the infectious disease practitioner. *Clin Infect Dis* **52**: 1038–45.

Donlan, R.M. and Costerton, J.W. (2002) Biofilms: survival mechanisms of clinically relevant microorganisms. *Clin Microbiol Rev* **15**: 167–193.

Dortet, L., Anguel, N., Fortineau, N., Richard, C., and Nordmann, P. (2013) In vivo acquired daptomycin resistance during treatment of methicillin-resistant *Staphylococcus aureus* endocarditis. *Int J Infect Dis* **17**: e1076–e1077.

Firth, N., Apisiridej, S., Berg, T., O'Rourke, B.A., Curnock, S., Dyke, K.G., and

Skurray, R.A. (2000) Replication of staphylococcal multiresistance plasmids. *J Bacteriol* **182**: 2170–8.

Firth, N., Jensen, S.O., Kwong, S.M., Skurray, R.A., and Ramsay, J.P. (2018) Staphylococcal plasmids, transposable and integrative elements. *Microbiol Spectr* **6**.

Fischer, A., Kambara, K., Meyer, H., Stenz, L., Bonetti, E.J., Girard, M., *et al*. (2014) GdpS contributes to *Staphylococcus aureus* biofilm formation by regulation of eDNA release. *Int J Med Microbiol* **304**: 284–299.

Frost, L.S., Leplae, R., Summers, A.O., and Toussaint, A. (2005) Mobile genetic elements: the agents of open source evolution. *Nat Rev Microbiol* **3**: 722–732.

Galié, S., García-Gutiérrez, C., Miguélez, E.M., Villar, C.J., and Lombó, F. (2018) Biofilms in the food industry: health aspects and control methods. *Front Microbiol* **9**.

Galperin, M.Y. (2005) A census of membrane-bound and intracellular signal transduction proteins in bacteria: bacterial IQ, extroverts and introverts. *BMC Microbiol* **5**: 35.

Galperin, M.Y. (2006) Structural classification of bacterial response regulators: diversity of output domains and domain combinations. *J Bacteriol* **188**: 4169–4182.

Galperin, M.Y., Nikolskaya, A.N., and Koonin, E.V. (2001) Novel domains of the prokaryotic two-component signal transduction systems. *FEMS Microbiol Lett* **203**: 11–21.

Garneau, J.E., Dupuis, M.È., Villion, M., Romero, D.A., Barrangou, R., Boyaval, P., *et al*. (2010) The CRISPR/*cas* bacterial immune system cleaves bacteriophage and plasmid DNA. *Nature* **468**: 67–71.

Geoghegan, J.A., Corrigan, R.M., Gruszka, D.T., Speziale, P., O'Gara, J.P., Potts, J.R., and Foster, T.J. (2010) Role of surface protein SasG in biofilm formation by *Staphylococcus aureus*. *J Bacteriol* **192**: 5663–5673.

Godde, J.S. and Bickerton, A. (2006) The repetitive DNA elements called CRISPRs and their associated genes: evidence of horizontal transfer among prokaryotes. *J Mol Evol* **62**: 718–729.

Goerke, C., Pantucek, R., Holtfreter, S., Schulte, B., Zink, M., Grumann, D., *et al*. (2009) Diversity of prophages in dominant *Staphylococcus aureus* clonal lineages. *J Bacteriol* **191**: 3462–3468.

Götz, F. (2002) *Staphylococcus* and biofilms. *Mol Microbiol* **43**: 1367–1378.

Götz, F. (1990) *Staphylococcus carnosus*: a new host organism for gene cloning and protein production. *J Appl Bacteriol* **69**: 49S-53S.

Grissa, I., Vergnaud, G., and Pourcel, C. (2007) The CRISPRdb database and tools to display CRISPRs and to generate dictionaries of spacers and repeats. *BMC Bioinformatics* **8**: 172.

Grundmann, H., Aires-de-Sousa, M., Boyce, J., and Tiemersma, E. (2006) Emergence and resurgence of meticillin-resistant *Staphylococcus aureus* as a public-health threat. *Lancet* **368**: 874–885.

Gu, B., Kelesidis, T., Tsiodras, S., Hindler, J., and Humphries, R.M. (2013) The emerging problem of linezolid-resistant *Staphylococcus*. *J Antimicrob Chemother* **68**: 4–11.

Haaber, J., Penadés, J.R., and Ingmer, H. (2017) Transfer of antibiotic resistance in *Staphylococcus aureus*. *Trends Microbiol* **25**: 893–905.

Haft, D.H., Selengut, J., Mongodin, E.F., and Nelson, K.E. (2005) A guild of 45 CRISPR-associated (Cas) protein families and multiple CRISPR/*cas* subtypes exist in prokaryotic genomes. *PLoS Comput Biol* **1**: 0474–0483.

Hall-Stoodley, L. and Stoodley, P. (2005) Biofilm formation and dispersal and the transmission of human pathogens. *Trends Microbiol* **13**: 7–10.

Heilmann, C., Schweitzer, O., Gerke, C., Vanittanakom, N., Mack, D., and Götz, F. (1996) Molecular basis of intercellular adhesion in the biofilm-forming *Staphylococcus epidermidis*. *Mol Microbiol* **20**: 1083–1091.

Hiramatsu, K., Aritaka, N., Hanaki, H., Kawasaki, S., Hosoda, Y., Hori, S., *et al*. (1997) Dissemination in Japanese hospitals of strains of *Staphylococcus aureus* heterogeneously resistant to vancomycin. *Lancet* **350**: 1670–1673.

Hiramatsu, K., Hanaki, H., Ino, T., Yabuta, K., Oguri, T., and Tenover, F.C. (1997) Methicillin-resistant *Staphylococcus aureus* clinical strain with reduced

vancomycin susceptibility. *J Antimicrob Chemother* **40**: 135–136.

Høiby, N., Bjarnsholt, T., Givskov, M., Molin, S., and Ciofu, O. (2010) Antibiotic resistance of bacterial biofilms. *Int J Antimicrob Agents* **35**: 322–332.

Holland, L.M., O'Donnell, S.T., Ryjenkov, D.A., Gomelsky, L., Slater, S.R., Fey, P.D., *et al*. (2008) A staphylococcal GGDEF domain protein regulates biofilm formation independently of cyclic dimeric GMP. *J Bacteriol* **190**: 5178–5189.

Horvath, P. and Barrangou, R. (2010) CRISPR/Cas, the immune system of bacteria and archaea. *Science* **327**: 167–170.

Howden, B.P., Davies, J.K., Johnson, P.D.R., Stinear, T.P., and Grayson, M.L. (2010) Reduced vancomycin susceptibility in *Staphylococcus aureus*, including vancomycin-intermediate and heterogeneous vancomycin-intermediate strains: Resistance mechanisms, laboratory detection, and clinical implications. *Clin Microbiol Rev* **23**: 99–139.

Hsu, P.D., Lander, E.S., and Zhang, F. (2014) Development and applications of CRISPR-Cas9 for genome engineering. *Cell* **157**: 1262–1278.

Jansen, R., Van Embden, J.D.A., Gaastra, W., and Schouls, L.M. (2002) Identification of genes that are associated with DNA repeats in prokaryotes. *Mol Microbiol* **43**: 1565–1575.

Jenal, U., Reinders, A., and Lori, C. (2017) Cyclic di-GMP: second messenger extraordinaire. *Nat Rev Microbiol* **15**: 271–284.

Jinek, M., Chylinski, K., Fonfara, I., Hauer, M., Doudna, J.A., and Charpentier, E. (2012) A programmable dual-RNA-guided DNA endonuclease in adaptive bacterial immunity. *Science* **337**: 816–821.

Kluytmans, J., Van Belkum, A., and Verbrugh, H. (1997) Nasal carriage of *Staphylococcus aureus*: epidemiology, underlying mechanisms, and associated risks. *Clin Microbiol Rev* **10**: 505–520.

Kuroda, M., Yamashita, A., Hirakawa, H., Kumano, M., Morikawa, K., Higashide, M., *et al*. (2005) Whole genome sequence of *Staphylococcus saprophyticus* reveals the pathogenesis of uncomplicated urinary tract infection. *Proc Natl Acad Sci USA* **102**: 13272–13277.

Kwan, T., Liu, J., DuBow, M., Gros, P., and Pelletier, J. (2005) The complete genomes and proteomes of 27 *Staphylococcus aureus* bacteriophages. *Proc Natl Acad Sci USA* **102**: 5174–5179.

Lasa, I. (2006) Towards the identification of the common features of bacterial biofilm development. *Int Microbiol* **9**: 21–28.

Lasa, I. and Penadés, J.R. (2006) Bap: a family of surface proteins involved in biofilm formation. *Res Microbiol* **157**: 99–107.

Latasa, C., Solano, C., Penadés, J.R., and Lasa, I. (2006) Biofilm-associated proteins. *Comptes Rendus - Biol* **329**: 849–857.

Lillestøl, R.K., Shah, S.A., Brügger, K., Redder, P., Phan, H., Christiansen, J., and Garrett, R.A. (2009) CRISPR families of the crenarchaeal genus *Sulfolobus*: bidirectional transcription and dynamic properties. *Mol Microbiol* **72**: 259–272.

Louwen, R., Staals, R.H.J., Endtz, H.P., van Baarlen, P., and van der Oost, J. (2014) The role of CRISPR-Cas systems in virulence of pathogenic bacteria. *Microbiol Mol Biol Rev* **78**: 74–88.

Lowder, B. V., Guinane, C.M., Zakour, N.L.B., Weinert, L.A., Conway-Morris, A., Cartwright, R.A., *et al*. (2009) Recent human-to-poultry host jump, adaptation, and pandemic spread of *Staphylococcus aureus*. *Proc Natl Acad Sci USA* **106**: 19545–19550.

Mack, D., Fischer, W., Krokotsch, A., Leopold, K., Hartmann, R., Egge, H., and Laufs, R. (1996) The intercellular adhesin involved in biofilm accumulation of *Staphylococcus epidermidis* is a linear β-1,6-linked glucosaminoglycan: purification and structural analysis. *J Bacteriol* **178**: 175–183.

MacLean, R.C. and San Millan, A. (2015) Microbial evolution: towards resolving the Plasmid Paradox. *Curr Biol* **25**: R764–R767.

Maiques, E., Úbeda, C., Campoy, S., Salvador, N., Lasa, Í., Novick, R.P., *et al*. (2006) β-lactam antibiotics induce the SOS response and horizontal transfer of virulence factors in *Staphylococcus aureus*. *J Bacteriol* **188**: 2726–2729.

Maiques, E., Úbeda, C., Tormo, M.Á., Ferrer, M.D., Lasa, Í., Novick, R.P., and Penadés, J.R. (2007) Role of staphylococcal phage and SaPI integrase in intra- and interspecies SaPI transfer. *J Bacteriol* **189**: 5608–5616.

Makarova, K.S., Grishin, N.V., Shabalina, S.A., Wolf, Y.I., and Koonin, E.V. (2006) A putative RNA-interference-based immune system in prokaryotes: computational analysis of the predicted enzymatic machinery, functional analogies with eukaryotic RNAi, and hypothetical mechanisms of action. *Biol Direct* **1**.

Makarova, K.S., Wolf, Y.I., Alkhnbashi, O.S., Costa, F., Shah, S.A., Saunders, S.J., *et al*. (2015) An updated evolutionary classification of CRISPR-Cas systems. *Nat Rev Microbiol* **13**: 722–736.

Malachowa, N. and Deleo, F.R. (2010) Mobile genetic elements of *Staphylococcus aureus*. *Cell Mol Life Sci* **67**: 3057–3071.

Marraffini, L.A. and Sontheimer, E.J. (2008) CRISPR interference limits horizontal gene transfer in staphylococci by targeting DNA. *Science* **322**: 1843–1845.

McCarthy, A.J., Loeffler, A., Witney, A.A., Gould, K.A., Lloyd, D.H., and Lindsay, J.A. (2014) Extensive horizontal gene transfer during *Staphylococcus aureus* co-colonization in vivo. *Genome Biol Evol* **6**: 2697–2708.

McKenney, D., Hübner, J., Muller, E., Wang, Y., Goldmann, D.A., and Pier, G.B. (1998) The *ica* locus of Staphylococcus epidermidis encodes production of the capsular polysaccharide/adhesin. *Infect Immun* **66**: 4711–4720.

McKenney, D., Pouliot, K.L., Wang, Y., Murthy, V., Ulrich, M., Döring, G., *et al*. (1999) Broadly protective vaccine for *Staphylococcus aureus* based on an in vivo-expressed antigen. *Science* **284**: 1523–1527.

Million-Weaver, S. and Camps, M. (2014) Mechanisms of plasmid segregation: have multicopy plasmids been overlooked? *Plasmid* **75**: 27–36.

Młynarczyk, A., Młynarczyk, G., and Jeljaszewicz, J. (1998) The genome of *Staphylococcus aureus*: a review. *Zentralbl Bakteriol* **287**: 277–314.

Mojica, F.J., Díez-Villaseñor, C., García-Martínez, J., and Soria, E. (2005) Intervening sequences of regularly spaced prokaryotic repeats derive from foreign genetic elements. *J Mol Evol* **60**: 174–182.

Morikawa, K., Takemura, A.J., Inose, Y., Tsai, M., Nguyen Thi, L.T., Ohta, T., and Msadek, T. (2012) Expression of a cryptic secondary sigma factor gene unveils natural competence for DNA transformation in *Staphylococcus aureus*. *PLoS*

Pathog **8**: e1003003.

Nicolella, C., Zolezzi, M., Rabino, M., Furfaro, M., and Rovatti, M. (2005) Development of particle-based biofilms for degradation of xenobiotic organic compounds. *Water Res* **39**: 2495–2504.

Novick, R.P. (1989) Staphylococcal plasmids and their replication. *Annu Rev Microbiol* **43**: 537–563.

Novick, R.P., Christie, G.E., and Penadés, J.R. (2010) The phage-related chromosomal islands of Gram-positive bacteria. *Nat Rev Microbiol* **8**: 541–551.

Novick, R.P. and Ram, G. (2017) Staphylococcal pathogenicity islands - movers and shakers in the genomic firmament. *Curr Opin Microbiol* **38**: 197–204.

Novick, R.P., Ross, H.F., Projan, S.J., Kornblum, J., Kreiswirth, B., and Moghazeh, S. (1993) Synthesis of staphylococcal virulence factors is controlled by a regulatory RNA molecule. *EMBO J* **12**: 3967–3975.

O'Brien, F.G., Ramsay, J.P., Monecke, S., Coombs, G.W., Robinson, O.J., Htet, Z., *et al*. (2015) *Staphylococcus aureus* plasmids without mobilization genes are mobilized by a novel conjugative plasmid from community isolates. *J Antimicrob Chemother* **70**: 649–52.

O'Gara, J.P. (2007) *ica* and beyond: biofilm mechanisms and regulation in *Staphylococcus epidermidis* and *Staphylococcus aureus*. *FEMS Microbiol Lett* **270**: 179–188.

O'Neill, A.J., Larsen, A.R., Skov, R., Henriksen, A.S., and Chopra, I. (2007) Characterization of the epidemic European fusidic acid-resistant impetigo clone of *Staphylococcus aureus*. *J Clin Microbiol* **45**: 1505–1510.

Ochman, H., Lawrence, J.G., and Grolsman, E.A. (2000) Lateral gene transfer and the nature of bacterial innovation. *Nature* **405**: 299–304.

Oram, M. and Black, L. (2011) Mechanisms of genome packaging. *Structural Virology*. RSC Publishing, 213–219.

Orr, M.W., Donaldson, G.P., Severin, G.B., Wang, J., Sintim, H.O., Waters, C.M., and Lee, V.T. (2015) Oligoribonuclease is the primary degradative enzyme for pGpG in *Pseudomonas aeruginosa* that is required for cyclic-di-GMP turnover.

Proc Natl Acad Sci USA **112**: E5048–E5057.

Penadés, J.R., Chen, J., Quiles-Puchalt, N., Carpena, N., and Novick, R.P. (2015) Bacteriophage-mediated spread of bacterial virulence genes. *Curr Opin Microbiol* **23**: 171–178.

Penadés, J.R. and Christie, G.E. (2015) The phage-inducible chromosomal islands: a family of highly evolved molecular parasites. *Annu Rev Virol* **2**: 181–201.

Pérez-Mendoza, D. and Sanjuán, J. (2016) Exploiting the commons: cyclic diguanylate regulation of bacterial exopolysaccharide production. *Curr Opin Microbiol* **30**: 36–43.

Périchon, B. and Courvalin, P. (2009) VanA-type vancomycin-resistant *Staphylococcus aureus*. *Antimicrob Agents Chemother* **53**: 4580–4587.

Phillips, G. and Funnell, B.E. Plasmid Biology (2004) American Society of Microbiology.

Pickar-Oliver, A. and Gersbach, C.A. (2019) The next generation of CRISPR–Cas technologies and applications. *Nat Rev Mol Cell Biol* **20**: 490–507.

Place, R.B., Hiestand, D., Gallmann, H.R., and Teuber, M. (2003) *Staphylococcus equorum* subsp. *linens*, subsp, nov., a starter culture component for surface ripened semi-hard cheeses. *Syst Appl Microbiol* **26**: 30–37.

Ram, G., Chen, J., Kumar, K., Ross, H.F., Ubeda, C., Damle, P.K., *et al*. (2012) Staphylococcal pathogenicity island interference with helper phage reproduction is a paradigm of molecular parasitism. *Proc Natl Acad Sci USA* **109**: 16300–16305.

Ram, G., Chen, J., Ross, H.F., Novick, R.P., and Musser, J.M. (2014) Precisely modulated pathogenicity island interference with late phage gene transcription. *Proc Natl Acad Sci USA* **111**: 14536–14541.

Ramsay, J.P. and Firth, N. (2017) Diverse mobilization strategies facilitate transfer of non-conjugative mobile genetic elements. *Curr Opin Microbiol* **38**: 1–9.

Ramsay, J.P., Kwong, S.M., Murphy, R.J.T., Yui Eto, K., Price, K.J., Nguyen, Q.T., *et al*. (2016) An updated view of plasmid conjugation and mobilization in *Staphylococcus*. *Mob Genet Elements* **6**: e1208317.

Ran, F.A., Cong, L., Yan, W.X., Scott, D.A., Gootenberg, J.S., Kriz, A.J., *et al*. (2015) In vivo genome editing using *Staphylococcus aureus* Cas9. *Nature* **520**: 186–191.

Rao, V.B. and Feiss, M. (2015) Mechanisms of DNA packaging by large double-stranded DNA viruses. *Annu Rev Virol* **2**: 351–378.

Römling, U. (2009) Rationalizing the evolution of EAL domain-based cyclic di-GMP-specific phosphodiesterases. *J Bacteriol* **191**: 4697–4700.

Römling, U., Galperin, M.Y., and Gomelsky, M. (2013) Cyclic di-GMP: the first 25 years of a universal bacterial second messenger. *Microbiol Mol Biol Rev* **77**: 1–52.

Rossi, F., Diaz, L., Wollam, A., Panesso, D., Zhou, Y., Rincon, S., *et al*. (2014) Transferable vancomycin resistance in a community-associated MRSA lineage. *N Engl J Med* **370**: 1524–1531.

Rouillon, C., Zhou, M., Zhang, J., Politis, A., Beilsten-Edmands, V., Cannone, G., *et al*. (2013) Structure of the CRISPR interference complex CSM reveals key similarities with cascade. *Mol Cell* **52**: 124–134.

Sampson, T.R. and Weiss, D.S. (2014) CRISPR-Cas systems: new players in gene regulation and bacterial physiology. *Front Cell Infect Microbiol* **4**: 37.

Schirmer, T. and Jenal, U. (2009) Structural and mechanistic determinants of c-di-GMP signalling. *Nat Rev Microbiol* **7**: 724–735.

Schwarz, S., Feßler, A.T., Hauschild, T., Kehrenberg, C., and Kadlec, K. (2011) Plasmid-mediated resistance to protein biosynthesis inhibitors in staphylococci. *Ann NY Acad Sci* **1241**: 82–103.

Schwarz, S., Shen, J., Wendlandt, S., Feßler, A.T., Wang, Y., Kadlec, K., and Wu, C.-M. (2014) Plasmid-mediated antimicrobial resistance in staphylococci and other Firmicutes. *Microbiol Spectr* **2**:.

Selva, L., Viana, D., Regev-Yochay, G., Trzcinski, K., Corpa, J.M., Lasa, Í., *et al*. (2009) Killing niche competitors by remote-control bacteriophage induction. *Proc Natl Acad Sci USA* **106**: 1234–1238.

Sengupta, M. and Austin, S. (2011) Prevalence and significance of plasmid maintenance functions in the virulence plasmids of pathogenic bacteria. *Infect Immun* **79**: 2502–2509.

Shang, F., Xue, T., Sun, H., Xing, L., Zhang, S., Yang, Z., *et al*. (2009) The *Staphylococcus aureus* GGDEF protein GdpS influences protein A gene expression in a c-di-GMP-independent manner. *Infect Immun*.

Sheehy, R.J. and Novick, R.P. (1975) Studies on plasmid replication. V. Replicative intermediates. *J Mol Biol* **93**: 237–253.

Shi, X. and Zhu, X. (2009) Biofilm formation and food safety in food industries. *Trends Food Sci Technol* **20**: 407–413.

Simm, R., Morr, M., Kader, A., Nimtz, M., and Römling, U. (2004) GGDEF and EAL domains inversely regulate cyclic di-GMP levels and transition from sessibility to motility. *Mol Microbiol* **53**: 1123–1134.

Singh, R., Paul, D., and Jain, R.K. (2006) Biofilms: implications in bioremediation. *Trends Microbiol* **14**: 389–397.

Sorek, R., Kunin, V., and Hugenholtz, P. (2008) CRISPR - a widespread system that provides acquired resistance against phages in bacteria and archaea. *Nat Rev Microbiol* **6**: 181–186.

Spratt, B.G. (1994) Resistance to antibiotics mediated by target alterations. *Science* **264**: 388–393.

Stelitano, V., Giardina, G., Paiardini, A., Castiglione, N., Cutruzzolà, F., and Rinaldo, S. (2013) C-di-GMP hydrolysis by *Pseudomonas aeruginosa* HD-GYP phosphodiesterases: analysis of the reaction mechanism and novel roles for pGpG. *PLoS One* **8**.

Taglialegna, A., Matilla-Cuenca, L., Dorado-Morales, P., Navarro, S., Ventura, S., Garnett, J.A., *et al*. (2020) The biofilm-associated surface protein Esp of *Enterococcus faecalis* forms amyloid-like fibers. *npj Biofilms Microbiomes* **6**: 1–12.

Taglialegna, A., Navarro, S., Ventura, S., Garnett, J.A., Matthews, S., Penades, J.R., *et al*. (2016) Staphylococcal Bap proteins build amyloid scaffold biofilm matrices in response to environmental signals. *PLOS Pathog* **12**: e1005711.

Tan, Y., Chu, A.H.Y., Bao, S., Hoang, D.A., Kebede, F.T., Xiong, W., *et al*. (2019) Rationally engineered *Staphylococcus aureus* Cas9 nucleases with high genome-wide specificity. *Proc Natl Acad Sci USA* **116**: 20969–20976.

Tojo, M., Yamashita, N., Goldmann, D.A., and Pier, G.B. (1988) Isolation and characterization of a capsular polysaccharide adhesin from *Staphylococcus epidermidis*. *J Infect Dis* **157**: 713–22.

Úbeda, C., Maiques, E., Knecht, E., Lasa, Í., Novick, R.P., and Penadés, J.R. (2005) Antibiotic-induced SOS response promotes horizontal dissemination of pathogenicity island-encoded virulence factors in staphylococci. *Mol Microbiol* **56**: 836–844.

Ubeda, C., Olivarez, N.P., Barry, P., Wang, H., Kong, X., Matthews, A., *et al*. (2009) Specificity of staphylococcal phage and SaPI DNA packaging as revealed by integrase and terminase mutations. *Mol Microbiol* **72**: 98–108.

Úbeda, C., Tormo, M.Á., Cucarella, C., Trotonda, P., Foster, T.J., Lasa, Í., and Penadés, J.R. (2003) Sip, an integrase protein with excision, circularization and integration activities, defines a new family of mobile *Staphylococcus aureus* pathogenicity islands. *Mol Microbiol* **49**: 193–210.

Ulrich, L.E., Koonin, E.V., and Zhulin, I.B. (2005) One-component systems dominate signal transduction in prokaryotes. *Trends Microbiol* **13**: 52–56.

Varga, M., Kuntová, L., Pantůček, R., Mašlaňová, I., Růžičková, V., and Doškař, J. (2012) Efficient transfer of antibiotic resistance plasmids by transduction within methicillin-resistant *Staphylococcus aureus* USA300 clone. *FEMS Microbiol Lett* **332**: 146–152.

Varga, M., Pantůček, R., Růžičková, V., and Doškař, J. (2016) Molecular characterization of a new efficiently transducing bacteriophage identified in meticillin-resistant *Staphylococcus aureus*. *J Gen Virol* **97**: 258–268.

Viana, D., Blanco, J., Tormo-Más, M.Á., Selva, L., Guinane, C.M., Baselga, R., *et al*. (2010) Adaptation of *Staphylococcus aureus* to ruminant and equine hosts involves SaPI-carried variants of von Willebrand factor-binding protein. *Mol Microbiol* **77**: 1583–1594.

Vuotto, C., Longo, F., and Donelli, G. (2014) Probiotics to counteract biofilm-associated infections: promising and conflicting data. *Int J Oral Sci* **6**: 189–194.

Walker, T.S., Bais, H.P., Déziel, E., Schweizer, H.P., Rahme, L.G., Fall, R., and Vivanco, J.M. (2004) *Pseudomonas aeruginosa*-plant root interactions.

Pathogenicity, biofilm formation, and root exudation. *Plant Physiol* **134**: 320–331.

Wang, R., Preamplume, G., Terns, M.P., Terns, R.M., and Li, H. (2011) Interaction of the Cas6 riboendonuclease with CRISPR RNAs: Recognition and cleavage. *Structure* **19**: 257–264.

Westra, E.R., Buckling, A., and Fineran, P.C. (2014) CRISPR-Cas systems: beyond adaptive immunity. *Nat Rev Microbiol* **12**: 317–326.

Westra, E.R., Swarts, D.C., Staals, R.H.J., Jore, M.M., Brouns, S.J.J., and van der Oost, J. (2012) The CRISPRs, they are a-changin': how prokaryotes generate adaptive immunity. *Annu Rev Genet* **46**: 311–339.

Whitchurch, C.B., Tolker-Nielsen, T., Ragas, P.C., and Mattick, J.S. (2002) Extracellular DNA required for bacterial biofilm formation. *Science* **295**: 1487.

Winkler, W.C., Cohen-Chalamish, S., and Breaker, R.R. (2002) An mRNA structure that controls gene expression by binding FMN. *Proc Natl Acad Sci USA* **99**: 15908–15913.

Winstel, V., Liang, C., Sanchez-Carballo, P., Steglich, M., Munar, M., Broker, B.M., *et al*. (2013) Wall teichoic acid structure governs horizontal gene transfer between major bacterial pathogens. *Nat Commun* **4**: 1–9.

Wladyka, B., Piejko, M., Bzowska, M., Pieta, P., Krzysik, M., Mazurek, Ł., *et al*. (2015) A peptide factor secreted by *Staphylococcus pseudintermedius* exhibits properties of both bacteriocins and virulence factors. *Sci Rep* **5**: 1–15.

Xia, G. and Wolz, C. (2014) Phages of *Staphylococcus aureus* and their impact on host evolution. *Infect Genet Evol* **21**: 593–601.

Yamaguchi, T., Hayashi, T., Takami, H., Ohnishi, M., Murata, T., Nakayama, K., *et al*. (2001) Complete nucleotide sequence of a *Staphylococcus aureus* exfoliative toxin B plasmid and identification of a novel ADP-ribosyltransferase, EDIN-C. *Infect Immun* **69**: 7760–7771.

Yoon, K.P., Misra, T.K., and Silver, S. (1991) Regulation of the *cadA* cadmium resistance determinant of *Staphylococcus aureus* plasmid pI258. *J Bacteriol* **173**: 7643–7649.

Yosef, I., Goren, M.G., and Qimron, U. (2012) Proteins and DNA elements essential for the CRISPR adaptation process in *Escherichia coli*. *Nucleic Acids Res* **40**: 5569–76.

Yourik, P., Fuchs, R.T., Mabuchi, M., Curcuru, J.L., and Robb, G.B. (2019) *Staphylococcus aureus* Cas9 is a multiple-turnover enzyme. *RNA* **25**: 35–44.

Zhang, J., Rouillon, C., Kerou, M., Reeks, J., Brugger, K., Graham, S., *et al*. (2012) Structure and mechanism of the CMR complex for CRISPR-mediated antiviral immunity. *Mol Cell* **45**: 303–313.

Zhu, T., Zhao, Y., Wu, Y., and Qu, D. (2017) The *Staphylococcus epidermidis gdpS* regulates biofilm formation independently of its protein-coding function. *Microb Pathog* **105**: 264–271.

Zhu, W., Clark, N.C., McDougal, L.K., Hageman, J., McDonald, L.C., and Patel, J.B. (2008) Vancomycin-resistant *Staphylococcus aureus* isolates associated with Inc18-like *vanA* plasmids in Michigan. *Antimicrob Agents Chemother* **52**: 452–457.

CHAPTER I

Elevated c-di-GMP levels promote biofilm formation and biodesulfurization capacity of *Rhodococcus erythropolis*

Summary

Bacterial biofilms provide high cell density and a superior adaptation and protection from stress conditions compared to planktonic cultures, making them a very promising approach for bioremediation. Several *Rhodococcus* strains can desulfurize dibenzothiophene (DBT), a major sulfur pollutant in fuels, reducing air pollution from fuel combustion. Despite multiple efforts to increase *Rhodococcus* biodesulfurization activity, there is still an urgent need to develop better biocatalysts. Here, we implemented a new approach that consisted in promoting *Rhodococcus erythropolis* biofilm formation through the heterologous expression of a diguanylate cyclase that led to the synthesis of the biofilm trigger molecule cyclic di-GMP (c-di-GMP). *R. erythropolis* biofilm cells displayed a significantly increased DBT desulfurization activity when compared to their planktonic counterparts. The improved biocatalyst formed a biofilm both under batch and continuous flow conditions which turns it into a promising candidate for the development of an efficient bioreactor for the removal of sulfur heterocycles present in fossil fuels.

Introduction

Bacterial biofilms are structured communities of bacterial cells enclosed in a self-produced polymeric matrix (Costerton *et al.*, 1999). Biofilms constitute a protected type of growth and thus, bacteria living in the form of biofilms are characterized by a superior resilience and robustness compared to planktonic cells that allows survival in hostile environments (Costerton *et al.*, 1999; Edel *et al.*, 2019). Such decreased susceptibility to environmental stressors together with the long-term activity shown by biofilm cells, the high microbial cell density, the ability to immobilize compounds and the easiness of separation of the end-product from the catalytic biomass, make biofilm systems a very practical and promising tool in bioremediation strategies (Singh *et al.*, 2006; Rosche *et al.*, 2009; Edel *et al.*, 2019). Fundamental to these properties is the role of the self-produced polymeric matrix that encases the cells of the biofilm and is mainly composed of polysaccharides, proteins, and extracellular DNA (eDNA) (Flemming *et al.*, 2016). Although the diversity in matrix composition and regulatory mechanisms controlling its synthesis is high, many diverse and phylogenetically distant bacterial species share common features that promote biofilm development such as the production of some exopolysaccharides (poly-β(1-6)-N-acetyl-glucosamine (PIA/PNAG), cellulose) (Cywes-Bentley *et al.*, 2013; Römling and Galperin, 2015), proteins with amyloid or amyloid-like conformation (Taglialegna, Lasa, *et al.*, 2016) and synthesis of the secondary messenger cyclic di-GMP (c-di-GMP) (Römling *et al.*, 2013).

Rhodococcus genus is a heterogeneous group of Gram-positive bacteria that present unique enzymatic capabilities of great biotechnological importance (Zampolli *et al.*,

2019). Amongst these bacteria, several strains of *Rhodococcus erythropolis* are considered as model organisms for biodesulfurization (BDS), an environmentally friendly method that aims at the removal of sulfur from refractory organic compounds of fossil fuels, at mild operating conditions, without lowering the calorific value of the fuel (Mohebali and Ball, 2016; Kilbane, 2017). This method is a complementary alternative to hydrodesulfurization (HDS), the most common technology used by refineries, that suffers from significant technical and economic limitations (Kilbane, 2006; Soleimani *et al.*, 2007). Removal of sulfur from crude oil products has great environmental impact, because fuel combustion results in sulfur dioxide emission into the environment, causing air pollution and acid rain. The *R. erythropolis* IGTS8 strain was the first bacterium in which the 4S pathway was reported (Gallagher *et al.*, 1993), by which dibenzothiophene (DBT), a major sulfur-containing aromatic compound in fuels that is recalcitrant to HDS, is converted to 2-hydroxybiphenyl (2HBP) and sulfite. The 4S pathway occurs via serial reactions in which two monooxygenases, DszC and DszA, and a desulfinase, DszB, are involved. The genes encoding these biodesulfurization enzymes are clustered in the *dszABC* operon present in a megaplasmid (Piddington *et al.*, 1995). Also, and since the monooxygenation reactions catalyzed by DszA and DszC require electrons, a fourth enzyme, the flavin reductase DszD, encoded by the chromosomal *dszD* gene, is needed for DBT desulfurization (Gray *et al.*, 1996). Desulfurization activity of naturally occurring bacterial cultures is very low due to different reasons, such as the lack of a *dszD* gene in the native *dsz* operon, the sulfate-mediated repression of the biodesulfurization operon (Li *et al.*, 1996), the poorly known transcriptional regulation of *dsz* genes (Kilbane, 2006), the inhibition, activity levels and restricted

substrate range of Dsz enzymes (Kilbane, 2006) and the limited solvent tolerance of the host cell (Kilbane, 2017). Thus, multiple efforts mostly based on genetic engineering of the *dsz* operon have been made to achieve higher desulfurization rates. However, the desulfurization levels reached by genetic manipulation are still inadequate to fulfill the industrial requirements and seem to be restricted by still unknown host factors. Therefore, it has long been proposed that modifications of other host functions are needed in order to develop desulfurization biocatalysts with higher specific activity (Kilbane, 2006; Martínez *et al.*, 2017; Wang *et al.*, 2017).

Taking into account the features of biofilm systems described above that make them especially suitable for the treatment of recalcitrant compounds and also, the fact that biofilm-dwelling microorganisms are widely accepted as being responsible for the majority of pollutant degradation in natural environments (Lear, 2016), in this work, we aimed at enhancing *R. erythropolis* biodesulfurization capacity by promoting its ability to form a biofilm. A selected strategy based on the overexpression of optimized *dsz* cassettes together with a heterologous diguanylate cyclase, named AdrA (Simm *et al.*, 2004), that drives the synthesis of elevated levels of the biofilm trigger molecule, c-di-GMP, highly promoted biofilm development under batch and continuous flow conditions and significantly improved specific desulfurization activity of *R. erythropolis* cells.

Experimental procedures

Bacterial strains, plasmids, oligonucleotides and culture conditions

Bacterial strains, plasmids and oligonucleotides used in this work are listed in Tables 1 and 2, respectively. *Escherichia coli* strains were routinely grown in LB broth (Condalab) at 37 °C. *R. erythropolis* strains were incubated in LB broth, or Basal Salt Medium (BSM) (Del Olmo *et al.*, 2005) at 30 °C. Media, when required, were supplemented with appropriate antibiotics at the following concentrations: ampicillin (Amp, 100 µg ml^{-1}), chloramphenicol (Cm, 34 µg ml^{-1}) and kanamycin (Km, 30 µg ml^{-1}). Bacteriological agar was used as gelling agent (VWR). A stock solution of 20 mg ml^{-1} thiostrepton (Sigma-Aldrich) in glacial acetic acid was prepared and added to cultures at 1 µg ml^{-1} to induce gene expression under the *tipA* promoter (P_{tipA}).

Table 1. Bacterial strains used in this study.

Strains	Relevant characteristics	MIC[a]	Reference/Source
Escherichia coli			
XL1Blue	*endA1 gyrA96*(*nalR*) *thi-1 recA1 relA1 lac glnV44* F'[::Tn10 *proAB+ lacIq* Δ(*lacZ*)M15] *hsdR17*(*rK-mK+*).	0797	Stratagene
BL21 (DE3)	Strain for heterologous expression and protein production.	0076	Novagen
Rhodococcus erythropolis			
IGTS8	Wild-type strain able to transform DBT into 2HBP via the 4S pathway.	5638	(Kilbane and Jackowski, 1992; Gallagher *et al.*, 1993)

Table 1. Bacterial strains used in this study. (cont.)

Strains	Relevant characteristics	MIC[a]	Reference/Source
***Salmonella enterica* subsp. *enterica* serovar Enteritidis**			
3934 *adrA*-3xFLAG	Wild-type clinical isolate expressing a 3xFLAG-tagged AdrA protein from the chromosome	2429	(Solano *et al.*, 2009)
3934 *adrA* D290N-3xFLAG	Wild-type clinical isolate expressing a 3xFLAG-tagged mutated AdrA protein from the chromosome. The mutated AdrA D290N version is unable to synthesize c-di-GMP.	4688	Laboratory of Microbial Pathogenesis (unpublished data)
Staphylococcus aureus			
15981	Clinical isolate. Biofilm positive strain.	0532	(Valle *et al.*, 2003)

[a] Number of each strain in the culture collection of the Laboratory of Microbial Pathogenesis, Navarrabiomed-Universidad Pública de Navarra.

Table 2. Plasmids and oligonucleotides used in this study.

Plasmid	Relevant characteristics	Reference/Source
pET46-Ek/LIC::*rbap_B*	Plasmid for rBap_B heterologous expression and production	(Taglialegna, Navarro, *et al.*, 2016)
pRC3	Plasmid for Dispersin B heterologous expression and production	(Ramasubbu *et al.*, 2005)
pJET1.2/blunt	Cloning vector	Thermo Scientific
pIZ*dszB1A1C1-D1*	pIZ1016 derivative plasmid expressing a synthetic *dszB1A1C1-D1* cassette	(Martínez, M. E.-S. Mohamed, *et al.*, 2016)
pTipQC1	Shuttle vector *Escherichia coli- Rhodococcus erythropolis*	(N. Nakashima and Tamura, 2004)
pTipQC1::*icaADBC*	pTipQC1 containing the *icaADBC* operon of *S. aureus* 15981 under the control of the inducible *tipA* promoter	This study
pTipQC1::*adrA*	pTipQC1 containing the *adrA* gene of *S.* Enteritidis 3934 tagged with the 3xFLAG epitope under the control of the inducible *tipA* promoter	This study

Table 2. Plasmids and oligonucleotides used in this study. (cont.)

Plasmid	Relevant characteristics	Reference/Source
pTipQC1::*adrA* D290N	pTipQC1 containing a mutated *adrA* gene of *S.* Enteritidis 3934, encoding for AdrA D290N and tagged with the 3xFLAG epitope under the control of the inducible *tipA* promoter	This study
pTipQC1::*dsz*-P*lacD*	pTipQC1 containing optimized *dszB1A1C1* genes organized as a transcriptional unit under the control of the inducible *tipA* promoter and also, *dszD1* under the *lac* promoter	This study
pTipQC1::*dsz*-P*lacD*-*adrA*	pTipQC1 containing optimized *dszB1A1C1* genes organized as a transcriptional unit under the control of the inducible *tipA* promoter and also, *dszD1* and the *adrA* gene tagged with the 3xFLAG epitope under the *lac* promoter	This study
pTipQC1::*dsz*-P*lacD*-*adrA-mCherry*	pTipQC1 containing optimized *dszB1A1C1* genes organized as a transcriptional unit under the control of the inducible *tipA* promoter and also, *dszD1*, the *adrA* gene tagged with the 3xFLAG epitope and the *mCherry* gene under the *lac* promoter	This study

Oligonucleotide	Sequence[a]
1	AGGAGATATACCATGGTTGCAATTTTTTAACTTTTTGCTTTTTTATCCTG
2	AGAGATCTAAGCTTGGATCCCCACTCCCATTGGCATTTACGA
13	**CCATGG**GCATGTTCCCAAAAATAATGAATG
17	**CTCGAG**TTACTATTTATCGTCGTCATC
40	**GAATTC**AAGCTTCTCGAGACGCGTTT
41	**GGATCC**ACTAGTTACGTAATCGATTT
42	**GGATCC**TTTGTTTAACTTTAAGAAGGAGATATACC
44	**GGATCC**TTTATCGTCGTCATCTTTGTAG
496	GATGACGACGATAAATAGTAACTCGAGAGGAGGTGAATAATGGTGAGC AAGGGCGAGGA
497	GG**GGATCC**TTACTTGTACAGCTCGTCCA

[a] Restriction enzymes sites and overlapping sequences for In-Fusion HD cloning are indicated in bold and underlined format, respectively.

DNA manipulations

Routine DNA manipulations were performed using standard procedures unless otherwise indicated. Oligonucleotides were synthesized by StabVida. Plasmids were purified using a Macherey Nagel plasmid purification kit. FastDigest restriction enzymes, Phusion DNA polymerase and Rapid DNA ligation kit (Thermo Scientific) were used according to the instructions of the manufacturer. All constructed plasmids were confirmed by Sanger sequencing.

Plasmids were transformed in *E. coli* and *R. erythropolis* by electroporation (0.1 cm cuvette; 200 Ω, 25 µF, 1.25 kV; Bio-Rad Gene Pulser X-Cell electroporator). Rhodococcal electrocompetent cells were generated as follows. *R. erythropolis* cells were incubated in LB medium for 48 h at 30 ˚C, diluted 1:200 in 100 ml of fresh LB broth and grown at 30 ˚C, 200 rpm, to an optical density (OD_{595nm}) of 0.7-0.8. Cells were cooled down on ice for 30 min, and then, washed twice, first with 50 ml and second with 2 ml of ice-cold 10% glycerol. Cells were finally resuspended in 250 µl of ice-cold 10% glycerol and stored in aliquots at -80 ˚C.

Construction of plasmids containing different genetic determinants involved in biofilm formation

To produce PIA/PNAG in R. erythropolis, the *icaADBC* operon of *Staphylococcus aureus* was amplified using oligonucleotides 1 and 2 and genomic DNA of the *S. aureus* 15981 strain as template (Valle *et al.*, 2003). Plasmid pTipQC1 (Nakashima and Tamura, 2004) was digested with NcoI and BamHI enzymes and the insert was

directionally cloned into pTipQC1 using the In-Fusion HD Cloning Kit (Takara), leading to pTipQC1::*icaADBC*.

The gene encoding for the diguanylate cyclase AdrA was amplified from the genome of *Salmonella enterica* subsp. *enterica* serovar Enteritidis (*S*. Enteritidis) 3934 *adrA*-3xFLAG strain (Solano et al., 2009), using primers 13 and 17. The PCR product was cloned into the pJET 1.2 vector (ThermoFisher Scientific), and then subcloned into the pTipQC1 plasmid digested with NcoI and XhoI enzymes leading to plasmid pTipQC1::*adrA*. An *adrA* mutated version, coding for a 3xFLAG tagged AdrA carrying a D290N substitution, was cloned into pTipQC1 following the same strategy as the one detailed above with the use of genomic DNA from the strain *S*. Enteritidis 3934 *adrA* D290N-3xFLAG (Table 1).

Construction of the *dsz-adrA* plasmid for enhanced biodesulfurization and biofilm formation

The synthetic *dszB1A1C1-D1* cassette was amplified from plasmid pIZ*dszB1A1C1-D1* (Martínez, M. E. S. Mohamed, *et al.*, 2016) using primers 40 and 41. The PCR product was cloned into the pJET 1.2 vector and then subcloned into the pTipQC1 plasmid digested with EcoRI and BamHI enzymes, leading to plasmid pTipQC1::*dsz*-P_{lac}*D*. *adrA*-3xFLAG together with the phage T7 gene 10 ribosome binding site (LG10-RBS) was amplified from plasmid pTipQC1::*adrA* using primers 42 and 44. The PCR product was cloned into the pJET 1.2 vector and then subcloned into pTipQC1::*dsz*-P_{lac}*D* digested with BamHI, leading to plasmid pTipQC1::*dsz*-P_{lac}*D*-*adrA*.

Fitness evaluation

R. erythropolis harboring plasmid pTipQC1, pTipQC1::*adrA*, pTipQC1::*adrA* D290N or pTipQC1::*dsz*-P_{lac}*D-adrA* were grown in LB Cm for 24 hours at 30 ˚C, and then diluted 1:100 in 5 ml of fresh LB Cm and incubated for 12 hours at 30 ˚C, 200 rpm. Thiostrepton was added and cultures were incubated for 12 hours at 30 ˚C, 200 rpm. Cultures were collected, centrifuged at 20,800 x g for 5 min and pellets were washed twice and resuspended in 1 ml HEPES buffer 50 mM pH 8.0 containing PMSF 1 mM. Bacteria were lysed using 100 µm acid-washed glass beads (Sigma) and a FastPrep cell disrupter (MP Biomedicals; speed 6, 45 s, twice). Samples were centrifuged for 10 min at 20,800 x g and 4 ˚C, supernatants were collected and protein quantification was carried out using a Bradford protein assay kit (Bio-Rad).

Biofilm assays

The B region of the biofilm associated protein (Bap) from Staphylococcus aureus was produced and purified as described elsewhere (Taglialegna, Navarro, *et al.*, 2016). This region polymerizes to form amyloid-like fibers under specific environmental conditions (acidic pH and low concentrations of calcium) to build the biofilm matrix. To induce bacterial aggregation and biofilm formation through the B region of Bap, a previously described protocol was used (Taglialegna, Navarro, *et al.*, 2016). Briefly, an overnight culture of *R. erythropolis* IGTS8 was diluted 1:100 in fresh LB medium containing glucose (0.25 % w/v) and rBap_B 2 µM was added. The culture was incubated for 24 h at 30 ˚C, 200 rpm and then, biofilm formation was visually inspected.

To analyse PIA/PNAG and c-di-GMP mediated biofilms, overnight cultures of *R. erythropolis* IGTS8 carrying pTipQC1, pTipQC1::*icaADBC*, pTipQC1::*adrA*, pTipQC1::*adrA* D290N, pTipQC1::*dsz*-P$_{lac}$*D* or pTipQC1::*dsz*-P$_{lac}$*D-adrA* and grown in LB Cm were diluted 1:100 in 4 ml of fresh LB Cm medium and incubated for 12 hours at 30 ˚C, 200 rpm. Thiostrepton was then added, cultures were further incubated for 12 hours at 30 ˚C, 200 rpm, and biofilm formation was visually examined.

Biofilm formation under flow conditions was analyzed using microfermenters (Pasteur Institute's laboratory of Fermentation) with a continuous 40 ml h^{-1} flow of LB Cm and constant aeration with sterile compressed air (0.3 bar) (Ghigo, 2001). Polystyrene and silicone rubber disk coupons (Biosurface Technologies Corporation) were fixed to the internal microfermenter glass slides (spatulas) and served as biofilm substrata. Microfermenter starter cultures of *R. erythropolis* pTipQC1::*dsz*-P$_{lac}$*D* and *R. erythropolis* pTipQC1::*dsz*-P$_{lac}$*D-adrA* strains were grown in LB Cm for 24 hours at 30 ˚C and 200 rpm, and then diluted 1:100 in fresh LB Cm and incubated again for 24 hours at 30 ˚C, 200 rpm. Each microfermenter was subsequently inoculated with 250 µl of the corresponding strain. Biofilm development was recorded after 48 h of incubation at 30 ˚C.

Construction of a reporter strain expressing mCherry and biofilm CLSM imaging

To construct a *R. erythropolis* biofilm forming strain expressing the gene encoding the red fluorescent protein mCherry, *adrA*-3xFLAG together with the phage T7 gene

10 ribosome binding site (LG10-RBS) was amplified from plasmid pTipQC1::*adrA* using primers 42 and 44. The gene encoding mCherry was amplified from pAD1-cCherry (Balestrino *et al.*, 2010) using primers 496 and 497. The two aforementioned PCR fragments were fused through overlapping PCR using primers 42 and 497, cloned into the pJET 1.2 vector and then subcloned into pTipQC1::*dsz*-P$_{lac}$*D* digested with BamHI, leading to plasmid pTipQC1::*dsz*-P$_{lac}$*D-adrA*-mCherry.

Plasmid pTipQC1::*dsz*-P$_{lac}$*D-adrA*-mCherry was transformed into *R. erythropolis* IGTS8. The resulting strain was grown under flow conditions using the microfermenter system described above and a polystyrene disk coupon as substrate. After biofilm development, the coupon was rinsed with PBS and placed upside down on a 35 mm glass bottom dish (1.5 coverslip, 14 mm glass diameter, uncoated; MatTek). Confocal laser scanning microscopy (CLSM) images were acquired at 0.27 µm z intervals using a Zeiss LSM 800 confocal system. mCherry was detected using a diode laser for excitation at 561 nm and emission from 565 to 700 nm was collected. Images were obtained using a 63 x/1.4 objective. The biofilm images were processed using Zeiss Zen software (Zeiss).

Activity of dispersing enzymes on the biofilm formed by *R. erythropolis* pTipQC1::*dsz*-P$_{lac}$*D-adrA*

Dispersin B enzyme was purified from a recombinant *Escherichia coli* BL21 (DE3) strain carrying plasmid pRC3 as previously described (Ramasubbu *et al.*, 2005). After purification, fractions containing Dispersin B were dialyzed against ultrapure water at 4 ºC using a Slide-A-Lyzer Dialysis Cassette (ThermoFisher Scientific) with a

molecular mass cut-off of 10 kDa and subsequently lyophilized. Lyophilized Dispersin B was finally resuspended in Storage Buffer (50 mM sodium phosphate pH 5.8; 100 mM NaCl; 50% glycerol) at a concentration of 2 mg ml^{-1} and stored at –20 ºC. Protein concentration was determined with a Bradford protein assay kit (Bio-Rad).

The standard microtiter dish biofilm formation assay was performed as previously described with minor modifications (O'Toole *et al.*, 1999). Briefly, overnight cultures of *R. erythropolis* pTipQC1::*dsz*-P_{lac}*D* grown in LB Cm were diluted 1:100 in 1.5 ml of LB Cm and incubated for 72 hours at 30 ˚C and 200 rpm in a 24 flat-well microtiter plate (Costar). Liquid media was then removed, wells were gently washed twice with PBS and the biofilm formed as an adhered ring to the well wall was treated for 2 hours at 37 ˚C with: (i) 100 µg ml^{-1} proteinase K (Sigma) in 20 mM Tris pH 7.5, 100 mM NaCl (Kaplan *et al.*, 2004); (ii) 100 U ml^{-1} DNAse I (Sigma) in PBS (Sugimoto *et al.*, 2018); (iii) 40 µg ml^{-1} Dispersin B in PBS (Kaplan *et al.*, 2004); (iv) 5 mg ml^{-1} cellulase (from *Trichoderma viride*, Sigma) in 50 mM citrate buffer pH 4.6 (Trivedi *et al.*, 2016); (v) 10 mM sodium metaperiodate (Scharlau) in 50 mM sodium acetate buffer pH 4.5 (Kaplan *et al.*, 2004). Control wells were filled with each reaction buffer. After treatment, wells were gently washed twice with PBS and biofilms were stained with 2 ml of 0.25% crystal violet (VWR) for 5 min at room temperature. The excess crystal violet was removed and wells were washed twice with PBS and air dried. Crystal violet-stained cells were quantified by solubilizing the dye with 2 ml of ethanol-acetone (80:20, vol/vol) and determining the optical density at 595 nm (OD_{595nm}). Each treatment was evaluated in triplicate.

Phenotype on Congo red agar plates

Colony morphology on Congo red agar plates to monitor extracellular matrix production was evaluated using a modified medium from (Freeman *et al.*, 1989) (30 g l^{-1} tryptic soy broth (Condalab), 15 g l^{-1} agar, 0.8 g l^{-1} Congo red (Sigma) and 20 g l^{-1} sucrose). Strains were grown on LB Agar Cm for 72 hours at 30 ˚C, cells were harvested and resuspended in sterile water to an optical density (OD_{595nm}) of 0.5-0.6 and then, 20 µl drops were spotted on Congo red plates supplemented with Cm, with and without the thiostrepton inducer. Plates were incubated for 48 hours at 30 ˚C.

PIA/PNAG and AdrA detection by immunoblotting

R. erythropolis pTipQC1 and *R. erythropolis* pTipQC1::*icaADBC* were grown in LB Cm for 24 hours at 30 ˚C, and then diluted 1:100 in fresh LB Cm and incubated for 12 hours at 30 ˚C, 200 rpm. Thiostrepton was added and cultures were further incubated for 12 hours at 30 ˚C, 200 rpm. 2 ml of each culture were collected and PIA/PNAG was extracted and detected as described (Cramton *et al.*, 1999; Valle *et al.*, 2003). Briefly, cultures were centrifuged at 18,000 x g for 5 min. Pellets were resuspended in 50 µl of 0.5 M EDTA (pH 8.0) and suspensions were incubated for 5 min at 100 ˚C and centrifuged at 18,000 x g for 5 min. Each supernatant (40 µl) was incubated with 10 µl of proteinase K (20 mg ml^{-1}) (Sigma) for 30 min at 37 ˚C. After the addition of 10 µl of Tris-buffered saline (20 mM Tris-HCl, 150 mM NaCl [pH 7.4]) containing 0.01% bromophenol blue, 5 µl were spotted on a nitrocellulose membrane using a Bio-Dot microfiltration apparatus (Bio-Rad). The membrane was blocked overnight with 5% skimmed milk in phosphate-buffered saline (PBS) with

0.1% Tween 20, and incubated for 2 h with specific anti-PNAG antibodies diluted 1:10,000 (Maira-Litrán *et al.*, 2005). Bound antibodies were detected with peroxidase-conjugated goat anti-rabbit immuno-globulin G antibodies (Jackson ImmunoResearch Laboratories) diluted 1:10,000 and developed using the SuperSignal West Pico Chemiluminescent Substrate (Thermo Scientific). All extracts were analyzed on the same membrane.

Correct expression and translation of *adrA* in *R. erythropolis* pTipQC1::*adrA*, *R. erythropolis* pTipQC1::*adrA* D290N and *R. erythropolis* pTipQC1::*dsz*-P$_{lac}$*D-adrA* was monitored by Western blot as follows. Cultures were grown in LB Cm for 24 hours at 30 ˚C, and then diluted 1:100 in fresh LB Cm and incubated for 12 hours at 30 ˚C, 200 rpm. Thiostrepton was added and cultures were incubated for 12 hours at 30 ˚C, 200 rpm. 4 ml of each culture were collected, centrifuged at 20,800 x g for 5 min and pellets were washed twice and resuspended in 1 ml HEPES buffer 50 mM pH 8.0 containing PMSF 1 mM. Bacteria were lysed using 100 µm acid-washed glass beads (Sigma) and a FastPrep cell disrupter (MP Biomedicals; speed 6, 45 s, twice). Samples were centrifuged for 10 min at 20,800 x g and 4 ˚C and supernatants were collected. For normalization purposes, protein quantification was carried out using a Bradford protein assay kit (Bio-Rad). Equal amounts of protein per sample were loaded on a 12% stain-free acrylamide gel (Criterion Bio-Rad). Proteins were transferred onto Hybond-ECL nitrocellulose membranes (GE Healthcare) by electroblotting and then, membranes were blocked overnight in PBS containing 0.1% Tween 20 and 5% skimmed milk under shaking conditions and incubated with monoclonal anti-FLAG antibodies labelled with horseradish peroxidase (Sigma) diluted 1:1,000 in blocking

solution for 2 h at room temperature. Bands were developed with the SuperSignal West Pico Chemiluminescent Substrate (Thermo Scientific).

c-di-GMP extraction and measurement

Cultures were grown in LB Cm for 24 hours at 30 ˚C, and then diluted 1:100 in fresh LB Cm and incubated for 12 hours at 30 ˚C, 200 rpm. Thiostrepton was added and cultures were incubated for 12 hours at 30 ˚C, 200 rpm. 4 ml of each culture were collected and c-di-GMP extraction was carried out following a protocol described in (Bähre and Kaever, 2017). c-di-GMP measurements were performed by HPLC-coupled tandem mass spectrometry (LC-MS/MS). A duplicate of each culture was used to determine protein content for normalization purposes. Duplicates were centrifuged at 20,800 x g for 5 min and pellets were washed twice and resuspended in 1 ml HEPES buffer 50 mM pH 8.0. Bacteria were lysed using 100 µm acid-washed glass beads (Sigma) and a FastPrep cell disrupter (MP Biomedicals; speed 6, 45 s, twice). Samples were centrifuged for 10 min at 20,800 x g and 4 ˚C and supernatants were collected. A Bradford assay kit (Bio-Rad) was used for protein quantification. Intracellular levels of c-di-GMP from biological triplicates are shown as mean values of picomoles of c-di-GMP per milligram of protein.

Desulfurization assays

Cultures were grown in LB Cm for 24 hours at 30 ˚C, and then diluted 1:100 in fresh LB Cm and incubated for 24 hours at 30 ˚C, 200 rpm. Cultures were collected

and washed twice with BSM. Bacterial pellets were resuspended in 50 ml BSM Cm in a 250 ml Erlenmeyer flask at an OD_{595nm} of 0.1. Since cell cultures expressing AdrA showed an aggregated phenotype, normalization was further adjusted based on protein quantification. Cultures were grown for 24 hours at 30 ˚C, 200 rpm, and then thiostrepton was added to induce gene expression under the P_{tipA} promoter. Cultures were further incubated for 24 hours at 30 ˚C and cells were collected by centrifugation and washed twice with 50 mM HEPES buffer pH 8.0. Bacterial pellets were resuspended (30 ml) in 50 mM HEPES buffer pH 8.0 at an OD_{595nm} of 1. Normalization was further adjusted based on protein quantification. Then, each culture was split in three samples of 10 ml each in 100 ml Erlenmeyer flasks. These resting cells preparations were used for the BDS assays, which were performed after adding 25 µM DBT (25 mM stock solution in acetonitrile), at 200 rpm and 30 ˚C. At 0, 15 and 60 minutes of incubation, each ten ml sample was mixed with an equal volume of acetonitrile and centrifuged at 14,000 x g for 10 min to be analyzed by high-performance liquid chromatography (HPLC). All BDS experiments were conducted in triplicate.

Desulfurization activity was analyzed by calculating the 2HBP specific production rate defined as the quantity of 2HBP produced per hour per gram of dry cell weight [μmol_{2HBP}/g DCW/h] and conversion efficiency [$X_{2HBP}^{time\ (min)} = (C_{2HBP}^{time\ (\min)} / C_{DBT}^{0}) \times 100$] defined as the ratio of the 2HBP produced to the initial concentration of DBT (Del Olmo *et al.*, 2005).

HPLC was used as described (Martínez, M. E. S. Mohamed, *et al.*, 2016) to analyze the concentration of DBT and 2HBP employing a C18 column (Teknokroma C18

150 x 4.6 mm, 5 µm particles). The mobile phase was a mix of acetonitrile/water (55:45) at 1 ml min^{-1} flow rate. Peaks were monitored at 234 nm for DBT and 206 nm for 2HBP. Calibrations were performed using highly purified standards of each compound.

Statistics

Statistical analyses were performed with the GraphPad Prism 5.01 program. For single comparisons, data were analyzed using an unpaired, two-tailed Student's t-test. For multiple comparisons, a one-way analysis of variance (ANOVA) with Bonferroni or Dunnett's post-test was used. In all tests, p values of less than 0.05 were considered statistically significant. *$p < 0.05$, **$p < 0.01$, ***$p < 0.001$.

Results and discussion

Selection of an optimal strategy to induce biofilm formation in *Rhodococcus erythropolis* IGTS8

The *bap* gene of the bacterial pathogen *Staphylococcus aureus* encodes the biofilm associated protein (Bap), a cell wall-associated protein of 2,276 amino acids. This surface protein self-assembles, under conditions of low calcium concentrations and acidic pH, into aggregates with an amyloid-like conformation and promotes biofilm formation. One of the main features of this protein is its modular organization, being the B region (Bap_B) responsible for the formation of the amyloid-like fibers and thus sufficient to promote biofilm development (Taglialegna, Navarro, *et al.*, 2016). Based on a previous study where it was demonstrated that the exogenous addition of recombinant Bap_B (rBap_B) at a concentration of 2 µM is enough to drive biofilm formation in *S. aureus* (Taglialegna, Navarro, *et al.*, 2016), we purified rBap_B and then cultured *R. erythropolis* IGTS8 in LB medium supplemented with 0.25% glucose and 2 µM rBap_B for 24 hours at 30 ˚C. Under laboratory conditions, wildtype *R. erythropolis* showed a basal capability of forming a biofilm that could be observed as a labile ring of cells adhered to the glass wall (**Figure 1A**). This observation is in agreement with the characteristic hydrophobicity of *Rhodococcus* cells provided by fatty acids of the cell wall, whose composition changes in response to the surface to which *Rhodococcus* adheres, resulting in different biofilm architectures and biomass (De Carvalho and Da Fonseca, 2007; Rodrigues and de Carvalho, 2015). Results showed that addition of rBap_B did not lead to an increase in *Rhodococcus* biofilm formation with respect to the non-treated

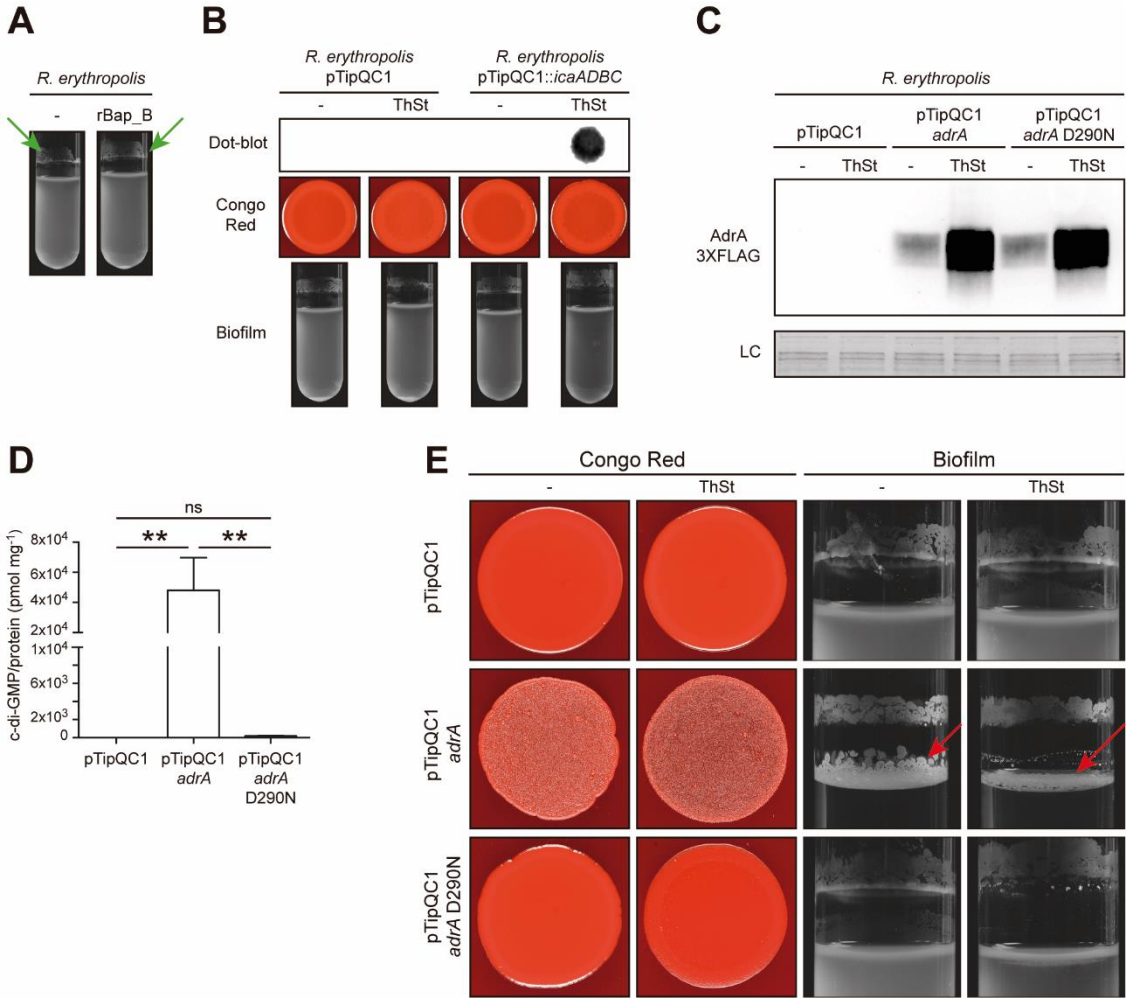

Figure 1. Evaluation of different strategies to promote *R. erythropolis* IGTS8 biofilm formation. (**A**) Biofilm phenotypes of the wild type strain in the absence or presence of 2 µM rBap_B after incubation in LB broth supplemented with 0.25 % glucose for 24 hours at 30 ˚C. Green arrows point to the basal biofilm that *R. erythropolis* forms under these conditions and that can be observed as a labile ring of cells adhered to the glass wall. (**B**) Analysis of PIA/PNAG exopolysaccharide production by dot-blot, colony morphology on Congo red agar and biofilm phenotype in LB medium of *R. erythropolis* containing the pTipQC1 empty plasmid or pTipQC1::*icaADBC* in the absence or presence of 1 µg ml^{-1} thiostrepton (ThSt). (**C**) Western blot showing AdrA levels in *R. erythropolis* containing the pTipQC1 empty plasmid, pTipQC1::*adrA* or pTipQC1::*adrA* D290N coding for an inactive AdrA protein, in the absence or presence of 1 µg ml^{-1} thiostrepton (ThSt). Anti-3xFLAG antibodies were

used to detect the AdrA 3xFLAG-tagged protein. A stain-free gel portion is shown as a loading control (LC). (**D**) *R. erythropolis* strains described in C were grown in LB containing 1 µg ml^{-1} thiostrepton. c-di-GMP was extracted, quantified by mass spectrometry and correlated to protein concentration. Data represent the mean ± standard deviation calculated from three independent experiments. Statistical significance was determined with one-way ANOVA followed by Bonferroni multiple comparison test. ***P* value < 0.01. ns; no significant difference. (**E**) Colony morphology on Congo red agar and biofilm phenotype in LB medium of the strains described in C. Red arrows point to the biofilm formed at the air-liquid interface by *R. erythropolis* pTipQC1::*adrA* both in the absence and presence of thiostrepton. Note that cultures become transparent since most bacteria are encased inside the biofilm formed at the interface.

culture (**Figure 1A**), probably because *Rhodococcus* growth does not result in medium acidification, a requisite for rBap_B mediated biofilm formation. We thus adjusted the pH of LB medium to 4.5 and used it to culture *R. erythropolis* in the presence of rBap_B. However, at this low pH *Rhodococcus* growth was arrested and therefore, this strategy for inducing biofilm formation was discarded.

PIA/PNAG, a homopolymer of N-acetylglucosamine, has been described as a conserved surface polysaccharide synthesized by several Gram-positive and Gram-negative bacteria to build the biofilm matrix (Cywes-Bentley *et al.*, 2013). In order to test a second strategy to promote biofilm formation in *R. erythropolis*, we amplified the *icaADBC* operon of *S. aureus*, which encodes the Ica proteins responsible for PIA/PNAG synthesis in this species (Cramton *et al.*, 1999), and cloned it into the pTipQC1 vector for its expression in *Rhodococcus* under the control of a thiostrepton inducible promoter (Nobutaka Nakashima and Tamura, 2004). *R. erythropolis* cells carrying either the empty pTipQC1 or the pTipQC1::*icaADBC* plasmid were incubated in LB broth, at 30˚C for 24 hours under shaking conditions in the absence or presence of thiostrepton and heterologous PIA/PNAG production was monitored using a dot-blot assay and an anti-PIA/PNAG antiserum. Results showed that *R. erythropolis* pTipQC1::*icaADBC* incubated in the presence of 1 µg ml^{-1} thiostrepton produced detectable levels of PIA/PNAG (**Figure 1B**). PIA/PNAG mediated biofilm formation has been associated to a rough colony morphology phenotype on solid media containing the Congo red dye (D. J. Freeman *et al.*, 1989). Also, the production of this exopolysaccharide in different species and the

subsequent biofilm formation can be visualized, after incubation in a glass tube under shaking conditions, as a ring of cells strongly adhered to the glass wall at the air–liquid interface (Valle *et al.*, 2003; Echeverz *et al.*, 2017). However, when these two phenotypes were investigated, *R. erythropolis* cells carrying the icaADBC operon showed a smooth morphotype on Congo red agar, indicative of non-biofilm producers, and were also unable to build a visible PIA/PNAG mediated biofilm in a glass tube, even under the presence of the thiostrepton inducer (**Figure 1B**). These results were unexpected, since we have previously shown that heterologous expression of the *pgaABCD* operon (responsible for PIA/PNAG synthesis in *Escherichia coli*) in *Salmonella* makes *Salmonella* capable of building a PIA/PNAG mediated biofilm (Echeverz *et al.*, 2017). In the present case, and although heterologous *icaADBC* expression in *R. erythropolis* IGTS8 drives PIA/PNAG synthesis, the resulting polysaccharide levels may be insufficient for inducing a significant biofilm development.

A third strategy for promoting biofilm formation focused on producing high levels of the intracellular dinucleotide c-di-GMP with the aim of inducing the synthesis of *Rhodococcus* own exopolysaccharides that may be part of the biofilm matrix (Pérez-Mendoza and Sanjuán, 2016). C-di-GMP is synthesized by enzymes called diguanylate cyclases harboring a GGDEF domain and is degraded by specific phosphodiesterases that contain an EAL or HD-GYP domain (Schirmer and Jenal, 2009). Thus, to promote c-di-GMP synthesis, we overexpressed in *R. erythropolis* the *adrA* gene from *Salmonella enterica* serovar Enteritidis, encoding a very active diguanylate cyclase and thus, able to synthesize c-di-GMP (Simm *et al.*, 2004). In

order to monitor *adrA* correct expression and translation in *Rhodococcus*, the *adrA* gene was amplified from a genetically modified *Salmonella* strain that encodes a labelled AdrA protein with a 3xFLAG translational fusion (Solano *et al.*, 2009) and was then cloned in the pTipQC1 plasmid. A Western blot assay confirmed the correct production of AdrA in *R. erythropolis* transformed with the pTipQC1::*adrA* plasmid (**Figure 1C**) that correlated with very high c-di-GMP levels in the *Rhodococcus* cytoplasm (**Figure 1D**). Notably, basal levels of AdrA were produced even in the absence of thiostrepton induction (**Figure 1C**). As a result of AdrA production, *R. erythropolis* pTipQC1::*adrA* cells, incubated both in the absence and presence of the inducer, showed a dry and rough colony phenotype on Congo red agar plates and formed a biofilm at the air-broth interface that encased most of the bacterial cells present in the culture (**Figure 1E**). Of note, the elevated AdrA synthesis and subsequent great c-di-GMP levels reached upon thiostrepton induction caused a marked negative effect in the *Rhodococcus* growth rate, that was much less pronounced in the absence of induction (**Figure 2**). Biofilm phenotypes were dependent on c-di-GMP synthesis, since transformation of *R. erythropolis* with pTipQC1::*adrA* D290N, producing an altered AdrA protein with a degenerate GGNEF motif (**Figure 1C**) and therefore, unable to synthesize c-di-GMP (**Figure 1D**), did not result in a biofilm associated phenotypic change (**Figure 1E**).

According to the results presented above, moderate AdrA overexpression and subsequent c-di-GMP production was chosen as an optimum strategy to induce biofilm development in *R. erythropolis* cells.

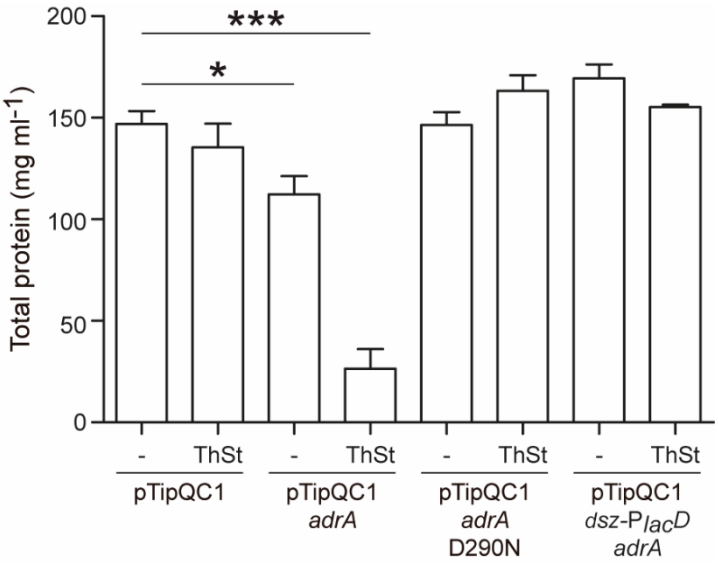

Figure 2. AdrA overexpression and subsequent very high c-di-GMP levels in *R. erythropolis* pTipQC1::*adrA* upon thiostrepton induction have a very significant negative impact on *Rhodococcus* growth. *R. erythropolis* strains harboring plasmid pTipQC1, pTipQC1::*adrA*, pTipQC1::*adrA* D290N or pTipQC1::*dsz*-P$_{lac}$*D-adrA* were grown in LB Cm for 24 hours at 30 ˚C, and then diluted 1:100 in fresh LB Cm and incubated for 12 hours at 30 ˚C, 200 rpm. Thiostrepton was added and cultures were incubated for 12 hours at 30 ˚C, 200 rpm. The control non-induced cultures were also incubated for 12 hours at 30 ˚C, 200 rpm. Cells were collected, lysed and the total protein content was calculated (µg ml^{-1}). Data were compared to the total protein content of the non-induced *R. erythropolis* pTipQC1 culture by one-way analysis of variance (ANOVA) with Dunnett's post-test. *P value < 0.05; ***P value < 0.001. Data represent the mean ± standard deviation calculated from two independent experiments performed in triplicate.

Engineering a *dsz-adrA* cassette that leads to moderate c-di-GMP production and biofilm formation in *R. erythropolis*

Based on a previous work where a synthetic *dsz* cassette for improved conversion of DBT into 2HBP was assembled and expressed in *Pseudomonas putida* (Martínez, M. E.-S. Mohamed, *et al.*, 2016), we constructed a pTipQC1 derived plasmid named pTipQC1::*dsz*-P_{lac}*D-adrA* (**Figure 3A**) to promote biofilm formation and *dsz* genes overexpression in *Rhodococcus* cells. This plasmid contained the synthetic *dszB1*, *dszA1* and *dszC1* genes arranged as an operon under the control of the *tipA* promoter, thus avoiding repression of transcription of the *dsz* native promoter in the presence of inorganic sulfate (Li *et al.*, 1996). Taking into account that increased expression of *dszD* has been reported to have a toxic effect (Galan *et al.*, 2000) and that, as stated above, AdrA production has to be tightly regulated to avoid a negative impact on growth, the cassette contains *dszD1* followed by the *adrA* gene, arranged as an operon, under control of the weak P_{lac} promoter and separated from the *dszB1A1C1* operon by a strong transcriptional terminator of the lambda phage (**Figure 3A**) (Martínez, M. E.-S. Mohamed, *et al.*, 2016). A second plasmid, pTipQC1::*dsz*-P_{lac}*D*, without the *adrA* gene was also constructed as a control to be used in biofilm and BDS analyses (**Figure 3A**).

Both plasmids were then introduced in *R. erythropolis* IGTS8 and AdrA production was evaluated by Western blot (**Figure 3B**). As expected, *R. erythropolis* pTipQC1::*dsz*-P_{lac}*D-adrA* cells produced moderate levels of AdrA, independently of thiostrepton induction. Western blot results were consistent with c-di-GMP quantities in the *Rhodococcus* cytoplasm (**Figure 3C**) that were fifty times lower than

when the *adrA* gene was expressed from the *tipA* promoter in the pTipQC1::*adrA* plasmid (**Figure 1D**). We finally evaluated biofilm related phenotypes and confirmed that such moderate levels of AdrA production did not have a negative impact on growth (**Figure 2**) and were enough for *R. erythropolis* pTipQC1::*dsz*-P$_{lac}$*D-adrA* cells to show a dry and rough colony phenotype on Congo red agar plates and to form a biofilm at the air-broth interface (**Figure 3D**). Hence, this strain was considered for subsequent analysis of DBT desulfurization improvement in relation to the control strain, *R. erythropolis* pTipQC1::*dsz*-P$_{lac}$*D*, that shows only basal natural levels of c-di-GMP (**Figure 3C**), and therefore stays in a planktonic physical state (**Figure 3D**).

R. erythropolis biofilm cells show a significantly improved capacity to convert DBT into 2HBP when compared to their planktonic counterparts

In order to test whether biofilm formation through AdrA overexpression in *R. erythropolis* enhances its biodesulfurization capacity, resting cell assays in aqueous phase were performed. To do so, cells (0.3 g dry cell weight per liter) were suspended in 50 mM HEPES buffer, 25 μM DBT was added and BDS was conducted at 30ºC. Triplicate samples were prepared for each strain so that at 0, 15 and 60 minutes of incubation, one sample of each strain was collected and DBT and 2HBP concentrations were determined. **Figure 4** shows the time courses for DBT utilization and 2HBP production (**Figure 4A**) and also the conversion efficiency of each strain, indicated as the ratio of 2HBP produced to the initial concentration of

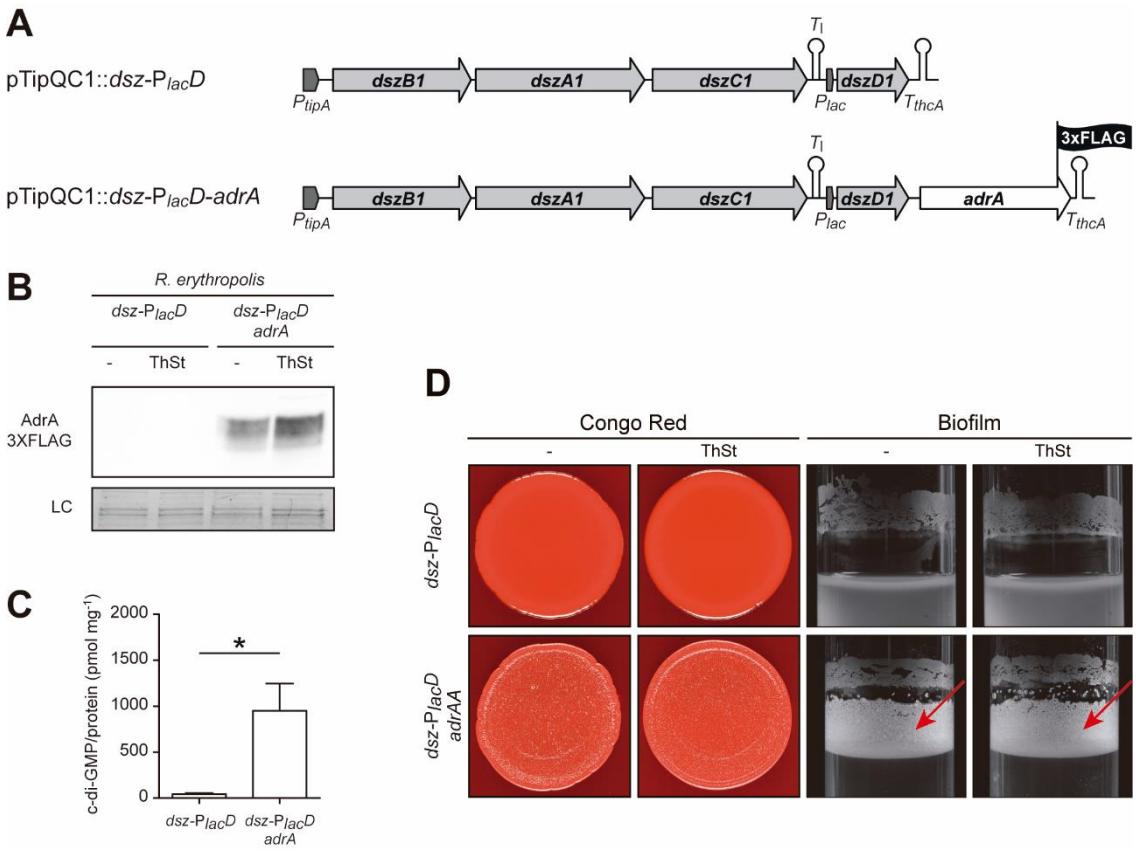

Figure 3. Construction and analysis of the biofilm formation capacity of *R. erythropolis* expressing *dsz* genes and *adrA*. (A) Schematic representation drawn to scale of the *dsz*-P*lacD* cassette alone or in combination with *adrA* that was cloned in the pTipQC1 plasmid. (B) Western blot showing AdrA levels in *R. erythropolis* carrying plasmids shown in A, and incubated in the absence or presence of 1 µg ml^{-1} thiostrepton (ThSt). Anti-3xFLAG antibodies were used to detect the AdrA 3xFLAG-tagged protein. A stain-free gel portion is shown as a loading control (LC). (C) *R. erythropolis* strains carrying plasmids shown in A were grown in LB containing 1 µg ml^{-1} thiostrepton. c-di-GMP was extracted, quantified by mass spectrometry and correlated to protein concentration. Data represent the mean ± standard deviation calculated from three independent experiments. Data were analyzed by using Student's *t* test. (D) Colony morphology on Congo red agar and biofilm phenotype in LB medium. Red arrows point to the biofilm formed at the air-liquid interface by *R. erythropolis* pTipQC1::*dsz*-P*lacD-adrA* both in the absence and presence of thiostrepton. Note that cultures become almost transparent since most bacteria are encased inside the biofilm formed at the interface.

DBT (**Figure 4B**). After 1 h of incubation, the conversion efficiency increased from a basal point of 20.8% shown by *R. erythropolis* harboring the empty pTipQC1 plasmid to 35.8% when control *R. erythropolis* pTipQC1::*dsz*-P$_{lac}$*D* planktonic cells were used. Remarkably, an almost complete conversion of DBT into 2HBP was achieved in the case of *R. erythropolis* pTipQC1::*dsz*-P$_{lac}$*D-adrA* biofilm cells (98.2%). Hence, these results demonstrated that biofilm formation through c-di-GMP production is a very productive alternative to the conventional strategy based on the sole overexpression of *dsz* genes. In fact, the specific desulfurization activity attained with the biofilm approach proposed in this study is 84.2 µmol2HBP/g DCW/h. This is the highest value described in the literature with either *Rhodococcus* or other bacterial species when performing microbial resting cell cultures in aqueous phase (Maghsoudi *et al.*, 2001; Del Olmo *et al.*, 2005; Martin *et al.*, 2005; Rashtchi *et al.*, 2006; Davoodi-Dehaghani *et al.*, 2010; Alves and Paixão, 2014; Ismail *et al.*, 2016; Martínez, M. E.-S. Mohamed, *et al.*, 2016; Dejaloud *et al.*, 2017). Additional research to confirm increased bioconversion efficiency may be focused on carrying out resting cells assays in a two-phase system where desulfurization activity is higher than in aqueous media (Davoodi-Dehaghani *et al.*, 2010).

Here, we increased the concentration of c-di-GMP through the overexpression of AdrA, a heterologous diguanylate cyclase. In this regard, *R. erythropolis* c-di-GMP signaling system is composed of fourteen proteins containing a GGDEF domain, four proteins containing both GGDEF and EAL domains and one protein containing an EAL domain (https://www.ncbi.nlm.nih.gov/Complete_Genomes/c-di-GMP.html).

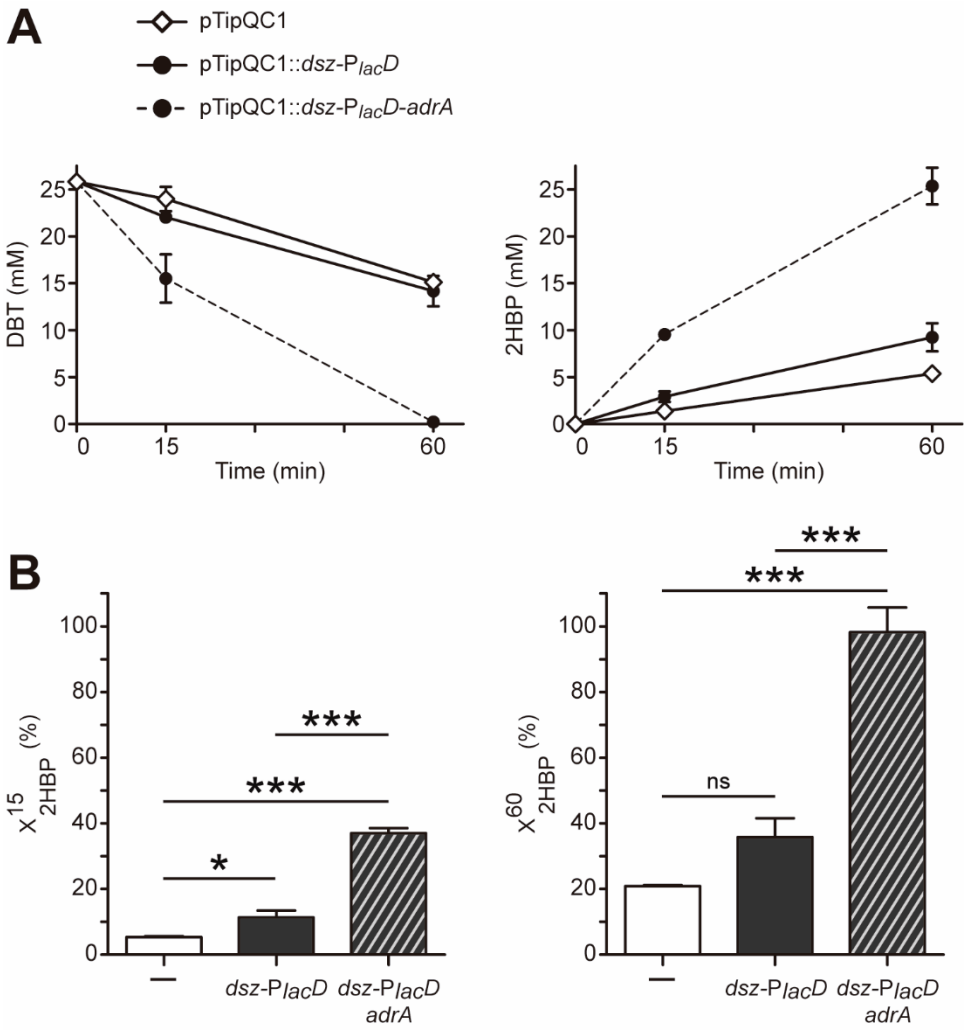

Figure 4. Conversion of DBT into 2HBP by *R. erythropolis* strains expressing the *dsz*-P$_{lacD}$ cassette alone (planktonic) or in combination with *adrA* (biofilm). Resting cells assays were carried out using 25 µM DBT as initial substrate. (A) DBT utilization (left) and 2HBP production (right) by resting cells at 15 and 60 min of desulfurization. (B) Conversion efficiency of DBT into 2HBP is denoted as the percentage of 2HBP production after 15 min (left) and 60 min (right) according to equation $X_{2HBP}^{time\ (min)} = (C_{2HBP}^{time\ (\mathrm{min})} / C_{DBT}^{0}) \times 100$. Data of *R. erythropolis* containing the pTipQC1 empty plasmid (-), *R. erythropolis* pTipQC1::*dsz*-P$_{lacD}$-*adrA* (*dsz*-P$_{lacD}$-*adrA*) and the control strain *R. erythropolis* pTipQC1::*dsz*-P$_{lacD}$ (*dsz*-P$_{lacD}$) were subjected to one-way analysis of variance (ANOVA) using Bonferroni post-test. **P* value < 0.05; ****P* value < 0.001. ns; no significant difference. Data represent the mean ± standard deviation calculated from three independent experiments.

Although the putative diguanylate cyclase or phosphodiesterase activity of these proteins has never been tested, further research might be dedicated to increase c-di-GMP levels by means of either overexpressing *Rhodococcus* GGDEF domain containing proteins or mutating EAL domain containing proteins through recently described genome editing systems (DeLorenzo *et al.*, 2018; Liang *et al.*, 2020). Also, future improvements of the recombinant strain might consider the insertion of the synthetic *dsz* cassette into the chromosome of the target host cell in order to avoid recombination events between the synthetic *dsz* genes present in the pTipQC1::*dsz*-P$_{lac}$*D-adrA* plasmid and the native genes.

With regard to the extracellular matrix composition of the biofilm formed by *R. erythropolis* pTipQC1::*dsz*-P$_{lac}$*D-adrA*, dispersion experiments with proteinase K (which degrades proteinaceous constituents of the matrix), sodium metaperiodate (which oxidizes polysaccharide bonds) and DNase (which digests matrix eDNA) showed that the biofilm was only sensitive to sodium metaperiodate, indicating that the major component of the biofilm matrix is of polysaccharide nature (**Figure 5**). Importantly, the identification of the exopolysaccharide that is being overproduced in *Rhodococcus* under elevated c-di-GMP conditions may inspire the generation of an engineered system to express such exopolysaccharide at will in order to tightly modulate *Rhodococcus* biofilm formation. In this sense, we treated *R. erythropolis* pTipQC1::*dsz*-P$_{lac}$*D-adrA* biofilm cells with Dispersin B, an enzyme produced by *Aggregatibacter actinomycetemcomitans* that specifically hydrolyzes the glycosidic linkages in PIA/PNAG (Kaplan *et al.*, 2004), and also with cellulase, that disrupts cellulose based biofilms (Solano *et al.*, 2002). However, none of the treatments

digested the extracellular matrix of the *R. erythropolis* pTipQC1::*dsz*-P$_{lac}$*D-adrA* biofilm (**Figure 5**), indicating that an exopolysaccharide of different nature is being produced by this strain to readily form a biofilm. The marine bacterium *R. erythropolis* PR4 is known to produce a fatty acid-containing extracellular polysaccharide (PR4 FACEPS) and an acidic extracellular polysaccharide named mucoidan, whose chemical composition and structure have been characterized (Urai *et al.*, 2007a, 2007b). The genetic determinants responsible for the synthesis of these exopolysaccharides and whether *R. erythropolis* IGTS8 produces them in response to c-di-GMP remains to be determined.

To our knowledge, this is one of the few studies performed to date that have shown c-di-GMP production as an optimal approach to enhance biofilm formation and subsequent bacterial biotransformation activities (Wu *et al.*, 2015; Benedetti *et al.*, 2016; Guo *et al.*, 2017; Hu *et al.*, 2019). Overall, our results evidence that increasing the levels of c-di-GMP might be a promising general strategy to enhance biodegradation kinetics of bacteria. Thus, this approach might have a significant impact on the biotechnological potential of *Rhodococcus* genus in ecological and bioremediation applications since it could be applied to boost many biodegradation capabilities of not only *R. erythropolis* but also other species.

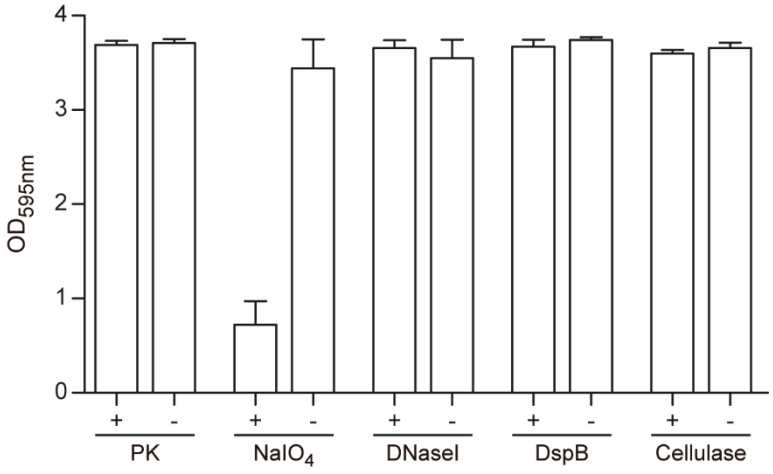

Figure 5. Analysis of the nature of the biofilm extracellular matrix produced by *R. erythropolis* pTipQC1::*dsz*-P*lac*D-*adrA* through biofilm treatment with dispersing agents. *R. erythropolis* pTipQC1::*dsz*-P*lac*D-*adrA* was grown in a 24 flat-well microtiter plate for 72 hours at 30 ˚C and 200 rpm. The biofilm attached to the well walls was treated for 2 hours at 37 ˚C with 100 µg ml^{-1} proteinase K (PK) in 20 mM Tris pH 7.5, 100 mM NaCl; 10 mM sodium metaperiodate ($NaIO_4$) in 50 mM sodium acetate buffer pH 4.5; 100 U ml^{-1} DNAse I in PBS; 40 µg ml^{-1} Dispersin B (DspB) in PBS and 5 mg ml^{-1} cellulase in 50 mM citrate buffer pH 4.6. Control wells (-) only contained the corresponding reaction buffer. After treatment, wells were washed and 0.25% crystal violet was added to stain non-dispersed biofilms. The amount of crystal violet-stained cells was quantified by solubilizing the dye in ethanol/acetone and determining the absorbance at 595 nm. Data represent the mean ± standard deviation calculated from three independent experiments. The biofilm formed by *R. erythropolis* pTipQC1::*dsz*-P*lac*D-*adrA* was only dispersed by sodium metaperiodate, indicating that an exopolysaccharide (neither PIA/PNAG nor cellulose) is the main component of the biofilm extracellular matrix.

R. erythropolis cells overproducing c-di-GMP form a biofilm on polystyrene and silicone surfaces under flow conditions inside microfermenters

Microbial cells immobilization in a reactor offers advantages such as superior operational stability, continuous processing and simpler separation from the reaction media for reuse (Soleimani *et al.*, 2007; Rosche *et al.*, 2009). Previous attempts to immobilize *R. erythropolis* cells include gel entrapment in resin polymers (Naito *et al.*, 2001) and decoration of bacteria with magnetic nanoparticles (Ansari *et al.*, 2009). However, these artificial immobilization approaches may show several limitations, such as the extra elaborate preparation steps that have a negative impact on costs, lower bacterial viability and restricted mass transfer through the immobilization matrix. Conversely, biofilms produce their own immobilization matrix and are naturally adapted to be viable within it (Rosche *et al.*, 2009). The above results indicated that c-di-GMP is able to induce *R. erythropolis* biofilm development in batch cultures. Next, we wondered whether c-di-GMP could also induce *R. erythropolis* biofilm development under continuous flow conditions that might be used to develop an engineered biofilm process for fuel desulfurization. For this, we assessed biofilm formation with the use of microfermenters, under continuous flow conditions and with a flow rate high enough to prevent planktonic growth (Ghigo, 2001). The microfermenters contain submerged, removable Pyrex slides, that serve as substratum for bacterial attachment. To test other types of surfaces apart from glass, polystyrene and silicone rubber disk coupons with a diameter of 12.7 mm were fixed on the glass slides (**Figure 6A**). Microfermenters were inoculated with either the biofilm catalytic strain *R. erythropolis* pTipQC1::*dsz*-P_{lac}*D-adrA* or the control non

biofilm forming strain *R. erythropolis* pTipQC1::*dsz*-P$_{lac}$*D*. After 48 hours of incubation at 30 ˚C, Pyrex slides were removed and biofilm formation on glass, polystyrene and silicone was visually inspected. Results showed that the *R. erythropolis* pTipQC1::*dsz*-P$_{lac}$*D-adrA* biocatalyst formed a very robust biofilm both on polystyrene and silicone surfaces whilst the control strain barely attached to these surfaces. None of the two strains was able to form a biofilm on the glass spatula (**Figure 6B**). In order to analyze biofilm structure, a derivative of *R. erythropolis* pTipQC1::*dsz*-P$_{lac}$*D-adrA* expressing the fluorescent mCherry protein was constructed. *R. erythropolis* pTipQC1::*dsz*-P$_{lac}$*D-adrA*-mCherry was incubated inside microfermenters and then, the biofilm formed on polystyrene coupons was inspected by confocal laser scanning microscopy (CLSM). Images confirmed the presence of a characteristic biofilm architecture that was many cells thick and showed a uniform substratum coverage (**Figure 6C**). Altogether, these results suggested that the engineered *R. erythropolis* biofilm forming strain constructed in this study could be used as an effective biocatalyst in the development of an efficient bioreactor for an improved BDS process.

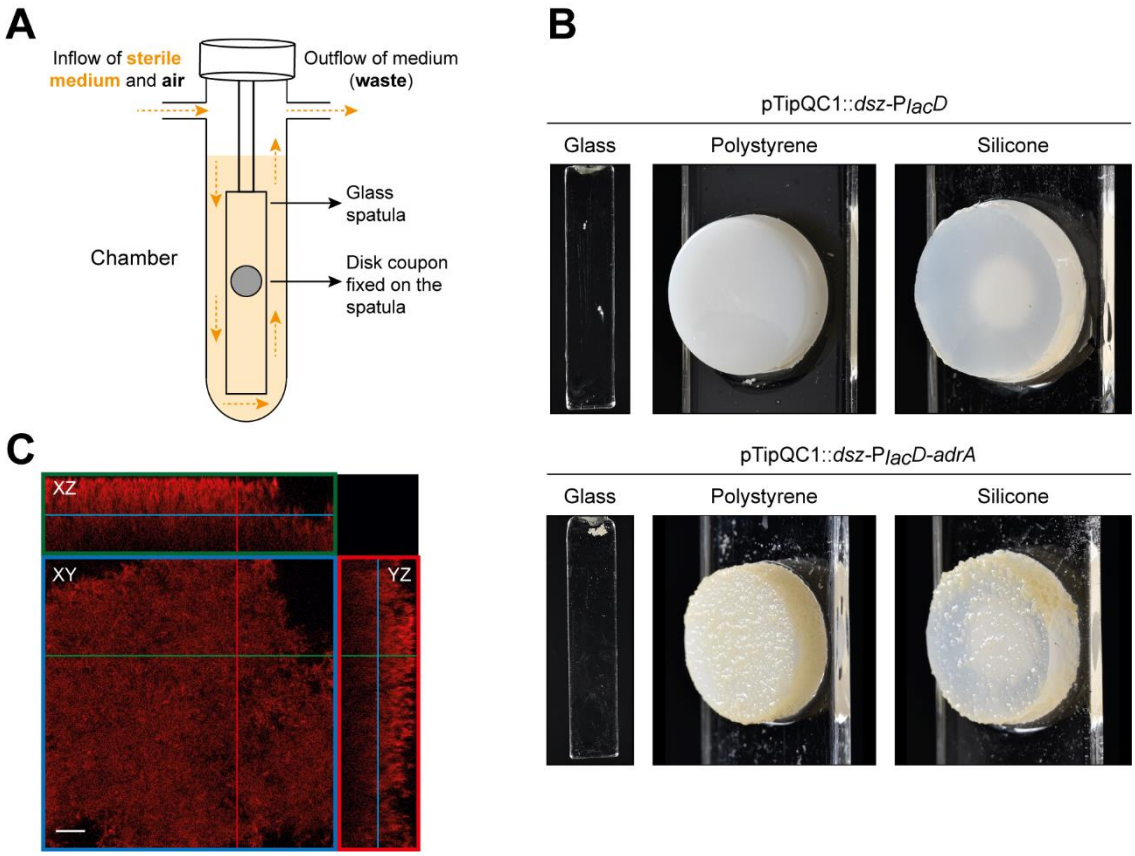

Figure 6. Biofilm formation on different surfaces by *R. erythropolis* pTipQC1::*dsz*-P$_{lac}$*D-adrA* grown under flow conditions inside microfermenters. (A) Schematic diagram of a microfermenter setup containing a glass spatula inside with a fixed 12.7 mm diameter disk coupon (depicted as a gray circle). (B) Images of the biofilm formed on the glass spatula (the entire spatula is shown), polystyrene and silicone rubber disk coupons by *R. erythropolis* pTipQC1::*dsz*-P$_{lac}$*D-adrA* and the control strain *R. erythropolis* pTipQC1::*dsz*-P$_{lac}$*D* after 48 hours of incubation at 30 ˚C under continuous flow conditions. (C) CLSM image of the top-down view (large panel, at 14 µm above the coupon surface) and orthogonal views (side panels) of the biofilm formed by *R. erythropolis* pTipQC1::*dsz*-P$_{lac}$*D-adrA-mCherry* on a polystyrene disk coupon after 48 hours of incubation at 30 ˚C under continuous flow conditions. Scale bar 10 µm. The experiment was performed in triplicate and a representative image is shown.

References

Alves, L. and Paixão, S.M. (2014) Fructophilic behaviour of *Gordonia alkanivorans* strain 1B during dibenzothiophene desulfurization process. *N Biotechnol* **31**: 73–79.

Ansari, F., Grigoriev, P., Libor, S., Tothill, I.E., and Ramsden, J.J. (2009) DBT degradation enhancement by decorating *Rhodococcus erythropolis* IGST8 with magnetic Fe_3O_4 nanoparticles. *Biotechnol Bioeng* **102**: 1505–1512.

Bähre, H. and Kaever, V. (2017) Identification and quantification of cyclic di-guanosine monophosphate and its linear metabolites by reversed-phase LC-MS/MS. In *Methods in molecular biology (Clifton, N.J.)*. pp. 45–58.

Balestrino, D., Anne Hamon, M., Dortet, L., Nahori, M.A., Pizarro-Cerda, J., Alignani, D., *et al*. (2010) Single-cell techniques using chromosomally tagged fluorescent bacteria to study *Listeria monocytogenes* infection processes. *Appl Environ Microbiol* **76**: 3625–3636.

Benedetti, I., de Lorenzo, V., and Nikel, P.I. (2016) Genetic programming of catalytic *Pseudomonas putida* biofilms for boosting biodegradation of haloalkanes. *Metab Eng* **33**: 109–118.

De Carvalho, C.C.C.R. and Da Fonseca, M.M.R. (2007) Preventing biofilm formation: promoting cell separation with terpenes. *FEMS Microbiol Ecol* **61**: 406–413.

Costerton, J.W., Stewart, P.S., and Greenberg, E.P. (1999) Bacterial biofilms: a common cause of persistent infections. *Science* **284**: 1318–1322.

Cramton, S.E., Gerke, C., Schnell, N.F., Nichols, W.W., and Götz, F. (1999) The intercellular adhesion (*ica*) locus is present in *Staphylococcus aureus* and is required for biofilm formation. *Infect Immun* **67**: 5427–5433.

Cywes-Bentley, C., Skurnik, D., Zaidi, Tanweer, Roux, D., Deoliveira, R.B., Garrett, W.S., *et al*. (2013) Antibody to a conserved antigenic target is protective against diverse prokaryotic and eukaryotic pathogens. *Proc Natl Acad Sci USA* **110**: E2209-18.

Davoodi-Dehaghani, F., Vosoughi, M., and Ziaee, A.A. (2010) Biodesulfurization of

dibenzothiophene by a newly isolated *Rhodococcus erythropolis* strain. *Bioresour Technol* **101**: 1102–1105.

Dejaloud, A., Vahabzadeh, F., and Habibi, A. (2017) *Ralstonia eutropha* as a biocatalyst for desulfurization of dibenzothiophene. *Bioprocess Biosyst Eng* **40**: 969–980.

DeLorenzo, D.M., Rottinghaus, A.G., Henson, W.R., and Moon, T.S. (2018) Molecular toolkit for gene expression control and genome modification in *Rhodococcus opacus* PD630. *ACS Synth Biol* **7**: 727–738.

Echeverz, M., García, B., Sabalza, A., Valle, J., Gabaldón, T., Solano, C., and Lasa, I. (2017) Lack of the PGA exopolysaccharide in *Salmonella* as an adaptive trait for survival in the host. *PLOS Genet* **13**: e1006816.

Edel, M., Horn, H., and Gescher, J. (2019) Biofilm systems as tools in biotechnological production. *Appl Microbiol Biotechnol* **103**: 5095–5103.

Flemming, H.C., Wingender, J., Szewzyk, U., Steinberg, P., Rice, S.A., and Kjelleberg, S. (2016) Biofilms: an emergent form of bacterial life. *Nat Rev Microbiol* **14**: 563–575.

Freeman, D. J., Falkiner, F.R., and Keane, C.T. (1989) New method for detecting slime production by coagulase negative staphylococci. *J Clin Pathol* **42**: 872–874.

Galan, B., Diaz, E., and Garcia, J.L. (2000) Enhancing desulphurization by engineering a flavin reductase-encoding gene cassette in recombinant biocatalysts. *Environ Microbiol* **2**: 687–694.

Gallagher, J., Olson, E.S., and Stanley, D.C. (1993) Microbial desulfurization of dibenzothiophene: a sulfur-specific pathway. *FEMS Microbiol Lett* **107**: 31–35.

Ghigo, J.M. (2001) Natural conjugative plasmids induce bacterial biofilm development. *Nature* **412**: 442–445.

Gray, K.A., Pogrebinsky, O.S., Mrachko, G.T., Xi, L., Monticello, D.J., and Squires, C.H. (1996) Molecular mechanisms of biocatalytic desulfurization of fossil fuels. *Nat Biotechnol* **14**: 1705–1709.

Guo, Y., Liu, S., Tang, X., and Yang, F. (2017) Role of c-di-GMP in anammox aggregation and systematic analysis of its turnover protein in *Candidatus Jettenia*

caeni. *Water Res* **113**: 181–190.

Hu, Y., Liu, X., Ren, A.T.M., Gu, J., and Cao, B. (2019) Optogenetic modulation of a catalytic biofilm for the biotransformation of indole into tryptophan. *Chem Sus Chem* **12**: 5142–5148.

Ismail, W., El-Sayed, W.S., Abdul Raheem, A.S., Mohamed, M.E., and El Nayal, A.M. (2016) Biocatalytic desulfurization capabilities of a mixed culture during non-destructive utilization of recalcitrant organosulfur compounds. *Front Microbiol* **7**: 266.

Kaplan, J.B., Ragunath, C., Velliyagounder, K., Fine, D.H., and Ramasubbu, N. (2004) Enzymatic detachment of *Staphylococcus epidermidis* biofilms. *Antimicrob Agents Chemother* **48**: 2633–2636.

Kilbane, J.J. (2017) Biodesulfurization: how to make it work? *Arab J Sci Eng* **42**: 1–9.

Kilbane, J.J. (2006) Microbial biocatalyst developments to upgrade fossil fuels. *Curr Opin Biotechnol* **17**: 305–314.

Kilbane, J.J. and Jackowski, K. (1992) Biodesulfurization of water-soluble coal-derived material by *Rhodococcus rhodochrous* IGTS8. *Biotechnol Bioeng* **40**: 1107–1114.

Lear, G. ed. (2016) Biofilms in bioremediation. Current research and emerging technologies, Caister Academic Press.

Li, M.Z., Squires, C.H., Monticello, D.J., and Childs, J.D. (1996) Genetic analysis of the *dsz* promoter and associated regulatory regions of *Rhodococcus erythropolis* IGTS8. *J Bacteriol* **178**: 6409–6418.

Liang, Y., Jiao, S., Wang, M., Yu, H., and Shen, Z. (2020) A CRISPR/Cas9-based genome editing system for *Rhodococcus ruber* TH. *Metab Eng* **57**: 13–22.

Maghsoudi, S., Vossoughi, M., Kheirolomoom, A., Tanaka, E., and Katoh, S. (2001) Biodesulfurization of hydrocarbons and diesel fuels by *Rhodococcus* sp. strain P32C1. *Biochem Eng J* **8**: 151–156.

Maira-Litran, T., Kropec, A., Goldmann, D.A., and Pier, G.B. (2005) Comparative opsonic and protective activities of *Staphylococcus aureus* conjugate vaccines containing native or deacetylated staphylococcal poly-N-acetyl-β-(1-6)-

glucosamine. *Infect Immun* **73**: 6752–6762.

Martin, A.B., Alcon, A., Santos, V.E., and Garcia-Ochoa, F. (2005) Production of a biocatalyst of *Pseudomonas putida* CECT5279 for DBT biodesulfurization: influence of the operational conditions. *Energy and Fuels* **19**: 775–782.

Martínez, I., El-Said Mohamed, M., Santos, V.E., García, J.L., García-Ochoa, F., and Díaz, E. (2017) Metabolic and process engineering for biodesulfurization in Gram-negative bacteria. *J Biotechnol* **262**: 47–55.

Martínez, I., Mohamed, M.E.-S., Rozas, D., García, J.L., and Díaz, E. (2016) Engineering synthetic bacterial consortia for enhanced desulfurization and revalorization of oil sulfur compounds. *Metab Eng* **35**: 46–54.

Mohebali, G. and Ball, A.S. (2016) Biodesulfurization of diesel fuels - Past, present and future perspectives. *Int Biodeterior Biodegrad* **110**: 163–180.

Naito, M., Kawamoto, T., Fujino, K., Kobayashi, M., Maruhashi, K., and Tanaka, A. (2001) Long-term repeated biodesulfurization by immobilized *Rhodococcus erythropolis* KA2-5-1 cells. *Appl Microbiol Biotechnol* **55**: 374–378.

Nakashima, Nobutaka and Tamura, T. (2004) Isolation and characterization of a rolling-circle-type plasmid from *Rhodococcus erythropolis* and application of the plasmid to multiple-recombinant-protein expression. *Appl Environ Microbiol* **70**: 5557–5568.

O'Toole, G.A., Pratt, L.A., Watnick, P.I., Newman, D.K., Weaver, V.B., and Kolter, R. (1999) Genetic approaches to study of biofilms. *Methods Enzymol* **310**: 91–109.

Del Olmo, C.H., Alcon, A., Santos, V.E., and Garcia-Ochoa, F. (2005) Modeling the production of a *Rhodococcus erythropolis* IGTS8 biocatalyst for DBT biodesulfurization: influence of media composition. *Enzyme Microb Technol* **37**: 157–166.

Pérez-Mendoza, D. and Sanjuán, J. (2016) Exploiting the commons: cyclic diguanylate regulation of bacterial exopolysaccharide production. *Curr Opin Microbiol* **30**: 36–43.

Piddington, C.S., Kovacevich, B.R., and Rambosek, J. (1995) Sequence and molecular characterization of a DNA region encoding the dibenzothiophene

desulfurization operon of *Rhodococcus* sp. strain IGTS8. *Appl Environ Microbiol* **61**: 468–475.

Ramasubbu, N., Thomas, L.M., Ragunath, C., and Kaplan, J.B. (2005) Structural analysis of dispersin B, a biofilm-releasing glycoside hydrolase from the periodontopathogen *Actinobacillus actinomycetemcomitans*. *J Mol Biol* **349**: 475–486.

Rashtchi, M., Mohebali, G.H., Akbarnejad, M.M., Towfighi, J., Rasekh, B., and Keytash, A. (2006) Analysis of biodesulfurization of model oil system by the bacterium, strain RIPI-22. *Biochem Eng J* **29**: 169–173.

Rodrigues, C.J.C. and de Carvalho, C.C.C.R. (2015) *Rhodococcus erythropolis* cells adapt their fatty acid composition during biofilm formation on metallic and non-metallic surfaces. *FEMS Microbiol Ecol* **91**: 135.

Römling, U. and Galperin, M.Y. (2015) Bacterial cellulose biosynthesis: diversity of operons, subunits, products, and functions. *Trends Microbiol* **23**: 545–557.

Römling, U., Galperin, M.Y., and Gomelsky, M. (2013) Cyclic di-GMP: the first 25 years of a universal bacterial second messenger. *Microbiol Mol Biol Rev* **77**: 1–52.

Rosche, B., Li, X.Z., Hauer, B., Schmid, A., and Buehler, K. (2009) Microbial biofilms: a concept for industrial catalysis? *Trends Biotechnol* **27**: 636–643.

Schirmer, T. and Jenal, U. (2009) Structural and mechanistic determinants of c-di-GMP signalling. *Nat Rev Microbiol* **7**: 724–735.

Simm, R., Morr, M., Kader, A., Nimtz, M., and Römling, U. (2004) GGDEF and EAL domains inversely regulate cyclic di-GMP levels and transition from sessibility to motility. *Mol Microbiol* **53**: 1123–1134.

Singh, R., Paul, D., and Jain, R.K. (2006) Biofilms: implications in bioremediation. *Trends Microbiol* **14**: 389–397.

Solano, C., García, B., Latasa, C., Toledo-Arana, A., Zorraquino, V., Valle, J., et al. (2009) Genetic reductionist approach for dissecting individual roles of GGDEF proteins within the c-di-GMP signaling network in *Salmonella*. *Proc Natl Acad Sci USA* **106**: 7997–8002.

Solano, C., García, B., Valle, J., Berasain, C., Ghigo, J.M., Gamazo, C., and Lasa, I.

(2002) Genetic analysis of *Salmonella* enteritidis biofilm formation: critical role of cellulose. *Mol Microbiol* **43**: 793–808.

Soleimani, M., Bassi, A., and Margaritis, A. (2007) Biodesulfurization of refractory organic sulfur compounds in fossil fuels. *Biotechnol Adv* **25**: 570–596.

Sugimoto, S., Sato, F., Miyakawa, R., Chiba, A., Onodera, S., Hori, S., and Mizunoe, Y. (2018) Broad impact of extracellular DNA on biofilm formation by clinically isolated Methicillin-resistant and -sensitive strains of *Staphylococcus aureus*. *Sci Rep* **8**:.

Taglialegna, A., Lasa, I., and Valle, J. (2016) Amyloid structures as biofilm matrix scaffolds. *J Bacteriol* **198**: 2579–2588.

Taglialegna, A., Navarro, S., Ventura, S., Garnett, J.A., Matthews, S., Penades, J.R., et al. (2016) Staphylococcal Bap proteins build amyloid scaffold biofilm matrices in response to environmental signals. *PLOS Pathog* **12**: e1005711.

Trivedi, A., Mavi, P.S., Bhatt, D., and Kumar, A. (2016) Thiol reductive stress induces cellulose-anchored biofilm formation in *Mycobacterium tuberculosis*. *Nat Commun* **7**: 1–15.

Urai, M., Yoshizaki, H., Anzai, H., Ogihara, J., Iwabuchi, N., Harayama, S., *et al*. (2007a) Structural analysis of an acidic, fatty acid ester-bonded extracellular polysaccharide produced by a pristane-assimilating marine bacterium, *Rhodococcus erythropolis* PR4. *Carbohydr Res* **342**: 933–942.

Urai, M., Yoshizaki, H., Anzai, H., Ogihara, J., Iwabuchi, N., Harayama, S., *et al*. (2007b) Structural analysis of mucoidan, an acidic extracellular polysaccharide produced by a pristane-assimilating marine bacterium, *Rhodococcus erythropolis* PR4. *Carbohydr Res* **342**: 927–932.

Valle, J., Toledo-Arana, A., Berasain, C., Ghigo, J.M., Amorena, B., Penadés, J.R., and Lasa, I. (2003) SarA and not σB is essential for biofilm development by *Staphylococcus aureus*. *Mol Microbiol* **48**: 1075–1087.

Wang, J., Butler, R.R., Wu, F., Pombert, J.-F., Kilbane, J.J., and Stark, B.C. (2017) Enhancement of microbial biodesulfurization via genetic engineering and adaptive evolution. *PLoS One* **12**: e0168833.

Wu, Y., Ding, Y., Cohen, Y., and Cao, B. (2015) Elevated level of the second

messenger c-di-GMP in *Comamonas testosteroni* enhances biofilm formation and biofilm-based biodegradation of 3-chloroaniline. *Appl Microbiol Biotechnol* **99**: 1967–1976.

Zampolli, J., Zeaiter, Z., Di Canito, A., and Di Gennaro, P. (2019) Genome analysis and -omics approaches provide new insights into the biodegradation potential of *Rhodococcus*. *Appl Microbiol Biotechnol* **103**: 1069–1080.

CHAPTER II

Fitness cost evolution of natural plasmids of *Staphylococcus aureus*

Summary

Plasmids have largely contributed to the spread of antimicrobial resistance genes among *Staphylococcus*. Knowledge about the fitness cost that plasmids confer on clinical staphylococcal isolates and the co-evolutionary dynamics that drive plasmid maintenance is still scarce. In this study, we aimed at analysing the initial fitness cost of plasmids in the bacterial pathogen *Staphylococcus aureus* and the plasmid-host adaptations that occur over time. For that, we first designed a CRISPR-based tool that enables the removal of native *S. aureus* plasmids and then transferred three different plasmids to the same background clinical cured strain. One of the plasmids, pUR2940, imposed a significant fitness cost to both the native and the new host. Experimental evolution in a non-selective medium resulted in a high rate pUR2940 loss and selected for clones with an alleviated fitness cost in which compensatory adaptation occurred via deletion of a 12.8 kb plasmid fragment, contained between two IS*Sau*10 insertion sequences and harbouring several antimicrobial resistance genes. Overall, our results describe the relevance of plasmid-borne insertion sequences in plasmid rearrangement and maintenance and suggest the potential benefits of reducing the use of antibiotics both in animal and clinical settings for the loss of clinical multidrug resistance plasmids.

Introduction

Plasmids are circular extrachromosomal DNA elements capable of semi-autonomous replication by recruiting host cell enzymes (Phillips and Funnell, 2004). Plasmids carry genes necessary for plasmid replication and transmission, and the so-called accessory genes that under specific environmental conditions provide beneficial traits such as antibiotic resistance, tolerance to heavy metals, virulence, metabolism of carbon sources, or root nodulation (Gogarten and Townsend, 2005). Many plasmids are large or found in high copy numbers and the logic suggests that in the absence of selection for plasmid-encoded traits, the fitness cost of plasmid carriage should be higher than its benefits and consequently, clones lacking the plasmid should outcompete the plasmid bearing population in few generations (Vogwill and MacLean, 2015; San Millan and MacLean, 2017). Some plasmids solve this puzzle by moving the beneficial genes to the bacterial chromosome and then, remaining as smaller plasmids or simply disappearing (Carroll and Wong, 2018). However, this strategy seems not to be the preferred solution, since plasmids containing accessory genes are widely distributed, indicating that mechanisms have been developed to persist in the host, independently of the presence of positive selection. In 2012, a seminal publication by Harrison and Brockhurst proposed that the paradox in plasmid persistence can be explained, at least in part, by compensatory mutations that the plasmid and the host accumulate over time to alleviate the fitness cost (Harrison and Brockhurst, 2012). Since then, several studies have pursued this line of investigation and found that host-plasmid coevolution is easily achievable in the laboratory through mutations that can occur in the plasmid, the bacterial

chromosome, or both (Millan *et al.*, 2014; San Millan *et al.*, 2014; Peña-Miller *et al.*, 2015; Harrison *et al.*, 2015). However, the rules governing plasmid fitness cost remain largely unexplored, and thus, it is not possible to predict the evolution of the same plasmid in different bacterial clones and the fitness effects of different plasmids in the same strain (Vogwill and MacLean, 2015).

Staphylococcus aureus is a major human pathogen routinely isolated as a commensal organism in more than a third of the human population. Most natural strains of *S. aureus* contain different types of mobile genetic elements (MGEs) including plasmids, transposons, insertion sequences, bacteriophages, and pathogenicity islands that facilitate the acquisition of genes encoding mechanisms of resistance against antimicrobials, biocides, and heavy metals (Lanza *et al.*, 2015). Regarding plasmids, most *S. aureus* clinical isolates harbor from one to three plasmids that can carry antibiotic and antiseptic resistance genes (responsible for resistance to β-lactams, tetracycline, erythromycin, kanamycin, vancomycin, trimethoprim, chloramphenicol, mupirocin, linezolid, teicoplanin, heavy metals, quaternary ammonium compounds, and chlorhexidine), which provide an advantage to the bacterium when the antibiotic and the biocide are present (Haaber *et al.*, 2017). Very often, the same plasmid accumulates multiple antimicrobial resistance genes, which increases the possibilities of selection for plasmid-encoded traits (McCarthy and Lindsay, 2012). Current knowledge about the fitness cost associated with the carriage of antibiotic resistance plasmids in *S. aureus* is scarce. The lab of J. Lindsay showed that differences in fitness between two prevalent methicillin-resistant *S. aureus* strains were unrelated to the presence of large antibiotic resistance

plasmids (Knight *et al.*, 2013). On the other hand, a recent study investigating the coevolution over the last 32 years of the pSK1 plasmid family in the Australian *S. aureus* ST239 MRSA clade revealed that pSK1 plasmid maintenance is linked to multiple structural variations caused by IS*256* and IS*257* insertion sequences (Baines *et al.*, 2019). In summary, we still have a limited understanding of how plasmids and *S. aureus* have coevolved in order to reduce the fitness cost that plasmid carriage produces when bacteria grow in an antibiotic-free environment, as occurs when patients finish the antibiotic treatment. This knowledge could have important consequences in the design of antibiotic management plans, especially if plasmid-borne bacteria show a lower fitness than plasmid-free bacteria in the absence of antibiotics.

In this work, we addressed the fitness cost and the mechanisms of coevolution of natural plasmids of *S. aureus*. For that, we generated a CRISPR-based tool to remove plasmids from natural isolates of *S. aureus*. One of the resulting plasmid-free strains was transformed with three different plasmids isolated from clinical *S. aureus* strains and then, the initial cost upon entering this new host was calculated and experimental evolution in the absence of selection was assayed. Our results showed that two plasmids did not produce any discernable cost and were stably maintained during evolution. On the contrary, a third plasmid caused a high fitness cost and was rapidly lost in the absence of selective pressure. Adaptation over time was dependent on plasmid rearrangements through plasmid-borne IS*Sau*10 insertion sequences and driven by the cost of a plasmid region comprising several antimicrobial resistance genes. These results indicate that insertion sequences-mediated loss of plasmid

resistance genes alleviates the cost associated with plasmid carriage in the absence of antibiotics and suggest that limiting antibiotic utilisation may select for mutated plasmid carrying clones that no longer confer resistance.

Experimental procedures

Bacterial strains, oligonucleotides and culture conditions

Bacterial strains, plasmids and oligonucleotides used in this work are listed in Table 1, 2 and 3, respectively. *Escherichia coli* strains were grown in Luria-Bertani medium (LB; Conda-Pronadisa) at 37 ˚C. *S. aureus* strains were routinely incubated in trypticase soy broth (TSB; Conda-Pronadisa) at 37 ˚C. Media, when required, were supplemented with appropriate antibiotics at the following concentrations: ampicillin (Amp, 100 µg ml^{-1}), chloramphenicol (Cm, 20 µg ml^{-1}), cadmium (Cd, 0.05 mM), erythromycin (Ery, 10 µg ml^{-1}) and lincomycin (Lin, 8 µg ml^{-1}). Bacteriological agar was used as gelling agent (VWR). A stock solution of 10 mg ml^{-1} anhydrotetracycline (Cayman Chemical Company) in dimethyl sulfoxide (DMSO) was prepared and added to cultures at 100 ng ml^{-1} to induce the expression of *cas9* (pEMPTY and derivatives).

Table 1. Bacterial strains used in this study.

Strains	Relevant characteristics	MIC[a]	Reference/Source
Escherichia coli			
IM01B	*mcrA* Δ(*mrr-hsdRMS-mcrBC*) φ80*lacZ*ΔM15 Δ*lacX*74 *recA*1 *araD*139 Δ(*ara-leu*)7697 *galU galK rpsL endA*1 *nupG* Δ*dcm* Ω*Phelp-hsdMS* (CC1-2) ΩPN25-*hsdS* (CC1-1). *E. coli* K12 DH10B derivative. Δ*dcm*. The *hsdMS* genes encoding methylase and specificity genes from *Staphylococcus aureus* MW2 clonal complex 1 were introduced into the chromosome at neutral locations via recombineering.	5694	(Monk *et al.*, 2015)

Table 1. Bacterial strains used in this study. (cont.)

Strains	Relevant characteristics	MIC[a]	Reference/Source
Staphylococcus aureus			
RN10359	RN450 lysogenic for 80α phage.	3337	(Úbeda, Barry, *et al.*, 2007)
RN4220	Restriction deficient derivative of 8325-4	99	(Peng *et al.*, 1988)
MW2	Community-acquired methicillin-resistant *Staphylococcus aureus* (CA-MRSA). Clonal lineage USA400 It contains pMW2. Cd^R	3566	(Baba *et al.*, 2002)
LAC	Community-acquired methicillin-resistant *Staphylococcus aureus* (CA-MRSA). Clonal lineage USA300. It contains pLAC-p03 and pLAC-p01. Cd^R	3413	(Voyich *et al.*, 2005)
N315	Hospital-acquired methicillin-resistant *Staphylococcus aureus* (LA-MRSA). Clonal lineage 5-Basal. It contains pN315. Cd^R	686	(Kuroda *et al.*, 2001)
C2940	Livestock-associated methicillin-resistant *Staphylococcus aureus* (LA-MRSA). Clonal lineage ST398. It contains pUR2940. Cd^R Ery^R	6706	(Lozano, Rezusta, *et al.*, 2012; Gómez-Sanz, Kadlec, Feßler, Zarazaga, *et al.*, 2013)
C1902	Livestock-associated methicillin-resistant *Staphylococcus aureus* (LA-MRSA). Clonal lineage ST398. It contains pUR1902. Cd^R Ery^R	6704	(Gómez-Sanz, Kadlec, Feßler, Zarazaga, *et al.*, 2013)
C3912	Livestock-associated methicillin- susceptible *Staphylococcus aureus* (LA-MSSA). Clonal lineage ST398. It contains pUR3912 integrated into the chromosome. Cd^R Ery^R	6710	(Gómez-Sanz, Zarazaga, *et al.*, 2013; Gómez-Sanz, Kadlec, Feßler, Billerbeck, *et al.*, 2013)
C2355	Livestock-associated methicillin-resistant *Staphylococcus aureus* (LA-MRSA). Clonal lineage ST398. It contains pUR2355. Lin^R	6712	(Lozano, Aspiroz, Rezusta, *et al.*, 2012)
C1841	Livestock-associated methicillin-resistant Staphylococcus aureus (LA-MRSA). Clonal lineage ST398. It contains pUR1841. Lin^R	6714	(Lozano, Aspiroz, Sáenz, et al., 2012)
RN4220 pMW2	RN4220 transformed with pMW2. Cd^R	7066	This study
RN4220 pLAC-p03	RN4220 transduced with pLAC-p03. Cd^R	7134	This study

Table 1. Bacterial strains used in this study. (cont.)

Strains	Relevant characteristics	MIC[a]	Reference/Source
RN4220 pN315	RN4220 transformed with pN315. Cd^R	7065	This study
C4864	RN4220 transformed with pUR2940. Cd^R Ery^R	6707	(Gómez-Sanz, Kadlec, Feßler, Zarazaga, *et al.*, 2013)
C4858	RN4220 transformed with pUR1902. Cd^R Ery^R	6705	(Gómez-Sanz, Kadlec, Feßler, Zarazaga, *et al.*, 2013)
C4863	RN4220 transformed with pUR3912. Cd^R Ery^R	6711	(Gómez-Sanz, Zarazaga, *et al.*, 2013)
C4043	RN4220 pUR2355. RN4220 strain transformed with plasmid pUR2355. Lin^R	6713	(Lozano, Aspiroz, Rezusta, *et al.*, 2012)
C4044	RN4220 transformed with pUR1841. Lin^R	6715	(Lozano, Aspiroz, Sáenz, *et al.*, 2012)
MW2 PF_{t0}	MW2 cured of plasmid pMW2	7068	This study
LAC PF_{t0}	LAC cured of plasmid pLAC-p01 and pLAC-p03	7131	This study
LAC PF_{t0} pLAC-p03	LAC PF_{t0} transformed with pLAC-p03	7177	This study
N315 PF_{t0}	N315 cured of plasmid pN315	7060	This study
C2940 PF_{t0}	C2940 cured of plasmid pUR2940. Cd^R	7058	This study
C1902 PFt0	C1902 cured of plasmid pUR1902	7057	This study
C1841 PFt0	C1841 cured of plasmid pUR1841	7059	This study
PFt0 $pMW2_{t0}$ C1	MW2 PF_{t0} transformed with plasmid pMW2. Clone 1. Cd^R	7090	This study
PFt0 $pMW2_{t0}$ C2	MW2 PF_{t0} transformed with plasmid pMW2. Clone 2. Cd^R	7138	This study
PFt0 $pMW2_{t0}$ C3	MW2 PF_{t0} transformed with plasmid pMW2. Clone 3. Cd^R	7139	This study
PFt0 $pUR2940_{t0}$ C1	MW2 PF_{t0} transformed with plasmid pUR2940. Clone 1. Cd^R Ery^R	7092	This study
PFt0 $pUR2940_{t0}$ C2	MW2 PF_{t0} transformed with plasmid pUR2940. Clone 2. Cd^R Ery^R	7140	This study

Table 1. Bacterial strains used in this study. (cont.)

Strains	Relevant characteristics	MIC[a]	Reference/Source
PF_{t0} $pUR2940_{t0}$ C3	MW2 PF_{t0} transformed with plasmid pUR2940. Clone 3. Cd^R Ery^R	7141	This study
PF_{t0} $pN315_{t0}$ C1	MW2 PF_{t0} transformed with plasmid pN315. Clone 1. Cd^R	7091	This study
PF_{t0} $pN315_{t0}$ C2	MW2 PF_{t0} transformed with plasmid pN315. Clone 2. Cd^R	7132	This study
PF_{t0} $pN315_{t0}$ C3	MW2 PF_{t0} transformed with plasmid pN315. Clone 3. Cd^R	7133	This study
PF_{t0} pLAC-$p03_{t0}$ C1	MW2 PF_{t0} transformed with plasmid pLAC-p03. Clone 1. Cd^R	7135	This study
PF_{t0} pLAC-$p03_{t0}$ C2	MW2 PF_{t0} transformed with plasmid pLAC-p03. Clone 2. Cd^R	7136	This study
PF_{t0} pLAC-$p03_{t0}$ C3	MW2 PF_{t0} transformed with plasmid pLAC-p03. Clone 3. Cd^R	7137	This study
PF_{t35} $pMW2_{t35}$ C1	PF_{t0} $pMW2_{t0}$ C1 evolved for 35 days under laboratory conditions. Cd^R	Evo10	This study
PF_{t35} $pMW2_{t35}$ C2	PF_{t0} $pMW2_{t0}$ C2 evolved for 35 days under laboratory conditions. Cd^R	Evo13	This study
PF_{t35} $pMW2_{t35}$ C3	PF_{t0} $pMW2_{t0}$ C3 evolved for 35 days under laboratory conditions. Cd^R	Evo16	This study
PF_{t35} $pUR2940_{t35}$ C1	PF_{t0} $pUR2940_{t0}$ C1 evolved for 35 days under laboratory conditions. Cd^R Ery^R	Evo19	This study
PF_{t35} $pUR2940_{t35}$ C2	PF_{t0} $pUR2940_{t0}$ C2 evolved for 35 days under laboratory conditions. Cd^R	Evo22	This study
PF_{t35} $pUR2940_{t35}$ C3	PF_{t0} $pUR2940_{t0}$ C3 evolved for 35 days under laboratory conditions. Cd^R	Evo25	This study
PF_{t35} $pN315_{t35}$ C1	PF_{t0} $pN315_{t0}$ C1 evolved for 35 days under laboratory conditions. Cd^R	Evo28	This study
PF_{t35} $pN315_{t35}$ C2	PF_{t0} $pN315_{t0}$ C2 evolved for 35 days under laboratory conditions. Cd^R	Evo31	This study
PF_{t35} $pN315_{t35}$ C3	PF_{t0} $pN315_{t0}$ C3 evolved for 35 days under laboratory conditions. Cd^R	Evo34	This study
PF_{t35} pLAC-$p03_{t35}$ C1	PF_{t0} pLAC-$p03_{t0}$ C1 evolved for 35 days under laboratory conditions. Cd^R	Evo37	This study
PF_{t35} pLAC-$p03_{t35}$ C2	PF_{t0} pLAC-$p03_{t0}$ C2 evolved for 35 days under laboratory conditions. Cd^R	Evo40	This study

Table 1. Bacterial strains used in this study. (cont.)

Strains	Relevant characteristics	MIC[a]	Reference/Source
PF_{t35} pLAC-$p03_{t35}$ C3	PF_{t0} pLAC-$p03_{t0}$ C3 evolved for 35 days under laboratory conditions. Cd^R	Evo43	This study
PF_{t35} C1	PF_{t35} $pUR2940_{t35}$ C1 cured of plasmid pUR2940	Evo62	This study
PF_{t35} C2	PF_{t35} $pUR2940_{t35}$ C2 cured of plasmid pUR2940	Evo63	This study
PF_{t35} C3	PF_{t35} $pUR2940_{t35}$ C3 cured of plasmid pUR2940	Evo64	This study
PF_{t35} C1 $pUR2940_{t0}$	PF_{t35} C1 transformed with plasmid isolated from PF_{t0} $pUR2940_{t0}$ C1. Cd^R Ery^R	Evo74	This study
PF_{t35} C2 $pUR2940_{t0}$	PF_{t35} C2 transformed with plasmid isolated from PF_{t0} $pUR2940_{t0}$ C2. Cd^R Ery^R	Evo75	This study
PF_{t35} C3 $pUR2940_{t0}$	PF_{t35} C3 transformed with plasmid isolated from PF_{t0} $pUR2940_{t0}$ C3. Cd^R Ery^R	Evo76	This study
PF_{t0} $pUR2940_{t35}$ C1	MW2 PF_{t0} transformed with plasmid isolated from PF_{t35} $pUR2940_{t35}$ C1. Cd^R Ery^R	Evo50	This study
PF_{t0} $pUR2940_{t35}$ C2	MW2 PF_{t0} transformed with plasmid isolated from PF_{t35} $pUR2940_{t35}$ C2. Cd^R	Evo51	This study
PF_{t0} $pUR2940_{t35}$ C3	MW2 PF_{t0} transformed with plasmid isolated from PF_{t35} $pUR2940_{t35}$ C3. CdR	Evo52	This study

[a] Number of each strain in the culture collection of the Laboratory of Microbial Pathogenesis, Navarrabiomed-Universidad Pública de Navarra.

Table 2. Plasmids used in this study.

Plasmid	Relevant characteristics	Size (pb)	Reference/Source
pJET1.2	Cloning vector. Amp^R	2974	Thermo Scientific
pFREE-Amp	Plasmid designed to remove plasmids from *E. coli*. CRISPR-Cas9-based curing. Amp^R	7804	(Lauritsen et al., 2017)
pRMC2	*E. coli* - *S. aureus* shuttle vector. Expression of genes from the anhydrotetracycline-inducible $P_{xyl/tetO}$ promoter. Amp^R Cm^R	6555	(Corrigan and Foster, 2009)
pCN38	*E. coli* - *S. aureus* shuttle vector. Amp^R Cm^R	5426	(Charpentier et al., 2004)
pMAD	*E. coli* - *S. aureus* shuttle vector containing a thermosensitive origin of replication for Gram-positive bacteria. Amp^R Ery^R	9666	(Arnaud et al., 2004)

Table 2. Plasmids used in this study. (cont.)

Plasmid	Relevant characteristics	Size (pb)	Reference/Source
pEMPTY	*E. coli* - *S. aureus* shuttle vector with the *cas9* gene expression under the $P_{xyl/tetO}$ promoter. Thermosensitive origin of replication for Gram-positive bacteria. Amp^R Cm^R	10497	This study
pEMPTY::sgRNA2	*E. coli* - *S. aureus* shuttle vector that allows CRISPR-Cas9-based rapid and efficient plasmid curing in *Staphylococcus aureus*. *cas9* gene expression under the $P_{xyl/tetO}$ promoter. sgRNA2 expression under SP01 promoter. Thermosensitive origin of replication for Gram-positive bacteria. Amp^R Cm^R	11271	This study
pMW2	Naturally occurring plasmid. Isolated from *S. aureus* MW2. Cd^R	20654	(Baba et al., 2002)
pUR2940	Naturally occurring plasmid. Isolated from *S. aureus* C2940. Cd^R Ery^R	23702	(Elena Gómez-Sanz et al., 2013)
pN315	Naturally occurring plasmid. Isolated from *S. aureus* N315. Cd^R	24653	(Kuroda et al., 2001)
pLAC-p03	Naturally occurring plasmid. Isolated from *S. aureus* LAC. Cd^R	27068	(Voyich et al., 2005)
pUR1902	Naturally occurring plasmid. Isolated from *S. aureus* C1902. Cd^R	≈2000	(Elena Gómez-Sanz et al., 2013)
pUR3912	Naturally occurring plasmid. Isolated from *S. aureus* C3912. Cd^R Ery^R	6176	(E. Gómez-Sanz et al., 2013; Gómez-sanz et al., 2013)
pUR1841	Naturally occurring plasmid. Isolated from *S. aureus* C1841. Lin^R	2361	(C. Lozano et al., 2012a)
pUR2355	Naturally occurring plasmid. Isolated from *S. aureus* C2355. Lin^R	7609	(Carmen Lozano et al., 2012; Monteiro et al., 2015)
$pUR2940_{t35}$ C1	Plasmid isolated from *S. aureus* PF_{t0} $pUR2940_{t0}$ C1 after being evolved under laboratory conditions for 35 days. Cd^R Ery^R	23702	This study
$pUR2940_{t35}$ C2	Plasmid isolated from *S. aureus* PF_{t0} $pUR2940_{t0}$ C2 after being evolved under laboratory conditions for 35 days. Cd^R	10822	This study

Table 2. Plasmids used in this study. (cont.)

Plasmid	Relevant characteristics	Size (pb)	Reference/Source
pUR2940$_{t35}$ C3	Plasmid isolated from *S. aureus* PF$_{t0}$ pUR2940$_{t0}$ C3 after being evolved under laboratory conditions for 35 days. Cd^{R}	12474	This study

Table 3. Oligonucleotides used in this study.

Oligonucleotide	Sequence (5'-3')[a]
Construction of pEMPTY and pEMPTY::sgRNA2	
191	**AAAAAATATTGACACTCTATCATTGATAGAGTATAATTAAAATAAGCTTG***AGATCT*TTaggaggatGATTATTTATGGATAAGAAATACTCAATAGGC
473	**GAGCTGGCGGCCGCTGCATG*CCTGCAGGGCGCGCCCTTAAGCCCGGG*TACCAGATCTCAAAAAACCCCTCAAGACCCGTTT**
119	CAAGCTTATTTTAATTATACTCTATCAATGATAGAGTGTCAATATTTTTTTTAG
195	**GGGTAACGCCAGGGTTTTCCCAGTCACGACGTTGTAAAACGACGGCCAGTGAATTC**CAGGTCGACGGTATCGATAAC
474	**AAACGGGTCTTGAGGGGTTTTTTGAGATCTGGTA*CCCGGGCTTAAGGGCGCGCCCTGCAG*GCATGCAGCGGCCGCCAGCTC**
189	**TTTCCGTGATGGTAACTTCACGGTAACCAAGATGTCGAGTTATCGATACCGTCGACCTG**GAATTCACTGGCCGTCGTTTT
257	**GTTGCGCAGCCTGAATGGCGAAT***GGCGCC*TGAGGGTTGCCAGAGTTAAAG
259	**CTTTCTTATCTTGATAATACCTAGGT***GGGCCCC*CCTCGATCCCGCAAGAGGCC
448	*CCCGGGCTTAAG*GTTGCGCACACCGACTAGCG
475	*GGCGCGCC*TTGACAAATTGCAGTAGGCATGACAAAATGGACTCACAAGTTTTGGGATTGTTAAGGGTTCCGGTTTTAGAGCTAGAAATAGCAAGTTAAAATAAGGCTAGTC
Checking plasmid presence	
217	CGTAAACGGATGCTGGCTAG
235	CGATTTTTGTGATGCTCGTCAGGG
280	TGAATGCAATTCAAAACAGTATATCAC
282	GTTCTCCATATGAGTTTAAAACTTCAG
253	CTGTTAAGTCATAACCAGAATG
255	ATGAAAATTAATAATGTAACAGAAAAG

Table 3. Oligonucleotides used in this study. (cont.)

Oligonucleotide	**Sequence** (5'-3')[a]
365	TGATGTGAAGTTGAAGCAACACTC
366	TGATGTGATCTGTGTACATGAGGA
437	GGATCATGTACACAACCATA
438	TTGTTCTGTGTTGTGTTCGA
Unveiling pUR2940$_{t35}$ C2 and C3 final structure	
412	GCATTTATTGGCTTGATTTTATCACCTGC
414	AGGGAAACAGGTTTTAGTTTATTCAGGTC

qPCR

Oligonucleotide	**Sequence (5'-3')**	**Target[b]**	**Size[c] (pb)**	**Tm[d]**	**Primer efficiency**
365	TGATGTGAAGTTGA AGCAACACTC	*cadX*	207	56	0.9284
366	TGATGTGATCTGTGT ACATGAGGA	*cadX*			
367	CAATAATACGCCGC GTTAAATCTG		205	57	0.9388
368	TCAATTAAGGGGTT TGCTGAAACG	*phoR*			
369	TTATGGTGCTGGGC AAATACA	*gyrB*	338	60	0.8188
370	CACCATGTAAACCA CCAGATA	*gyrB*			

[a] Overlapping sequences for In-Fusion HD cloning, primer annealing regions and restriction enzymes sites are indicated in bold, underlined format and italics, respectively. The SOD ribosome binding site is shown in lower case letters. The SP01 promoter, sgRNA2 and sgRNA scaffold extra sequence are highlighted in light, medium and dark gray, respectively.

[b] *cadX* (plasmid gene); *phoR* (chromosomal monocopy gene used to compare the ratio of plasmid and chromosomal DNA in all cases except in strain C2940); *gyrB* (chromosomal monocopy gene used to compare the ratio of plasmid and chromosomal DNA in strain C2940).

[c] Amplicon size.

[d]Melting temperatures used for the qPCR.

DNA manipulations

Routine DNA manipulations were performed using standard procedures unless otherwise indicated. Oligonucleotides were synthesized by StabVida (Caparica, Portugal). FastDigest restriction enzymes, Phusion DNA polymerase and Rapid DNA ligation kit (Thermo Scientific) were used according to the manufacturer's instructions. Plasmids were purified using a Macherey Nagel plasmid purification kit according to the manufacturer's protocol. To extract plasmids from *S. aureus*, an extra step was included to the established protocol: after resuspension in buffer A1 and previous to the addition of A2, the mixture was subjected to physical lysis using glass beads (FastPrep cell disrupter; 6 m s^{-1}, 40 seconds). Plasmids were transformed in *Escherichia coli* by electroporation (1 mm cuvette; 200Ω, 25μF, 1250V; Gene Pulser X-Cell electroporator). *S. aureus* competent cells were generated as previously described (Valle *et al.*, 2003). All plasmids, but pLAC-p03, were transformed in *Staphylococcus aureus* by electroporation (1mm cuvette; 100Ω, 25μF, 1250V; Gene Pulser X-Cell electroporator). All constructed plasmids were confirmed by Sanger sequencing.

Genomic DNA was extracted from 1 ml of overnight cultures grown in antibiotic-free TSB medium using GenElute Bacterial Genomic DNA Kit (Sigma) according to the manufacturer's protocol.

Moving pLAC-p03 to RN4220

Plasmids extracted from *S. aureus* LAC strain (pLAC-p01 and pLAC-p03) were transformed into the laboratory strain RN4220, generating a RN4220 strain

containing both plasmids, pLAC-p01 and pLAC-p03. 80α phage lysate was generated as specified in (Chen *et al.*, 2015). A culture of RN4220 pLAC-p01 pLAC-p03 was infected with the 80α lysate at a multiplicity of infection of 0.1 until complete lysis. RN4220 pLAC-p01 pLAC-p03 lysate was filtered (0.2 μm) and used to infect RN4220 wild type cells. Transductant selection was made in media containing 100 mM sodium citrate and 0.05 mM cadmium as selective agent. pLAC-p03 presence in Cd-resistant transductants was checked by plasmid extraction followed by PCR-amplification using oligonucleotides 365 and 366. The absence of pLAC-p01 was confirmed using primers 280 and 282.

Construction of pEMPTY::sgRNA2

The shuttle vector pEMPTY was constructed as follows. The *cas9* gene and the transcriptional terminator for bacteriophage T7 RNA polymerase were PCR-amplified from pFREE-Amp using primers 191 and 473 (Lauritsen *et al.*, 2017). The tetracycline-inducible promoter, $P_{xyl/tetO}$, was amplified using the pRMC2 plasmid as template and oligonucleotides 119 and 195 (Corrigan and Foster, 2009). A pCN38 backbone was amplified using oligonucleotides 474 and 189 (Charpentier *et al.*, 2004). Then, in-Fusion cloning (In-Fusion® HD Cloning Kit, Takara) was used to combine the three fragments described above. The resulting plasmid was linearized with ApaI and EheI and ligated to the temperature-sensitive origin of replication $pE194_{ts}$-ori amplified from pMAD (Arnaud *et al.*, 2004) using oligonucleotides 257 and 259, generating the thermo-sensitive plasmid pEMPTY.

The module containing the strong constitutive promoter SP01 directing the expression levels of the chimeric molecule composed of guide RNA 2 fused to the transactivating RNA (tracrRNA) was amplified from pFREE-Amp (Lauritsen *et al.*, 2017) using oligonucleotides 448 and 475. The amplification product was cloned into pJET1.2, digested with SmaI and AscI, gel purified and cloned into pEMPTY generating pEMPTY::sgRNA2.

sgRNA site identification and database generation

The sequences of 358 fully sequenced staphylococcal plasmids were retrieved from the RefSeq database (O'Leary *et al.*, 2016) (release 83). From those plasmids, sequences corresponding to origins of replication and origins of transfer (*oriTs*) were identified through conventional alignments using BLASTn against previously annotated *ori* sequences in the RefSeq files (NC_008356 (pLNU plasmids), NC_001995 (pSK plasmids), NC_001393 (pT181), NC_006974 (pACK6), NC_005566 (pSK639), NC_005243 (pC223) and NC_005127 (pUB101)), and previously identified *oriTs* (O'Brien *et al.*, 2015). Sequences corresponding to *rep* and *mob* genes were extracted using HMMER3 (Eddy, 2011) and MOBscan software (Garcillán-Barcia *et al.*, 2020). Specific plasmid-related sequences previously described in the scientific literature (Lozano *et al.*, 2012) were also considered.

The online platform *sgRNA scorer 2.0* (Chari *et al.*, 2017) was then used to predict and identify sgRNA activity on the previous plasmid-related sequences database. A score greater than or equal to 0.5, according to the platform classier, and virtual capability of action over 10 or more plasmids were the requirements established for

a target site to be selected. A database containing all this information can be found in Table S4.

Plasmid curing from *S. aureus*

S. aureus strains to be cured were transformed with 1 µg of pEMPTY::sgRNA2 plasmid. Recombinant bacteria were selected on solid media supplemented with 20 µg ml^{-1} Cm after 48-72 hours of incubation at 28 °C and pEMPTY::sgRNA2 presence was confirmed by PCR using primers 217 and 235. Positive clones were propagated in 5 ml of TSB containing 20 µg ml^{-1} Cm for 8 hours (200 rpm, 28 °C). 100 µl of these cultures were used to inoculate 15 ml of fresh TSB medium supplemented with 20 µg ml^{-1} Cm and 100 ng ml^{-1} anhydrotetracycline. After incubation for 16 hours at 200 rpm, 28 °C, serial dilutions of the cultures were plated on antibiotic-free TSA medium and also, TSA containing a selective agent (Cd, Ery or Lin) upon which plasmid-located genes are known to confer resistance. The presence/absence of natural plasmids was doubled checked in colonies isolated on the general medium by streaking them on general and selective medium and PCR-amplification. The presence of plasmids pMW2, pLAC-p03, pN315, pUR2940, pUR1902 and pUR3912 was checked using primers 365 and 366; presence of pUR1841 was checked using primers 253 and 255; presence of pUR2355 was checked using primers 437 and 438.

To remove pEMPTY::sgRNA2, a natural plasmid-free colony was grown in 15 ml of non-selective TSB medium for 16 hours at 37 °C under shaking conditions. Serial dilutions of the culture were made and plated on antibiotic-free TSA medium and medium containing 20 µg ml^{-1} Cm. Colonies obtained on antibiotic-free TSA were

doubled checked for pEMPTY::sgRNA2 absence by streaking them on general and selective medium and PCR-amplification (primers 217 and 235).

Fitness evaluation

Overnight cultures were diluted to an OD_{595nm} of 0.1 in fresh TSB medium. 5 µl of the adjusted cultures were used to inoculate 195 µl of fresh TSB medium using 96 multi-well plates (Thermo Scientific). Growth kinetics were assayed using a Synergy H1 Hybrid Multi-Mode Microplate Reader (Biotek). No-selective TSB medium was used in all cases. Growth data (OD_{595nm}) was collected every 15 minutes for 24 hours at 37 °C under shaking conditions (fast orbital shaking: 425 cpm). 10 technical replicates were used for each of the tested strains. All the experiments were repeated at least three times.

Two parameters were extracted from growth dynamics: the area under the growth curve (culture total growth), and the duration of the lag phase (Hall *et al*., 2014). The mathematical procedure followed to calculate the area under the growth curve consisted in integrating the OD_{595nm} values generated from time 0 to 6.5 hours for each culture. To determine the length of the lag phase, the maximum slope of the growth curve based on 5 consecutive time points was considered as the entrance in the exponential phase of growth.

Evolution assays

Three plasmid-carrying clones selected from three independent transformation rounds of the parental plasmid-free strain MW2 PF_{t0} with plasmids $pMW2_{t0}$, $pUR2940_{t0}$, $pN315_{t0}$ and $pLAC\text{-}p03_{t0}$ were propagated in 3 ml of antibiotic-free TSB medium and every 12 hours, 3 µl of each culture were transferred to 3 ml of fresh TSB medium for a total duration of 35 days. At the end of the evolution process, cultures were plated on TSA medium containing 0.05 mM cadmium and a resistant colony was selected for each culture.

Evolution of strain MW2 PF_{t0} transformed with evolved $pUR2940_{t35}$ plasmids and strain C2940 was performed as described above but for a period of 14 days.

Monitoring of plasmid carrying cells during the evolution assays

Every 7 days, evolving cultures were serially diluted and plated on TSA and TSA containing 0.05 mM Cd or 10 µg ml^{-1} Ery in the case of C2940 strain. According to the number of resistant colonies, the percentage of plasmid-carrying colonies was calculated. Also, PCR-amplification (primers 365 and 366) was randomly performed to discard the emergence of spontaneous mutants on TSA supplemented with Cd and ensure plasmid presence.

Quantification of plasmid copy number

Plasmid copy number was determined by quantitative polymerase chain reaction (qPCR) using a QuantStudio 12K Flex Real-Time PCR System (Life Technologies) and Power SYBR™ Green PCR Master Mix (Applied Biosystems™) at a final DNA concentration of 0.2 ng μl^{-1}. For that, DNA extraction was performed with the GenElute Bacterial Genomic DNA Kit (Sigma), quantified and 1 µg of genomic DNA was digested with 1µl of FastDigest EcoRI for 2 hours at 37 ˚C. EcoRI was inactivated at 80 ºC for 15 min. qPCR was performed for each extraction in triplicate. The amplification conditions were: initial denaturation for 10 min at 95 ºC, followed by 40 cycles of denaturation for 15 s at 95 ºC, annealing (Table S3-qPCR) and extension for 1 min at 57 ºC. After the amplification was complete, a melting curve analysis was performed by cooling the reaction to 60 ºC and then heating slowly to 95 ºC. Primers used for analysis are described in Table S3-qPCR. To calculate the copy number of plasmid per chromosome, the following formula (Millan *et al.*, 2014) was used:

$$cn = \frac{(1 + Ec)^{Ctc}}{(1 + Ep)^{Ctp}} \text{ x } \frac{Sc}{Sp}$$

where cn is the plasmid copy number per chromosome, Sc and Sp are the sizes of the chromosomal and plasmid amplicons (in bp), Ec and Ep are the efficiencies of the chromosomal and plasmid qPCRs (relative to 1) and Ctc and Ctp are the threshold cycles of the chromosomal and plasmid reactions, respectively.

To calculate primer efficiency, serial dilutions of the MW2 wild type EcoRI digested genomic DNA were used to create a standard curve for each pair of primers.

The first point of the curve was the dilution 10^{-2}. Three technical replicates were made for each point. The average cycle threshold (Ct) was obtained for each point and plotted against the $\log_{10}$ of each sample dilution. The slope of the regression was obtained and the efficiency of the primers was calculated using the following formula (San Millan *et al.*, 2014):

$$\text{Efficiency (\%)} = (10^{-\frac{1}{\text{Slope}}} - 1) \text{ x } 100$$

Next-generation sequencing and data processing

Deep sequencing on DNA samples was performed by MicrobesNG (Birmingham, UK) using Illumina technology. Genome assembly and plasmid reconstruction were performed with PLACNETw (Vielva *et al.*, 2017; de Toro *et al.*, 2020). Short-read sequence data were mapped to reference strain *S. aureus* MW2 (NC_003923.1) or reference plasmid pUR2940 (HF583292.1) by using Snippy (v4.3.6) (https://github.com/tseemann/snippy). Genomes and variant calling files were visualized using IGV (Robinson *et al.*, 2011). BLAST Ring Image Generator (BRIG) was used for comparing plasmid variants (Alikhan *et al.*, 2011).

Statistics

Statistical analyses were performed with the GraphPad Prism 5.01 program. A one-way analysis of variance combined with the Bonferroni multiple *post hoc* test was used to analyze statistical significance in the study of the initial fitness cost after MW2

PF_{t0} transformation with different plasmids. A nonparametric Mann-Whitney U test was used to assess differences in the analysis of plasmid copy number and fitness cost. Differences with a *P* value < 0.05 were considered significant. Box plots show median (horizontal black lines), lower and upper quartiles, and extreme values (whiskers).

Results

Curing of naturally occurring plasmids of *S. aureus* using a CRISPR-Cas9 system

In order to develop an efficient plasmid curing tool for *S. aureus*, we constructed a plasmid that enables CRISPR-Cas9 precise targeting of *S. aureus* plasmids DNA. For that, the *cas9* gene was cloned downstream the tetracycline-inducible promoter $P_{xyl/tetO}$ inside a pCN38 backbone in which the replication origin was changed by the temperature-sensitive origin of replication $pE194_{ts}$-ori, leading to a thermo-sensitive plasmid that we named pEMPTY (**Figure S1**). Then, to identify guide RNAs that target the majority of natural plasmids found in *S. aureus*, we searched for fully sequenced plasmids from the *Staphylococcus* genus in NCBI RefSeq database. Replication origins, oriTs and *rep* and *mob* genes, which codify replication-initiatiation proteins and relaxases respectively, were queried using the *sgRNA scorer 2.0* online platform (Chari et al., 2017) to predict guide RNA activity on input sequences. Only those target sequences that were present in ten or more plasmids with a score equal to or greater than 0.5 were selected (Table S1; included as an appendix in digital format). From these, the sequence targeted by guide RNA 2 (gRNA2) was selected since it was found in 56% of *S. aureus* plasmids. Then, gRNA2 was fused to the trans-activating RNA (tracrRNA) and cloned under control of the constitutive strong promoter SP01 in pEMPTY plasmid leading to the final thermo-sensitive plasmid curing tool pEMPTY::sgRNA2 (**Figures 1A and S1**).

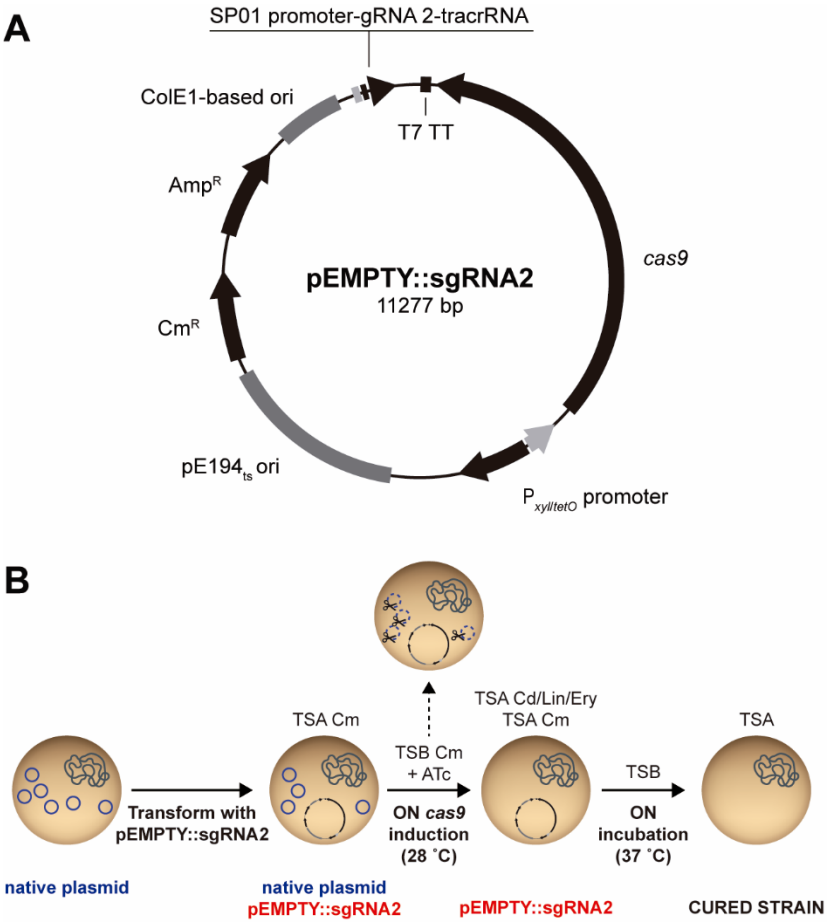

Figure 1. Plasmid map of pEMPTY::sgRNA2 and plasmid curing process in *S. aureus* using the pEMPTY::sgRNA2 system. A. The shuttle vector pEMPTY::sgRNA2 contains the *cas9* gene downstream the tetracycline-inducible promoter $P_{xyl/tetO}$ to guarantee regulation of curing functionality, the temperature-sensitive origin of replication $pE194_{ts}$-ori that allows the loss of the vector system by increasing the temperature to 37 ºC, and a small guide RNA, consisting of the guide RNA number two that targets *S. aureus* plasmids fused to the scaffold tracrRNA sequence, downstream the constitutive SP01 promoter. B. pEMPTY::sgRNA2 is transformed into a *S. aureus* strain containing the target plasmid for curing and transformants are selected on medium containing chloramphenicol as selective agent. Cells are transferred into liquid TSB medium containing chloramphenicol and anhydrotetracycline (ATc) and the culture is incubated overnight at 28 ºC to allow *cas9* gene expression and thus, cleavage of target plasmids directed by guide RNA 2. The culture is plated on TSA containing chloramphenicol and antibiotic (cadmium, lincomycin or erythromycin) selective TSA and cured cells are identified by antibiotic sensitivity and PCR screening. A colony of cured cells is incubated overnight in non-selective TSB medium at 37 ˚C and the culture is plated on non-selective TSA and incubated overnight at 37 ˚C to select a cured colony that has lost plasmid pEMPTY::sgRNA2.

To test the efficiency of our plasmid-curing system, we firstly transformed the *S. aureus* RN4220 strain with seven unrelated plasmids of similar size and diverse origins targeted by sgRNA2 (pMW2, pUR2940, pN315, pLAC-p03, pUR1902, pUR3912 and pUR1841). Also, plasmid pUR2355 was used as a control of plasmid curing unavailability because it does not contain the gRNA2 target DNA sequence. *S. aureus* RN4220 plasmid bearing strains were transformed with pEMPTY::sgRNA2, *cas9* expression was induced with anhydrotetracycline and bacteria were plated on general TSA medium and TSA containing a selective agent to calculate curing rates (**Figure 1B**). All *S. aureus* RN4220 derivatives but the control strain bearing pUR2355 became sensitive to the selective agent with plasmid curing efficiencies that ranged between 96-100% of the total population (Table 4).

Next, we evaluated the efficacy of pEMPTY::sgRNA2 for curing plasmids in their original wildtype strains where transformation efficiencies can be compromised. In all the strains, our system showed plasmid curing rates similar to those previously obtained in the laboratory strain RN4220 (Table 4).

Altogether, these results demonstrate that pEMPTY::sgRNA2 can be efficiently used for curing of naturally occurring plasmids from *S. aureus* isolates of diverse origins. The replacement of sgRNA2 by a different guide RNA would allow the removal of those plasmids that are not targeted by sgRNA2.

Table 4. Plasmid curing efficiencies achieved with the use of pEMPTY::sgRNA2

Strain	Curing efficiency (%)
RN4220 pMW2	99.9
RN4220 pUR2940	99.7
RN4220 pN315	100
RN4220 pLAC-p03	100
RN4220 pUR1902	99.9
RN4220 pUR3912	98.3
RN4220 pUR1841	99.9
RN4220 pUR2355[a]	0
MW2	100
C2940	96.1
N315	98
LAC	96.1
C1902	100
C3912[b]	Killed
C1841	100
C2355[a]	0

[a] plasmid pUR2355 does not contain the guide RNA 2 target DNA sequence

[b] plasmid pUR3912 integrated in the chromosome

Evaluation of the fitness cost and evolutionary adaptation associated with plasmid carriage in *S. aureus*

The pEMPTY::sgRNA2 plasmid-curing tool enables to approach the study of the fitness of clones with and without a particular plasmid and also, it permits to construct new bacterium-plasmid associations. Thus, aiming to investigate the fitness cost produced by different plasmids in a cured *S. aureus* strain, we transformed the plasmid-free derivative of *S. aureus* MW2 strain (MW2 PF_{t0}) with plasmids pUR2940, pN315 and pLAC-p03 (**Figures 2A and S2**). These plasmids are from *S. aureus* strains representative of livestock-associated (C2940), hospital (N315) and community (LAC) environments. Also, MW2 PF_{t0} was transformed with its own original pMW2 plasmid as a control of neutral fitness cost (**Figures 2A and S2**). Three plasmid-carrying clones selected from three independent transformation rounds were studied in each case (**Figure 2B**). Analysis of the initial fitness cost, measured as the differences in both the area under the growth curve and the duration of the lag phase between MW2 PFt_0 and plasmid-bearing clones, revealed that only plasmid pUR2940 caused a significant decrease in the area under the growth curve and also a delay in the lag phase (**Figure 3**).

In order to analyze the evolution of newly acquired plasmids over time in the absence of selection, we propagated the MW2 plasmid-carrying strains in antibiotic-free culture medium for 35 days, diluting the culture (1:1000) every 12 hours, which corresponds to approximately 640 generations of bacterial evolution by the end of

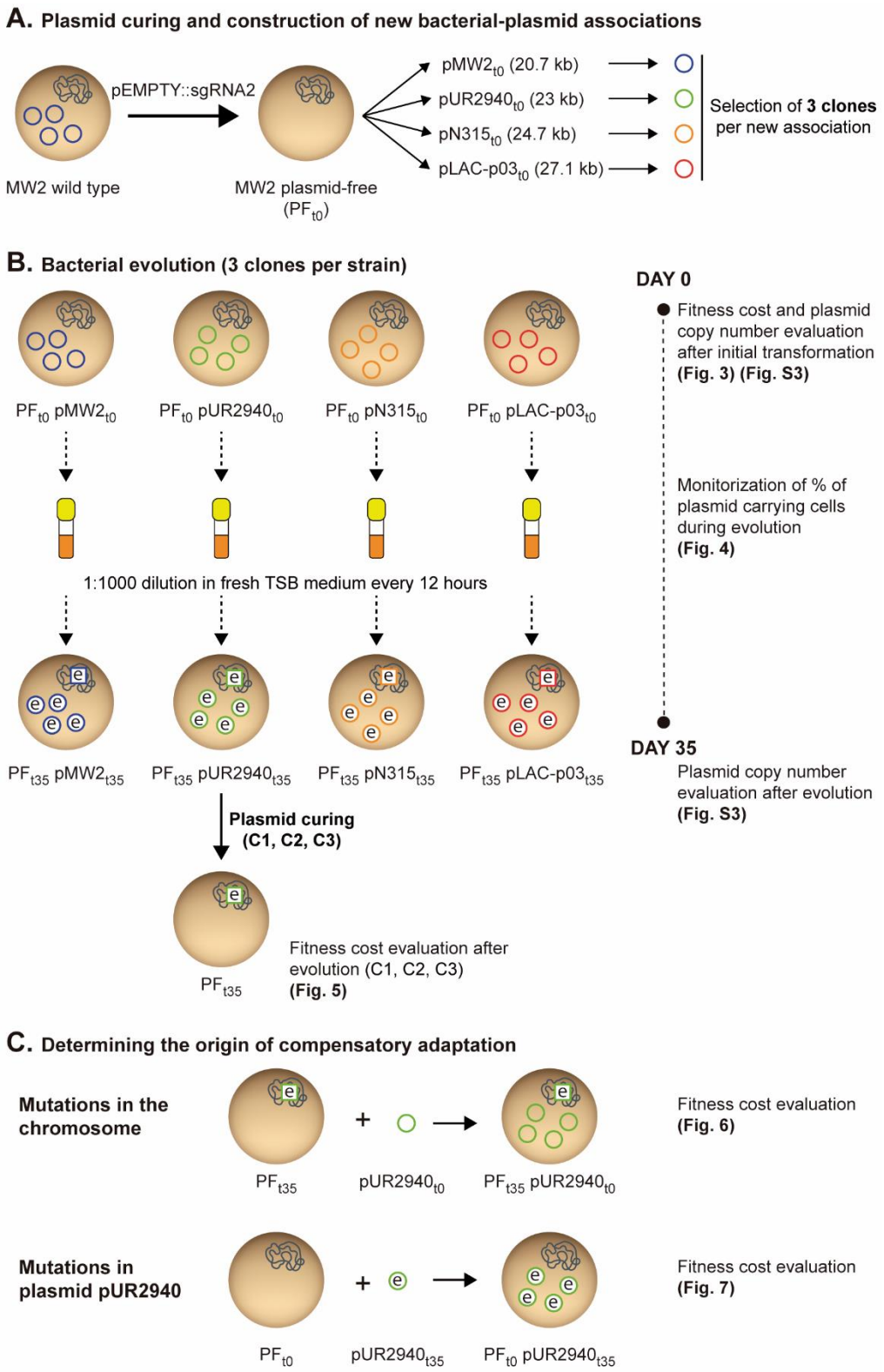

Figure 2. Experimental design of the evolution process of *S. aureus* MW2 plasmid-containing clones and analysis of the compensatory adaptation to plasmid pUR2940.

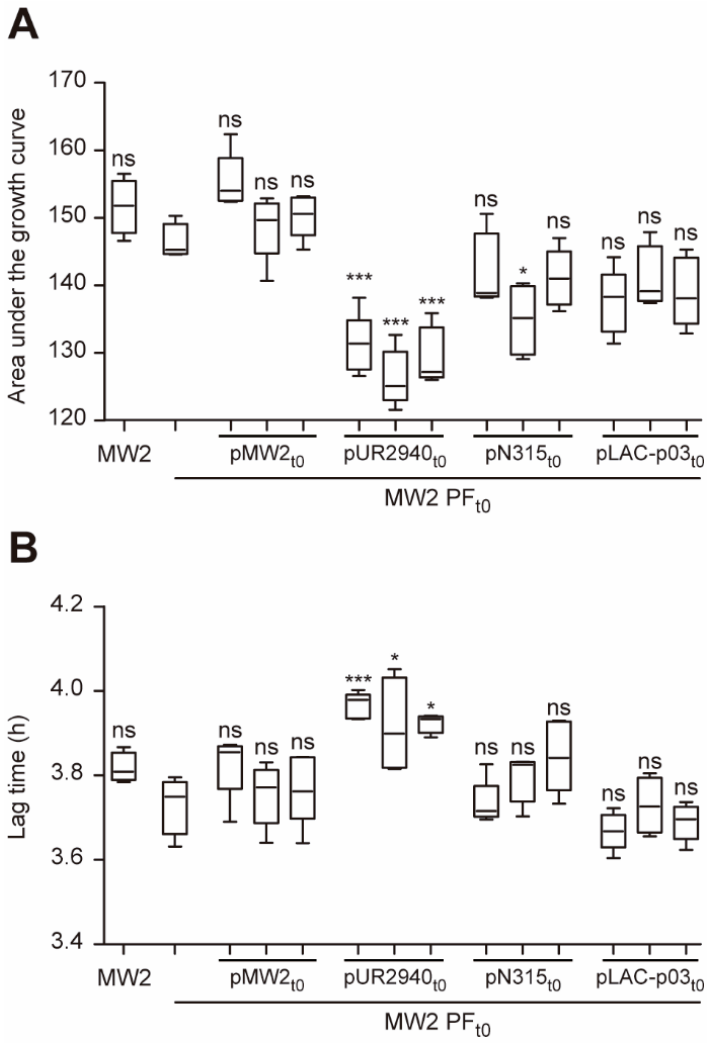

Figure 3. Initial fitness cost after MW2 transformation with plasmids pMW2, pUR2940, PN315 and pLAC-p03. Fitness of plasmid-free MW2 (MW2 PF_{to}) was compared with that of the wild type MW2 strain and MW2 PF_{t0} transformed with plasmids pMW2, pUR2940, pN315 and pLAC-p03 (three independently transformed clones were analyzed). A. The area under the growth curve and B. the duration of the lag phase are shown. Data were collected during growth in TSB medium for 24 hours at 37 ˚C under shaking conditions. Ten technical replicates were used for each of the tested strains and experiments were repeated three times. Plasmid pUR2940 produced a significant cost in cured MW2 strain. Statistical analysis was assessed using a one-way analysis of variance combined with the Bonferroni multiple *post-hoc* test. **P* value < 0.05; ****P* value < 0.001. ns; no significant difference.

the experiment (**Figure 2B**). At day 35, cultures were plated on TSA medium containing 0.05 mM cadmium and one plasmid-bearing clone was isolated from each culture.

Evaluation of the dynamics of plasmid carriage over the 35 days of the experiment showed that whilst the control plasmid pMW2 and also plasmids pN315 and pLAC-p03 were stably maintained by the entire population, the frequency of pUR2940 plasmid-carrying cells rapidly declined, with almost 100% of the population of all three evolved clones being plasmid-free by the end of the assay (**Figure 4**). On the other hand, analysis of the plasmid copy number in all MW2 plasmid-bearing clones at the beginning of the evolution process and also in isolated plasmid-carrying clones at the end of the experiment showed that plasmid copy number did not change during bacterial evolution in all cases (**Figure S3**). Altogether these results showed that, from the three plasmids analyzed, pUR2940 produced an evident cost in MW2 strain that contributed to a decline of the plasmid frequency in the population over time.

Next, to discern whether the pUR2940 plasmid still produced a cost in the small population that carried the plasmid at the end of the evolution process or compensatory adaptation had taken place, pUR2940 was cured in MW2 pUR2940 evolved clones (MW2 PF_{t35} $pUR2940_{t35}$) and fitness of evolved plasmid-bearing clones was compared to that of their respective cured clones (MW2 PF_{t35}) (**Figures 2B and 5A**). Results showed that pUR2940 did no longer produced a cost in two out of the three clones analyzed, indicating that compensatory adaptation had occurred during evolution to overcome the cost associated with pUR2940 carriage (**Figure 5B**).

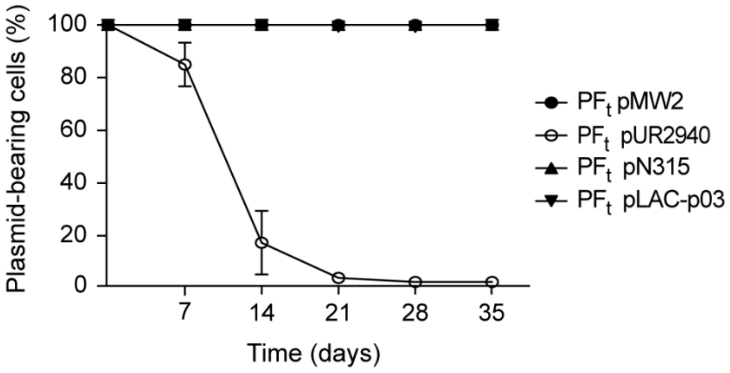

Figure 4. Plasmid stability in the bacterial populating during the evolution process. Proportion of plasmid-bearing bacteria is shown as a function of the evolution time. Every seven days during the evolution process, cultures of the three clones corresponding to each MW2 PF strain transformed with plasmids pMW2, pUR2940, PN315 and pLAC-p03 were plated on TSA medium. 100 colonies from each culture were streaked on TSA and TSA containing 0.05 mM Cd as plasmid selective agent. The number of total and also resistant colonies was counted and the percentage of plasmid carrying colonies was calculated. Data represent the mean and standard deviation of values obtained from the three individual clones analyzed in each case.

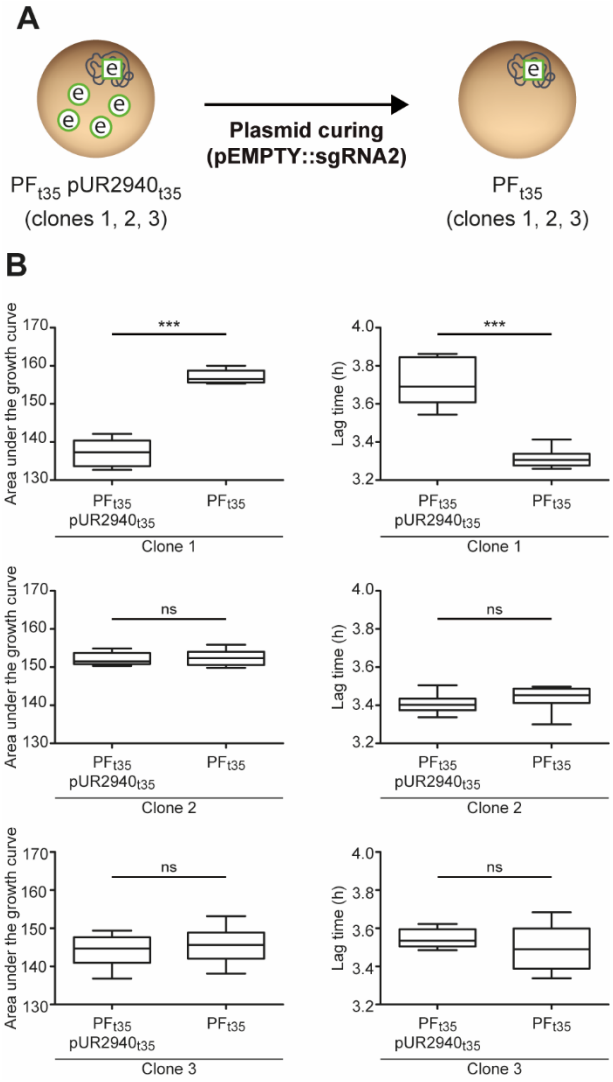

Figure 5. Final fitness cost of plasmid pUR2940 in strain MW2 after the evolution process. A. To elucidate if, in the evolved populations, plasmid pUR2940 still imposed a cost, the three MW2 pUR2940 evolved clones (MW2 PF_{t35} $pUR2940_{t35}$ C1, C2 and C3) were cured, leading to their respective cured clones MW2 PF_{t35} C1, C2 and C3, and fitness was compared. B. The area under the growth curve (left) and the duration of the lag phase (right) are shown. Data were collected during growth in TSB medium for 24 hours at 37 ˚C under shaking conditions. Ten technical replicates were used for each of the tested strains and experiments were repeated three times. The evolved plasmid $pUR2940_{t35}$ still produced a significant cost in the evolved clone 1 (plasmid curing in this clone resulted in an increase in the area under the growth curve and a decrease in the lag time). On the contrary, pUR2940 associated cost was compensated in evolved clones number two and three (plasmid curing in these two clones did not result in a fitness increase). Statistical analysis was assessed using the Mann-Whitney *U* test. ****P* value < 0.001. ns; no significant difference.

Elucidation of the genetic basis of compensation of the cost produced by plasmid pUR2940

To get an insight into the genetic basis of MW2 compensatory adaptation to plasmid pUR2940 present in evolved MW2 PF_{t35} $pUR2940_{t35}$ clones, two strategies were followed (DelaFuente *et al.*, 2020) (**Figure 2C**). First, to analyze the contribution of chromosomal modifications to plasmid cost alleviation, we transformed the evolved cured clones (MW2 PF_{t35}) with the ancestral $pUR2940_{t0}$ plasmid and fitness was compared prior to and after transformation with the plasmid (**Figure 6A**). All three evolved cured clones transformed with ancestral $pUR2940_{t0}$ showed low fitness compared to their non-transformed counterparts (clear decrease in the area under the growth curve and a delay in the lag phase) (**Figure 6B**). These results suggested that chromosomal modifications were not involved in pUR2940 carriage adaptation. Second, to investigate the contribution of pUR2940 plasmid mutations to cost alleviation, we transformed the ancestral MW2 plasmid-free strain, MW2 PF_{t0}, with the different $pUR2940_{t35}$ plasmids isolated from the three evolved MW2 PF_{t35} $pUR2940_{t35}$ clones (**Figure 7A**). pUR2940 isolated from the evolved adapted MW2 PF_{t35} $pUR2940_{t35}$ clones two and three did not produce a cost when transformed in the ancestral MW2 plasmid-free strain (**Figure 7B**). On the contrary, the pUR2940 plasmid variant producing a fitness cost in the evolved MW2 PF_{t35} $pUR2940_{t35}$ clone one, also produced a cost when it was transformed in the ancestral MW2 plasmid-free strain. Altogether, these results suggested that compensatory adaptation to plasmid pUR2940 present in evolved MW2 PF_{t35} $pUR2940_{t35}$ can occur through mutations in plasmid pUR2940 during the evolution process.

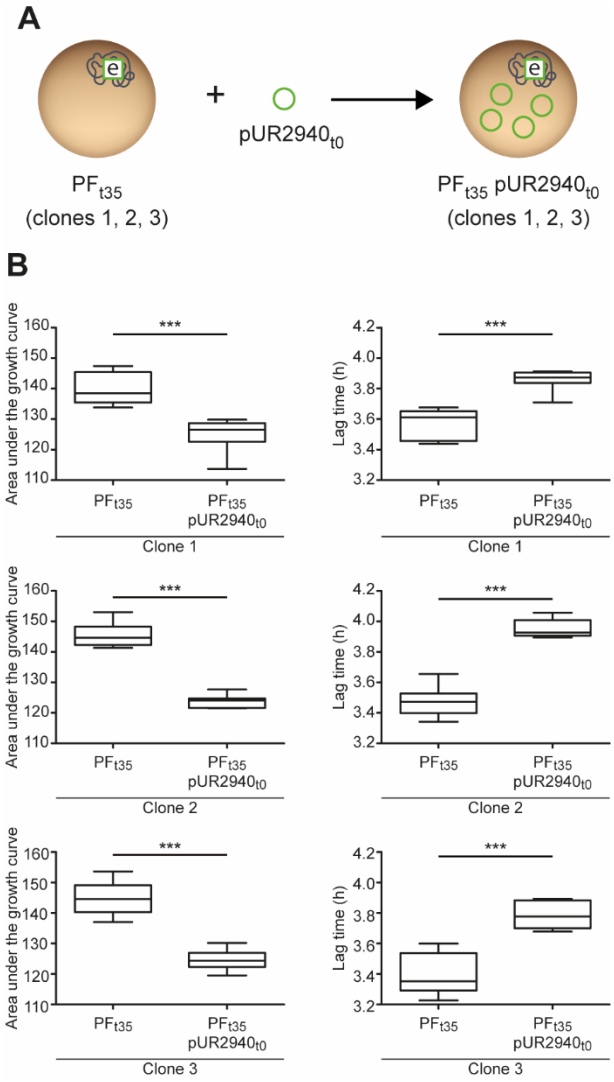

Figure 6. Compensatory adaptation to pUR2940 is not based on changes in the chromosome of host MW2 bacteria. A. The first strategy to analyze the origin of MW2 compensatory adaptation to pUR2940 is depicted. Evolved cured clones MW2 PF_{t35} C1, C2 and C3 were transformed with the ancestral $pUR2940_{t0}$ plasmid. B. Fitness of evolved cured clones MW2 PF_{t35} C1, C2 and C3 was compared with that of transformed clones with ancestral $pUR2940_{t0}$. The area under the growth curve (left) and the duration of the lag phase (right) are shown. Data were collected during growth in TSB medium for 24 hours at 37 ˚C under shaking conditions. Ten technical replicates were used for each of the tested strains and experiments were repeated three times. The ancestral plasmid produced a significant cost in all three cured evolved clones (decrease in the area under the growth curve and increase in the lag time). Statistical analysis was assessed using the Mann-Whitney *U* test. **P* value < 0.05; ***P* value < 0.01; ****P* value < 0.001.

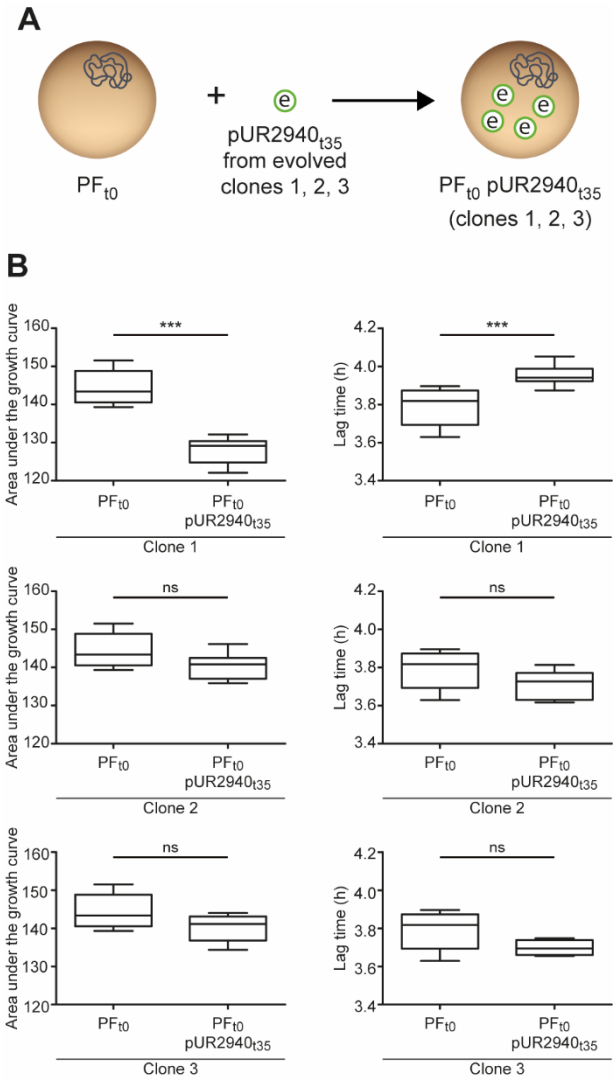

Figure 7. Compensatory adaptation of MW2 to pUR2940 in clones number two and three is due to changes in pUR2940. A. The second strategy to analyze the origin of MW2 compensatory adaptation to pUR2940 is depicted. The ancestral MW2 plasmid-free strain, MW2 PF_{t0}, was transformed with $pUR2940_{t35}$ plasmids isolated from the three evolved MW2 PF_{t35} $pUR2940_{t35}$ clones. B. Fitness of ancestral MW2 PFt_0 was compared before and after transformation with $pUR2940_{t35}$ from evolved clones. The area under the growth curve (left) and the duration of the lag phase (right) are shown. Data were collected during growth in TSB medium for 24 hours at 37 ˚C under shaking conditions. Ten technical replicates were used for each of the tested strains and experiments were repeated three times. $pUR2940_{t35}$ from the non-adapted evolved clone number one produced a significant cost in the ancestral MW2 strain (decrease in the area under the growth curve and increase in the lag time). On the contrary, $pUR2940_{t35}$ from the adapted evolved clones number two and three did not produce a cost in the ancestral MW2 strain. Statistical analysis was assessed using the Mann-Whitney *U* test. **P* value < 0.05; ***P* value < 0.01; ****P* value < 0.001.

To investigate the changes in pUR2940$_{t35}$ responsible for the adaptation, we sequenced the pUR2940$_{t35}$ variants isolated from the two evolved adapted clones and compared the retrieved sequences to that of pUR2940$_{t35}$ isolated from the non-adapted clone and also to the ancestral plasmid pUR2940$_{t0}$. As predicted by the fitness experiments, no mutations were found in the plasmid from the non-adapted clone whilst a fragment of 12,880 bp was lost in both plasmid variants isolated from adapted clones (**Figure 8**). Its loss seemed the result of homologous recombination involving two copies of the insertion sequence IS*Sau10*. This fragment was not found as an independent replicative unit (it includes replication initiation protein genes) and neither was inserted into the host chromosome of the evolved strain. Notably, the lost fragment contains genes that provide resistance to macrolides, lincosamides and streptogramin B (*ermC* and *ermT*), trimethoprim (*dfrK*) and tetracycline (*tetL*). This fragment also includes the MOB$_V$ relaxase gene and thus, the conjugative mobilisation of these evolved plasmid variants would be impaired.

Finally, in order to confirm that this new plasmid variant was indeed completely stable in the MW2 strain, we propagated ancestral MW2 PF$_{t0}$ transformed with pUR2940$_{t35}$ evolved plasmids for fourteen days, following the previously described evolution process (**Figure 2B**). After fourteen days of evolution, the percentage of plasmid carriage was calculated, and as expected, the two new adapted variants pUR2940$_{t35}$ were present in 100% of the population whereas the non-adapted plasmid pUR2940$_{t35}$ was almost lost (4% of plasmid-bearing bacteria). Overall, these results demonstrated that pUR2940 plasmid reorganization is needed to alleviate the cost produced in the MW2 strain.

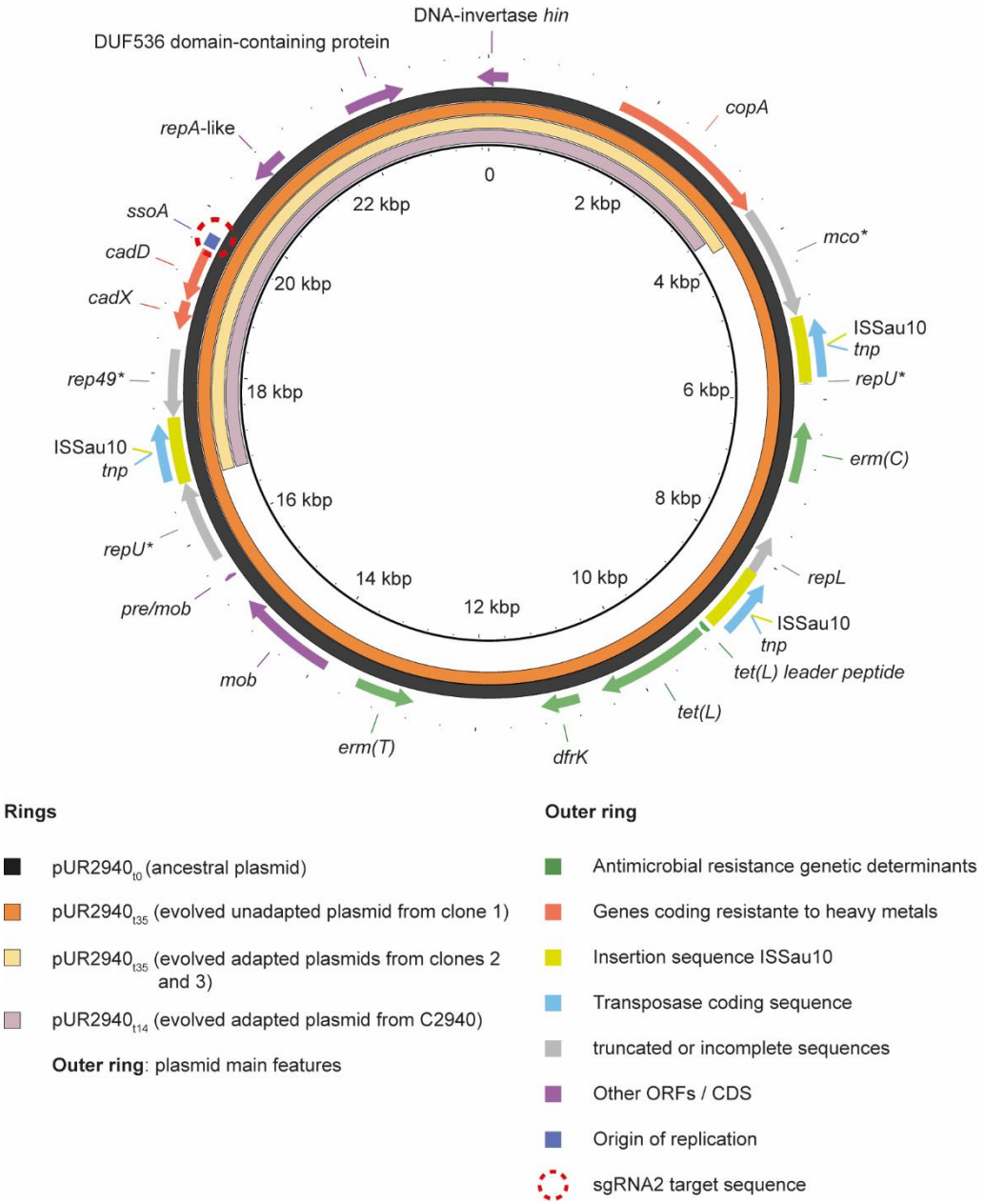

Figure 8. Comparison of the ancestral plasmid pUR2940$_{t0}$, evolved plasmids pUR2940$_{t35}$ from MW2 evolved clones number 1, 2 and 3 and evolved plasmid pUR2940$_{t14}$ isolated from evolved strain C2940. Image visualization was carried out with BLAST Ring Image Generator (BRIG) which shows similarity between the central reference sequence pUR2940$_{t0}$ and the other variants as concentric rings.

pUR2940 also imposes a cost in its natural host that can be compensated via IS*Sau*10 mediated deletion of plasmid antimicrobial resistance genes

The above results indicated that the pUR2940 plasmid produces a noticeable cost in MW2 strain that can be alleviated through plasmid rearrangement when cultured in the absence of antibiotic pressure. Based on this, we wondered whether pUR2940 also imposes a cost in the original *S. aureus* strain (C2940) under conditions in which plasmid genes do not provide any benefit to the host. A comparison of the fitness of C2940 strain and its respective cured derivative, when grown in the absence of selection, confirmed that pUR2940 produces a significant cost in its original host (**Figure 9**). Indeed, when C2940 was propagated in liquid medium without antibiotics for fourteen days, only 4.6% of the cells retained the ancestral plasmid. Given that C2940 strain shows an intrinsic high resistance to cadmium (Gómez-Sanz *et al.*, 2013), we were unable to select cadmium resistant and erythromycin sensitive clones, which would presumably harbor an evolved pUR2940 plasmid. To analyze if reorganized pUR2940 variants appear during C2940 evolution in the absence of selection, a plasmid extraction was performed from the whole evolved culture after fourteen days of propagation in TSB medium and the PCR product of primers 412 and 414 was examined through agarose gel electrophoresis. A band with a size of the expected evolved pUR2940 plasmid was excised and analysed by sequencing, which retrieved data showing a deletion of a fragment similar to the one occurring in pUR2940$_{t35}$ isolated from MW2 evolved adapted clones (**Figure 8**). Hence, these results confirmed the occurrence of pUR2940 reorganization via IS*Sau*10 insertion sequence that leads to the loss of antimicrobial resistance genes when C2940 strain encounters an antibiotic-free environment.

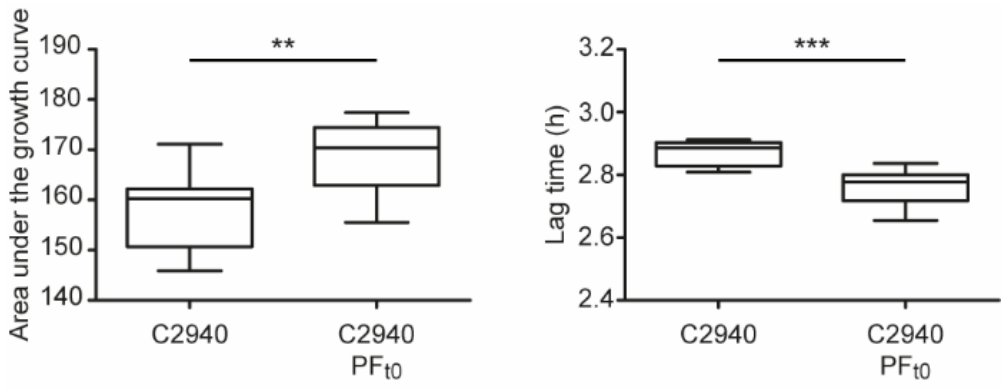

Figure 9. Fitness cost of plasmid pUR2940 in its original host, strain C2940. Fitness of strain C2940 was compared with that of its plasmid-free derivative C2940 PF_{t0}. A. The area under the growth curve and B. the duration of the lag phase are shown. Data were collected during growth in TSB medium for 24 hours at 37 ˚C under shaking conditions. Ten technical replicates were used and experiments were repeated three times. Plasmid pUR2940 produced a significant cost in its original host. Statistical analysis was assessed using the Mann-Whitney *U* test. ***P* value < 0.01; ****P* value < 0.001.

Discussion

Location of genes in plasmids rather than in the chromosome offers benefits to bacteria because it allows higher levels of gene expression, different versions of a gene to coexist in the same cell (heterozygosity) which eases the evolution by increasing the mutation rate; and facilitates the exchange of genes and the acquisition of new capacities (Rodriguez-Beltran *et al.*, 2018). However, the presence of a plasmid also imposes a fitness cost and therefore, the fact that plasmids are so abundant in bacteria living in competitive environments when the selection pressure has disappeared, for instance, a patient after finishing the antibiotic treatment, seems counterintuitive. Most of our current understanding about the fitness cost caused by plasmids has been obtained with bacteria of the *Pseudomonas* genus and it is important to examine whether similar rules govern plasmid evolution in other clinically relevant bacterial species (Millan *et al.*, 2014; San Millan *et al.*, 2014; Harrison *et al.*, 2015). In this study, we have investigated the fitness cost associated with plasmid carriage in clinical isolates of *S. aureus*, where these mobile genetic elements are major agents in the dissemination of multidrug resistance determinants.

The best method to demonstrate the relationship between the presence of the plasmid and fitness cost is the elimination of the plasmid (curing) from the bacterial population. The cost should disappear in cured derivatives and reappear when the plasmid is reintroduced into the cured strain. Plasmid curing has been traditionally performed by prolonged bacterial growth in the presence of chemical and physical agents, some of which introduce mutations in the DNA or interfere specifically with its replication (Lauritsen *et al.*, 2017). The risk of these strategies is that they favor the

accumulation of mutations, something that is incompatible with investigating the molecular basis of plasmid fitness cost. We have addressed this methodological limitation by generating a CRISPR-based tool (the pEMPTY plasmid) that only requires the transformation of a given strain to remove the existing plasmid. In the present study, we have used a guide RNA that targets 56% of the currently known plasmids in *S. aureus*. An easy way to expand the chance of plasmid targeting would be to include additional sgRNA in the pEMPTY plasmid.

We used a clinical *S. aureus* strain in which we removed its native plasmid (plasmid-free *S. aureus* MW2) to simulate the scenario of the physical arrival of a plasmid into a new host. The analysis of the fitness cost produced upon arrival revealed somewhat surprising results showing that two plasmids (pN315 and pLAC-p03) did not cause any noticeable cost. These two plasmids are slightly larger than the native MW2 plasmid and contain a different set of antimicrobial resistance genes. A reasonable explanation for these results is that during the adaptive evolution of *S. aureus* MW2 to its native plasmid, bacteria accumulated chromosomal changes to alleviate the cost associated with plasmid carriage and thus, the introduction of a new plasmid does not require additional co-evolution steps. Besides, pMW2, pN315 and pLAC-p03 encode toxin-antitoxin systems that could prevent plasmid loss even in the absence of selective pressure, while pN315 and pMW2 encode bacteriocins that could provide a competitive advantage to the plasmid-bearing cells. In contrast, plasmid pUR2940 produced a strong fitness cost both to its native host and the new *S. aureus* MW2 PF_{t0} strain. pUR2940 is a multirresistant plasmid isolated from a human methicillin-resistant *S. aureus* of the clonal lineage ST398 that carries several

antibiotic resistance genes that confer protection against macrolides, lincosamin and streptogramin B, trimethoprim and tetracycline, a cadmium resistance determinant and three copies of the IS*Sau*10 insertion sequence (Gómez-Sanz *et al.*, 2013). In the absence of selective pressure, the plasmid was very unstable and less than 1% of the population contained the plasmid after 21 days of growth in non-selecting conditions. Neither toxin-antitoxin systems nor bacteriocins are encoded in pUR2940. Coevolution of the plasmid and the host through serial passages in antibiotic-free medium selected for plasmids that had lost a 12.8 kb plasmid region, flanked by two IS*Sau*10 elements and that comprises all the antibiotic resistance genes. The sequencing results suggest that deletion occurs via intramolecular recombination between two IS*Sau*10 insertion sequences, without subsequent integration in the host chromosome. IS*Sau*10 belongs to the IS*6*/IS*26* family (Harmer and Hall, 2019), which has been shown to be involved in the mobilization of antibiotic resistance genes in Gram-negative bacteria (Harmer *et al.*, 2014; Porse *et al.*, 2016). Thus, alleviation of the plasmid fitness cost comes at the expense of losing all the antibiotic resistance determinants. A question raised by these results is how the deleted region causes such a strong fitness cost to the host. It is unsurprising that antibiotic resistance genes provide a selective advantage in the presence of antibiotics, but it is less clear why their presence is so costly with little or no selective pressure. One possibility is that these genes are expressed at very high levels so that transcription, translation and/or the subsequent interactions between the proteins responsible for antibiotic resistance and cellular networks affect bacterial physiology. Alternatively, it is possible that the transposase encoded by the IS may interact with other mobile genetic elements carried in the bacterial genome and produce a

reduction in bacterial fitness (San Millan and MacLean, 2017). The resulting new evolved plasmid showed no detectable fitness cost, at least with the resolution of the growth measurements used in our study. This plasmid, in the future, might provide a backbone for the entry of a new carriage. The IS*Sau10* copy that remains in the evolved plasmid variants could be a platform to promote cointegration of another molecule also containing an IS*Sau10* copy via the conservative transposition route or homologous recombination. Importantly, results showing that plasmid pUR2940 causes a fitness cost in its native *S. aureus* strain indicate that long-term coevolution between the host and the plasmid has not yet occurred. Also, the fact that strain C2940 harbors the non-evolved pUR2940 plasmid suggests that the selective pressure encountered by this strain in different environments has been high enough to prevent the loss of antimicrobial resistance determinants from the plasmid (Peña-Miller *et al.*, 2015; Wein *et al.*, 2020).

Further investigations using *in vivo* animal models are necessary to confirm that insertion sequence and transposon mediated deletion is a general strategy to reduce the fitness cost of multidrug plasmid carriage in the absence of antibiotics. This knowledge is critical to predict the evolution of plasmids containing insertion sequence elements together with multidrug resistant genes and may have a significant impact on the choice of antibiotic regimens in order to decrease the probability of plasmid persistence.

References

Alikhan, N.F., Petty, N.K., Ben Zakour, N.L., and Beatson, S.A. (2011) BLAST Ring Image Generator (BRIG): simple prokaryote genome comparisons. *BMC Genomics* **12**: 402.

Arnaud, M., Chastanet, A., and Débarbouillé, M. (2004) New vector for efficient allelic replacement in naturally nontransformable, low-GC-content, Gram-positive bacteria. *Appl Environ Microbiol* **70**: 6887–6891.

Baba, T., Takeuchi, F., Kuroda, M., Yuzawa, H., Aoki, K., Oguchi, A., *et al*. (2002) Genome and virulence determinants of high virulence community-acquired MRSA. *Lancet* **359**: 1819–1827.

Baines, S.L., Jensen, S.O., Firth, N., da Silva, A.G., Seemann, T., Carter, G.P., *et al*. (2019) Remodeling of pSK1 family plasmids and enhanced chlorhexidine tolerance in a dominant hospital lineage of methicillin-resistant *Staphylococcus aureus*. *Antimicrob Agents Chemother* **63**: 299.

Carroll, A.C. and Wong, A. (2018) Plasmid persistence: costs, benefits, and the plasmid paradox. *Can J Microbiol.* **64**: 293–304.

Chari, R., Yeo, N.C., Chavez, A., and Church, G.M. (2017) sgRNA Scorer 2.0: a species independent model to predict CRISPR/Cas9 activity. *ACS Synth Biol* **6**: 902–904.

Charpentier, E., Anton, A.I., Barry, P., Alfonso, B., Fang, Y., and Novick, R.P. (2004) Novel cassette-based shuttle vector system for Gram-positive bacteria. *Appl Environ Microbiol* **70**: 6076–6085.

Chen, J., Ram, G., Penadés, J.R., Brown, S., and Novick, R.P. (2015) Pathogenicity island-directed transfer of unlinked chromosomal virulence genes. *Mol Cell* **57**: 138–149.

Corrigan, R.M. and Foster, T.J. (2009) An improved tetracycline-inducible expression vector for *Staphylococcus aureus*. *Plasmid* **61**: 126–129.

DelaFuente, J., Rodriguez-Beltran, J., and San Millan, A. (2020) Methods to study fitness and compensatory adaptation in plasmid-carrying bacteria. In, *Methods in Molecular Biology*. pp. 371–382.

Eddy, S.R. (2011) Accelerated profile HMM searches. *PLoS Comput Biol* **7**: 1002195.

Garcillán-Barcia, M.P., Redondo-Salvo, S., Vielva, L., and la Cruz, de, F. (2020) MOBscan: automated annotation of MOB relaxases. In, *Methods in Molecular Biology*. pp. 295–308.

Gogarten, J.P. and Townsend, J.P. (2005) Horizontal gene transfer, genome innovation and evolution. *Nat Rev Micro* **3**: 679–687.

Gómez-Sanz, E., Kadlec, K., Feßler, A.T., Billerbeck, C., Zarazaga, M., Schwarz, S., and Torres, C. (2013) Analysis of a novel *erm*(T)- and *cadDX*-carrying plasmid from methicillin-susceptible *Staphylococcus aureus* ST398-t571 of human origin. *J Antimicrob Chemother* **68**: 471–473.

Gómez-Sanz, E., Kadlec, K., Feßler, A.T., Zarazaga, M., Torres, C., and Schwarz, S. (2013) Novel *erm*(T)-carrying multiresistance plasmids from porcine and human isolates of methicillin-resistant *Staphylococcus aureus* ST398 that also harbor cadmium and copper resistance determinants. *Antimicrob Agents Chemother* **57**: 3275–3282.

Gómez-Sanz, E., Zarazaga, M., Kadlec, K., Schwarz, S., and Torres, C. (2013) Chromosomal integration of the novel plasmid pUR3912 from methicillin-susceptible *Staphylococcus aureus* ST398 of human origin. *Clin Microbiol Infect* **19**: E519–22.

Haaber, J., Penadés, J.R., and Ingmer, H. (2017) Transfer of antibiotic resistance in *Staphylococcus aureus*. *Trends Microbiol* **25**: 893–905.

Hall, B.G., Acar, H., Nandipati, A., and Barlow, M. (2014) Growth rates made easy. *Mol Biol Evol* **31**: 232–238.

Harmer, C.J. and Hall, R.M. (2019) An analysis of the IS6/IS26 family of insertion sequences: is it a single family? *Microb Genomics* **5**:.

Harmer, C.J., Moran, R.A., and Hall, R.M. (2014) Movement of IS26-associated antibiotic resistance genes occurs via a translocatable unit that includes a single IS26 and preferentially inserts adjacent to another IS26. *mBio* **5**: e01801–14.

Harrison, E. and Brockhurst, M.A. (2012) Plasmid-mediated horizontal gene transfer is a coevolutionary process. *Trends Microbiol* **20**: 262–267.

Harrison, E., Guymer, D., Spiers, A.J., Paterson, S., and Brockhurst, M.A. (2015) Parallel compensatory evolution stabilizes plasmids across the parasitism-mutualism continuum. *Curr Biol* **25**: 2034–2039.

Knight, G.M., Budd, E.L., and Lindsay, J.A. (2013) Large mobile genetic elements carrying resistance genes that do not confer a fitness burden in healthcare-associated meticillin-resistant *Staphylococcus aureus*. *Microbiology* **159**: 1661–1672.

Kuroda, M., Ohta, T., Uchiyama, I., Baba, T., Yuzawa, H., Kobayashi, I., *et al*. (2001) Whole genome sequencing of meticillin-resistant *Staphylococcus aureus*. *Lancet* **357**: 1225–1240.

Lanza, V.F., Tedim, A.P., Martínez, J.L., Baquero, F., and Coque, T.M. (2015) The plasmidome of firmicutes: impact on the emergence and the spread of resistance to antimicrobials. *Microbiol Spectr* **3**: PLAS–0039–2014.

Lauritsen, I., Porse, A., Sommer, M.O.A., and Nørholm, M.H.H. (2017) A versatile one-step CRISPR-Cas9 based approach to plasmid-curing. *Microb Cell Fact.* **16**: 1–10.

Lozano, C., Aspiroz, C., Rezusta, A., Gómez-Sanz, E., Simon, C., Gómez, P., *et al*. (2012) Identification of novel *vga*(A)-carrying plasmids and a Tn*5406*-like transposon in meticillin-resistant *Staphylococcus aureus* and *Staphylococcus epidermidis* of human and animal origin. *Int J Antimicrob Agents* **40**: 306–312.

Lozano, C., Aspiroz, C., Sáenz, Y., Ruiz-García, M., Royo-García, G., Gómez-Sanz, E., *et al*. (2012) Genetic environment and location of the *lnu*(A) and *lnu*(B) genes in methicillin-resistant *Staphylococcus aureus* and other staphylococci of animal and human origin. *J Antimicrob Chemother* **67**: 2804–2808.

Lozano, C., García-Migura, L., Aspiroz, C., Zarazaga, M., Torres, C., and Aarestrup, F.M. (2012) Expansion of a plasmid classification system for Gram-positive bacteria and determination of the diversity of plasmids in *Staphylococcus aureus* strains of human, animal, and food origins. *Appl Environ Microbiol* **78**: 5948–5955.

Lozano, C., Rezusta, A., Gómez, P., Gómez-Sanz, E., Báez, N., Martin-saco, G., *et al*. (2012) High prevalence of *spa* types associated with the clonal lineage CC398 among tetracycline-resistant methicillin-resistant *Staphylococcus aureus* strains in a Spanish hospital. *J Antimicrob Chemother* **67**: 330–334.

McCarthy, A.J. and Lindsay, J.A. (2012) The distribution of plasmids that carry virulence and resistance genes in *Staphylococcus aureus* is lineage associated. *BMC Microbiol* **12**: 1–8.

Millan, A.S., Peña-Miller, R., Toll-Riera, M., Halbert, Z.V., McLean, A.R., Cooper, B.S., and MacLean, R.C. (2014) Positive selection and compensatory adaptation interact to stabilize non-transmissible plasmids. *Nat Commun* **5**: 5208.

Monk, I.R., Tree, J.J., Howden, B.P., Stinear, T.P., and Foster, T.J. (2015) Complete bypass of restriction systems for major *Staphylococcus aureus* lineages. *mBio* **6**: 1–12.

O'Brien, F.G., Eto, K.Y., Murphy, R.J.T., Fairhurst, H.M., Coombs, G.W., Grubb, W.B., and Ramsay, J.P. (2015) Origin-of-transfer sequences facilitate mobilisation of non-conjugative antimicrobial-resistance plasmids in *Staphylococcus aureus*. *Nucleic Acids Res* **43**: 7971–7983.

O'Leary, N.A., Wright, M.W., Brister, J.R., Ciufo, S., Haddad, D., McVeigh, R., *et al*. (2016) Reference sequence (RefSeq) database at NCBI: current status, taxonomic expansion, and functional annotation. *Nucleic Acids Res* **44**: D733–D745.

Peng, H.L., Novick, R.P., Kreiswirth, B., Kornblum, J., and Schlievert, P. (1988) Cloning, characterization, and sequencing of an accessory gene regulator (*agr*) in *Staphylococcus aureus*. *J Bacteriol* **170**: 4365–4372.

Peña-Miller, R., Rodríguez-González, R., MacLean, R.C., and San Millan, A. (2015) Evaluating the effect of horizontal transmission on the stability of plasmids under different selection regimes. *Mob Genet Elements* **5**: 29–33.

Phillips, G. and Funnell, B.E. (2004) Plasmid Biology. American Society for Microbiology.

Porse, A., Schønning, K., Munck, C., and Sommer, M.O.A. (2016) Survival and evolution of a large multidrug resistance plasmid in new clinical bacterial hosts. *Mol Biol Evol* **33**: 2860–2873.

Robinson, J.T., Thorvaldsdóttir, H., Winckler, W., Guttman, M., Lander, E.S., Getz, G., and Mesirov, J.P. (2011) Integrative genomics viewer. *Nat Biotechnol* **29**: 24–26.

Rodriguez-Beltran, J., Hernandez-Beltran, J.C.R., DelaFuente, J., Escudero, J.A., Fuentes-Hernandez, A., MacLean, R.C., *et al*. (2018) Multicopy plasmids allow bacteria to escape from fitness trade-offs during evolutionary innovation. *Nature Ecology & Evolution* **2**: 873–881.

San Millan, A. and MacLean, R.C. (2017) Fitness costs of plasmids: a limit to plasmid transmission. *Microbiol Spectr* **5**: 1–12.

San Millan, A., Heilbron, K., and MacLean, R.C. (2014) Positive epistasis between co-infecting plasmids promotes plasmid survival in bacterial populations. *ISME J* **8**: 601–612.

Ubeda, C., Barry, P., Penadés, J.R., and Novick, R.P. (2007) A pathogenicity island replicon in *Staphylococcus aureus* replicates as an unstable plasmid. *Proc Natl Acad Sci USA* **104**: 14182–14188.

Valle, J., Toledo-Arana, A., Berasain, C., Ghigo, J.-M., Amorena, B., Penadés, J.R., and Lasa, I. (2003) SarA and not sigmaB is essential for biofilm development by *Staphylococcus aureus*. *Mol Microbiol* **48**: 1075–1087.

Vielva, L., De Toro, M., Lanza, V.F., and De La Cruz, F. (2017) PLACNETw: a web-based tool for plasmid reconstruction from bacterial genomes. *Bioinformatics* **33**: 3796–3798.

Voyich, J.M., Braughton, K.R., Sturdevant, D.E., Whitney, A.R., Saïd-Salim, B., Porcella, S.F., *et al*. (2005) Insights into mechanisms used by *Staphylococcus aureus* to avoid destruction by human neutrophils. *J Immunol* **175**: 3907–3919.

Vogwill, T. and MacLean, R.C. (2015) The genetic basis of the fitness costs of antimicrobial resistance: a meta-analysis approach. *Evol Appl* **8**: 284–295.

Wein, T., Wang, Y., Hülter, N.F., Hammerschmidt, K., and Dagan, T. (2020) Antibiotics interfere with the evolution of plasmid stability. *Curr Biol* **30**: 1–7.

Supplementary information

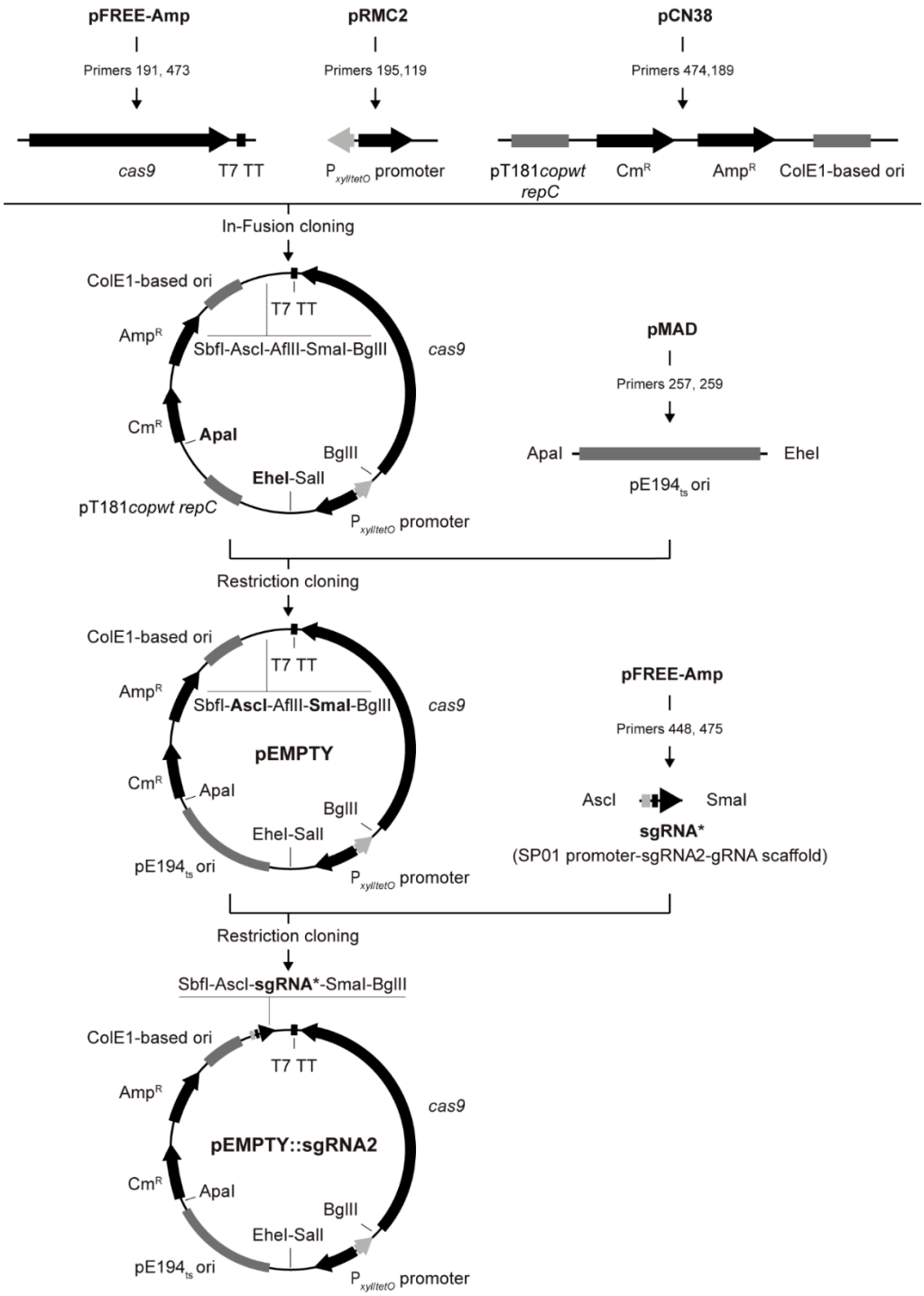

Figure 1. Schematic representation of construction of the pEMPTY::sgRNA2 plasmid.

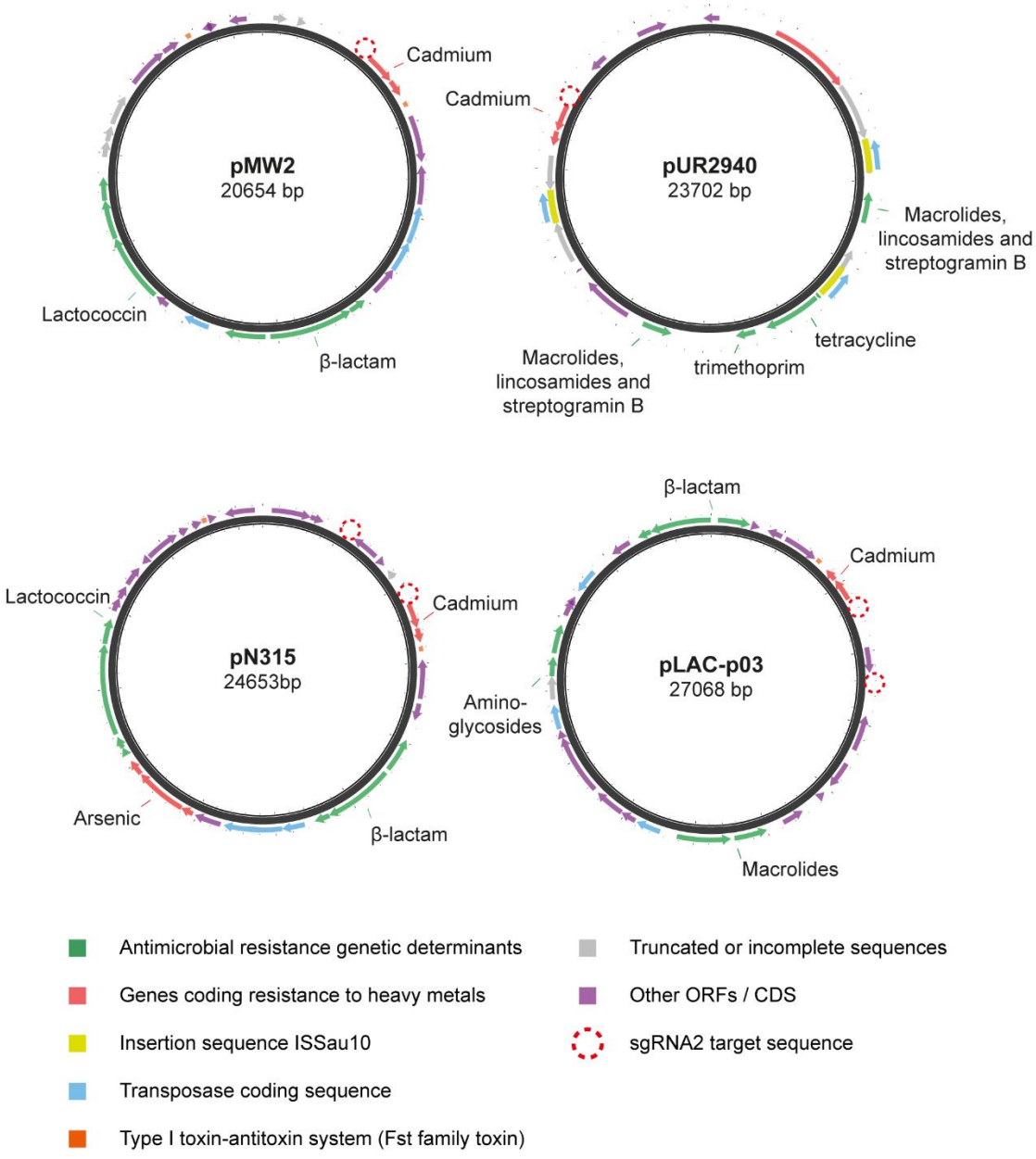

Figure S2. Maps of plasmids pMW2, pUR2940, pN315 and pLAC-p03. Images were generated with the BLAST Ring Image Generator (BRIG) using plasmid sequences retrieved from the NCBI RefSeq database.

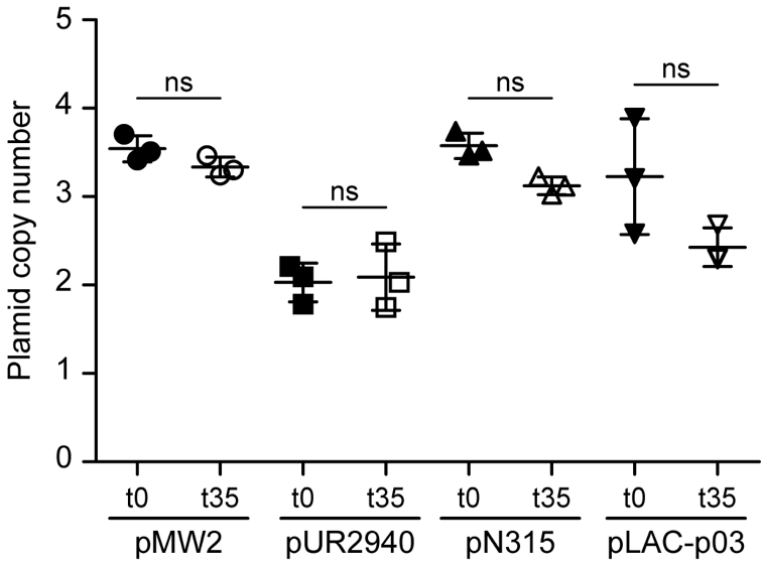

Figure S3. Plasmid copy number at day 0 and day 35 of the evolution process. Number of pMW2, pUR2940, pN315 and pLAC-p03 copies per cell in the three ancestral MW2 transformed clones (day 0) and the three MW2 plasmid-carrying evolved clones (day 35) were determined by qPCR. Data represent the mean and standard deviation of values obtained from the three individual clones analyzed in each case. Experiments were carried out in triplicates. Statistical analysis was carried out using a Mann-Whitney *U* test. ns; no significant difference.

CHAPTER III

Synergistic antibacterial effect of antibiotics and engineered pathogenicity islands carrying CRISPR on *Staphylococcus aureus*

Summary

Staphylococcus aureus continues to cause life-threatening infections in both hospital and community settings. Bacteria from this species have become increasingly resistant to antibiotics, especially β-lactams and aminoglycosides, and their infections are, in many cases, untreatable. With the aim of exploring a novel therapeutic approach, we choose a modified *Staphylococcus aureus* Pathogenicity Islands (SaPIs) carrying a CRISPR-Cas9 module to improved antibiotic treatment both *in-vitro* and *in-vivo*. We generated the recombinant SaPIs carrying a constitutive CRISPR-Cas9 system using homology recombination in yeast. The synthetic SaPI-elements were tested in combination with ceftaroline, linezolid, vancomycin and daptomycin to inactivate *S. aureus*. Results showed a synergistic effect between $SaPI_{CRISPR}$ and linezolid, demonstrating the potential of this association to combat *Staphylococcus*-mediated infections. Based on these results, we propose $SaPI_{CRISPR}$ as a promising candidate to administered simultaneously with antibiotics to combat persistent or antibiotic-resistant infections.

Introduction

The emergence of multidrug-resistant pathogens and the subsequent decrease of antibiotics effectiveness is a global health issue. The rapid dissemination of antimicrobial-resistant strains is due to the widespread use of antibiotics and the subsequent strong selective pressure bacteria are subjected to, especially in livestock and clinical-related facilities (Levy and Bonnie, 2004).

Development of alternative treatment modalities has become one of the highest priorities of modern medicine. Bacteriophages, or phages, are viruses that invade bacterial cells. Typically, they consist of an outer protein hull enclosing genetic material. Some phages, known as lytic, destroy their target bacteria by replicating inside and, in the process of releasing mature virion particles, lysing the host cell (Rohwer and Segall, 2015). These phages are similar to antibiotics in that they have antibacterial activity. Theoretically, phages present some advantages over antibiotics because they can be used against antibiotic-resistant strains and non-growing bacteria (e.g. those found inside a biofilm). Moreover, phages are taxa specific and, therefore, dysbiosis and chances of developing secondary infections are avoided (Sulakvelidze, 2005; Del Pozo *et al.*, 2007; Harada *et al.*, 2018). Nevertheless, phage therapy also has some drawbacks. Phages can, via generalized transduction, mobilize bacterial resident genes, such as antibiotic resistance or virulence determinants, and the possibility of lysogenization may render the culture immune to future treatments with the same or related phages (Penadés *et al.*, 2015; Bondy-Denomy *et al.*, 2016).

Mobile pathogenicity islands (PIs) are phage satellites that maintain an intimate relationship with certain bacteriophages whose lifecycles they parasite. Following

infection by a helper phage or SOS induction of a helper prophage, the PI genome excises from the bacterial chromosome, using PI-coded integrase (*int)* and excision functions (*xis*) (Úbeda *et al.*, 2003; Mir-Sanchis *et al.*, 2012), it replicates extensively using its own replicon (Úbeda, Barry, *et al.*, 2007), and then, it is efficiently packaged into infectious particles composed of phage virion proteins (Tallent *et al.*, 2007; Tormo *et al.*, 2008; Quiles-Puchalt *et al.*, 2014). Some SaPIs encode capsid morphogenesis functions that remodel the phage capsid to fit their smaller genomes (Úbeda, Maiques, *et al.*, 2007; Carpena *et al.*, 2016) while others simply use full-size phage capsids (for a recent review, see (Novick *et al.*, 2010; Penadés and Christie, 2015). SaPIs cannot replicate in the absence of the helper phage. This is a key issue because it restricts the amount of infected bacteria to the initial number of SaPI particles administered but at the same time limits the mobilization of genes among the microbial population (Penadés and Christie, 2015). Furthermore, because no interference mechanisms between SaPIs have been described up to date, several rounds of treatment using the same SaPI may be applied (Penadés and Christie, 2015).

Staphylococcus aureus has been listed by the World Health Organization as a species for which new antibiotics are urgently needed (Mulani *et al.*, 2019). Traditional antibiotic treatment for *S. aureus*-associated infections includes methicillin and vancomycin. However, since the rise of methicillin and vancomycin-resistant strains, their use has been compromised (Chambers and DeLeo, 2009). Alternatives, ranging from the discovery of new antimicrobials to the combined used of antibiotics with other biological agents, such as phages have already been proposed

(Tacconelli *et al.*, 2018; Kebriaei *et al.*, 2020). Moreover, based on the potential benefits os SaPI usage in phage therapy strategies, the group of R. Novick recently proposed the use of modified pathogenicity islands as alternative anti-staphylococcal therapeutic agents (Ram *et al.*, 2018).

In this work, we investigate whether modified SaPIs carrying a CRISPR-*cas9* system targeting bacterial conserved chromosomal regions are able to improve antibiotic efficiency. For that, we used a previously described yeast-mediated recombineering strategy to generate custom-made SaPIs containing a bactericidal cargo (Ibarra-Chávez *et al.*, 2020). The results revealed that these synthetic SaPIs, administered in a bacteria/particle ratio of 1 to 10, showed a synergistic activity when used in combination with certain antibiotics against *S. aureus*.

Experimental procedures

Bacterial strains, oligonucleotides and culture conditions

Bacterial strains, plasmids and oligonucleotides used in this work are listed in Table 1, 2 and 3, respectively. *Escherichia coli* strains were grown in Luria-Bertani medium (LB; Conda-Pronadisa) at 37 ˚C. *S. aureus* strains were routinely incubated in trypticase soy broth (TSB; Conda-Pronadisa) at 37 ˚C. *S. cerevisiae* was grown either in yeast extract – peptone – dextrose (YPD; Sigma-Aldrich), 2x YPD or synthetic defined (SD) medium at 30 ˚C. A stock solution of 10x SD was prepared (6.8 g of Yeast Nitrogen Base Without Amino Acids (Sigma-Aldrich), 50 g of glucose (VWR) and 1.92 g of Yeast Synthetic Drop-out Medium Supplements (Sigma-Aldrich) in 100 ml of distilled water), filter-sterilized and stored at 2-8 ˚C. Media, when required, were supplemented with appropriate antibiotics at the following concentrations: ampicillin (Amp, 100 µg ml^{-1}), erythromycin (Ery, 10 µg ml^{-1}), chloramphenicol (Cm, 20 µg ml^{-1}), tetracycline (Tet, 3 µg ml^{-1}), ceftaroline (0.38 µg ml^{-1}), linezolid (2 µg ml^{-1}), vancomycin (1.5 µg ml^{-1}) and daptomycin (0.75 µg ml^{-1}). Ceftaroline *in-vitro* activation was carried out by treating 0.05 mg with 1 U of Alkaline Phosphatase (FastAP, Thermo Scientific) for 1 hour at 37 ˚C. In the case of daptomycin, the physiological levels of calcium needed for the antibiotic to work (50 mg l^{-1}) are supplied by the SaPI solvent (phage buffer). Bacteriological agar was used as gelling agent (VWR).

Table 1. Bacterial strains used in this study.

Strains	Relevant characteristics	MIC[a]	Reference/Source
Escherichia coli			
IM01B	*mcrA* Δ(*mrr-hsdRMS-mcrBC*) φ80*lacZ*ΔM15 Δ*lacX*74 *recA*1 *araD*139 Δ(*ara-leu*)7697 *galU galK rpsL endA*1 *nupG* Δ*dcm* Ω*Phelp-hsdMS* (CC1-2) ΩPN25-*hsdS* (CC1-1). *E. coli* K12 DH10B derivative. Δ*dcm* (gene encoding cytosine methylation). The *hsdMS* genes encoding methylase and specificity genes from *Staphylococcus aureus* MW2 clonal complex 1 were introduced into the chromosome at neutral locations via recombineering.	5694	(Monk *et al.*, 2015)
NovaBlue GigaSingles™ Cells	*endA1 hsdR17* (r_{K12}^- m_{K12}^+) *supE44 thi-1 recA1 gyrA96 relA1 lac* F′[*proA*$^+$*B*$^+$ *lacI*^{q}*ZΔM15*::Tn*10*] (Tet^R)		Novagen
Saccharomyces cerevisiae			
BY23849	MATa *leu2*Δ0 *ura3*Δ0 *his3*-Δ1 *met15*Δ0	07692	Toh-e, Akio: Research Center for Pathogenic Fungi Chiba University
Staphylococcus aureus			
RN10359	RN450 lysogenic for 80α phage.	3337	(Úbeda, Barry, *et al.*, 2007)
RN4220	Laboratory strain. 8325-4 derivative. Restriction defective.	99	(Peng *et al.*, 1988)
RN4220 SaPIbov2 *bap*::*tetM*	RN4220 derivative. Strain containing the SaPIbov2 pathogenicity island marked with a tetracycline resistance cassette in the *bap* gene.	JP2129	(Ram *et al.*, 2012)
RN4220 Δ*rsaE*	RN4220 derivative. Mutant for the gene coding the sRNA RsaE.	7406	This study
RN4220 Δ*rsaI*	RN4220 derivative. Mutant for the gene coding the sRNA RsaI.	07725	This study
RN4220 Δ*rsaH*	RN4220 derivative. Mutant for the gene coding the sRNA RsaH.	07733	This study
RN4220 Δ*rsaE* Δ*rsaH* Δ*rsaI*	RN4220 derivative. Mutant for the genes coding the sRNA RsaE, RsaH, RsaI.	4093	This study

Table 1. Bacterial strains used in this study. (cont.)

Strains	Relevant characteristics	MIC[a]	Reference/Source
RN4220 80α Δ*terS*	RN4220 lysogenized by 80α. Phage mutant for the gene coding the small terminase subunit.	07706	(Úbeda *et al.*, 2009)
RN450 80α::*ermC*	RN450 (phage-cured 8325-4 derivative) lysogenized by 80α. Phage marked with an erythromycin resistance cassette.	JP6399	(Manning *et al.*, 2018)
RN4220 80α Δ*terS*::*ermC*	RN4220 lysogenized by 80α. Phage mutant for the gene coding the small terminase subunit. Phage marked with an erythromycin resistance cassette.	07711	This study
RN4220 80α Δ*terS*::*ermC* pCN51(Cm^R)::P$_{cad}$-*terS*$_{80α}$-TT	RN4220 lysogenized by 80α Δ*terS*::*ermC*. Strain containing a plasmid that constitutively expresses the wildtype 80α *terS* gene.	07716	This study
RN4220 80α Δ*terS*::*ermC* SaPIbov2::P$_{blaZ}$-cas system-sgRNA2-*tetM*	RN4220 lysogenized by 80α Δ*terS*::*ermC* and SaPIbov2. The pathogenicity island constitutively expresses the *Steptococcus pyogenes cas9* gene and the sgRNA2.	08017	This study
RN4220 Δ*rsaE* 80α Δ*terS*::*ermC* SaPIbov2::P$_{blaZ}$-cas system-sgRNA$_{rsaE}$-*tetM*	RN4220 Δ*rsaE* lysogenized by 80α Δ*terS*::*ermC* and SaPIbov2. The pathogenicity island constitutively expresses the *Steptococcus pyogenes cas9* gene and the sgRNA targeting *rsaE*.	08018	This study
RN4220 Δ*rsaH* 80α Δ*terS*::*ermC* SaPIbov2::P$_{blaZ}$-cas system-sgRNA$_{rsaH}$-*tetM*	RN4220 Δ*rsaH* lysogenized by 80α Δ*terS*::*ermC* and SaPIbov2. The pathogenicity island constitutively expresses the *Steptococcus pyogenes cas9* gene and the sgRNA targeting *rsaH*.	08019	This study
RN4220 Δ*rsaI* 80α Δ*terS*::*ermC* SaPIbov2::P$_{blaZ}$-cas system-sgRNA$_{rsaI}$-*tetM*	RN4220 Δ*rsaI* lysogenized by 80α Δ*terS*::*ermC* and SaPIbov2. The pathogenicity island constitutively expresses the *Steptococcus pyogenes cas9* gene and the sgRNA targeting *rsaI*.	08020	This study

[a] Number of each strain in the culture collection of the Laboratory of Microbial Pathogenesis, Navarrabiomed-Universidad Pública de Navarra.

Table 2. Plasmids used in this study.

Plasmid	Relevant characteristics	Reference/Source
pEMPTY$_0$	*E. coli* - *S. aureus* shuttle vector. pEMPTY predecessor. No thermosensitive version. Amp^R Cm^R	Charpter II. Unpublished data
pEMPTY$_0$::sgRNA2	*E. coli* - *S. aureus* shuttle vector. It allows rapid and efficient plasmid curing in *Staphylococcus aureus*. Amp^R Cm^R	This study
pEMPTY$_0$::sgRNA$_{rsaE}$	*E. coli* - *S. aureus* shuttle vector. sgRNA targets the gene coding RsaE. Amp^R Cm^R	This study
pEMPTY$_0$::sgRNA$_{rsaH}$	*E. coli* - *S. aureus* shuttle vector. sgRNA targets the gene coding RsaH. Amp^R Cm^R	This study
pEMPTY$_0$::sgRNA$_{rsaI}$	*E. coli* - *S. aureus* shuttle vector. sgRNA targets the gene coding RsaI. Amp^R Cm^R	This study
pFREE-Amp	Plasmid design to remove plasmids from *E. coli*. CRISPR-Cas9-based curing. Amp^R	(Lauritsen *et al.*, 2017)
pRN6680	pBluescriptΩ2.9-kb pMVN6 SmaI-HindII [*tetA*(M)]. Amp^R Tet^R	(Charpentier, Ana I Anton, *et al.*, 2004)
pMAD	*E. coli* - *S. aureus* shuttle vector. The plasmid contains a thermosensitive origin of replication for Gram-positive bacteria and the *bgaB* gene that encodes a ß-galactosidase, reporter of plasmid presence. Amp^R Ery^R	(Arnaud *et al.*, 2004)
pMAD_lic	pMAD modified plasmid for inserting DNA fragments using a ligase independent cloning. Amp^R Ery^R	(Burgui *et al.*, 2018)
pMAD_lic::*rsaE*	pMAD_lic plasmid containing the regions needed for deletion of the *rsaE* gene. Amp^R Ery^R	This study
pMAD::*rsaH*	pMAD plasmid containing the regions needed for deletion of the *rsaH* gene. Amp^R Ery^R	This study
pMAD::*rsaI*	pMAD plasmid containing the regions needed for deletion of the *rsaI* gene. Amp^R Ery^R	This study
pCN40	*E. coli* - *S. aureus* shuttle vector. The plasmid contains the strong constitutive promoter P$_{blaZ}$. Amp^R Ery^R	(Charpentier, Ana I. Anton, et al., 2004)
pCN38	*E. coli* - *S. aureus* shuttle cloning vector. Amp^R Cm^R	(Charpentier, Ana I. Anton, et al., 2004)
pCN51	*E. coli* - *S. aureus* shuttle vector. The plasmid contains the leaky constitutive promoter P$_{cad}$. Amp^R Ery^R	(Charpentier, Ana I. Anton, et al., 2004)

Table 2. Plasmids used in this study. (cont.)

Plasmid	Relevant characteristics	Reference/Source
pAUR112	*E. coli* - *S. cerevisiae* shuttle vector. YAC, yeast artificial chromosome, high capacity vector. Amp^R *ura3* AbA^R	TaKaRa
pAUR112::SaPIbov2 ::P_{blaZ}-cas system-sgRNA2-*tetM*	pAUR112 containing a modified SaPIbov2. sgRNA2. Amp^R *ura3*	This study
pAUR112::SaPIbov2 ::P_{blaZ}-cas system-sgRNA$_{rsaE}$-*tetM*	pAUR112 containing a modified SaPIbov2. sgRNA$_{rsaE.}$ Amp^R *ura3*	This study
pAUR112::SaPIbov2 ::P_{blaZ}-cas system-sgRNA$_{rsaH}$-*tetM*	pAUR112 containing a modified SaPIbov2. sgRNA$_{rsaH.}$ Amp^R *ura3*	This study
pAUR112::SaPIbov2 ::P_{blaZ}-cas system-sgRNA$_{rsaI}$-*tetM*	pAUR112 containing a modified SaPIbov2. sgRNA$_{rsaI.}$ Amp^R *ura3*	This study
pCN51(CmR)::P_{cad}-*ter*$S_{80\alpha}$-TT	*E. coli* - *S. aureus* shuttle vector. pCN51 derivative: Ery to Cm resistance cassette substitution. It contains the gene coding the 80α small terminase subunit under the control of the pCN51 cadmium inducible promoter. Amp^R Cm^R	José R. Penadés' Lab (unpublished data)

Table 3. Oligonucleotides used in this study.

Oligonucleotide	Sequence
pEMPTY derivatives	
247	CTGCAGTTGACAAATTGCAGTAGGCATGACAAAATGGACTCACAAGTTTTGGGATTGTTAAGGGTTCCGGTTTTAGAGCTAGAAATAGCAAGTTAAAATAAGGCTAGTC
294	GGCTGCAGTTGACAAATTGCAGTAGGCATGACAAAATGGACTCAGGGAGAAATTTTTCACTTCAAACAAAGGTTTTAGAGCTAGAAATAGCAAG
E7	GGCTGCAGTTGACAAATTGCAGTAGGCATGACAAAATGGACTCAAGGTAAAAATTTGACTCCCTTTAGTAGGTTTTAGAGCTAGAAATAGCAAG
E15	GGCTGCAGTTGACAAATTGCAGTAGGCATGACAAAATGGACTCATTATTACTTACTTTCCTTTCTATTTGTGTTTTAGAGCTAGAAATAGCAAG
245	CCCGGGTTAATTAAGTTGCGCACACCGACTAGCG
pMAD::*rsaE*	
330	GACGACGACAAGAGTCTATTTTTGTCGCTGAAGTTG
332	CACTTCCCTCTTATTAAAAAAGAACATGTTCATAATATAACATGCTATCTCTAC

Table 3. Oligonucleotides used in this study. (cont.)

Oligonucleotide	Sequence
334	ATGTTCTTTTTTAATAAGAGGGAAGTG
336	GAGGAGAAGCCCGGTCCGAAAGCTTGAAAATTGATTTG
346	AAATTCCAACCGTCAAATTC
348	GATTTAGAAGTATTTAAAGACGAC
pMAD::*rsaH*	
E1	GGGGATCCAAACGTTCCCATTGATACAC
E2	GGTTTAAGTGTTGTGTTAAAAGATACAATTCAAAAAAAGTTATTGAC
E3	CTTTTAACACAACACTTAAACC
E4	GGCCATGGTCTGCATTTTCTTTTTGACGC
E5	CCGATGACAACTCGTGTACCT
E6	AATCTAGCTCATTCTGCTCT
pMAD::*rsaI*	
E9	GGCCATGGCTTAATTCCATTACAAAAAGCACC
E10	CGCTTACATTTTAAAAAAGATTGTTATGCATAAAATGAAGAAGTCTTC
E11	CAATCTTTTTTAAAATGTAAGCG
E12	GGGAATTCATAAAAGTCCATGCGTTTAAG
E13	TAACGATGGTGGTTCTTCC
E14	GTCATATGTTGTGTGTCATC
pAUR112 derivatives	
404	GGAATGGTTACCGGGAATTTGTAATTTGCGTTATTCTTTCCTCTGGATC CTC
410	GCCATTTCCATATTTGTCGTTCTCCCACTGATGGGCACTTTCTCGAA
E50	TTCGAGAAAGTGCCCATCAGTGGGAGAACGACAAATATGGAAATGGC
E17	CCTTTTAAAAGCAGGATTTAG
E18	CTAAATCCTGCTTTTAAAAGG
E19	ACTTCACTATAACCATCACC
E20	GGTGATGGTTATAGTGAAGT
452	TGTAGCATGTATTGTGATAGC
422	ACATGCTACACCAGGTCGACCATGCAGCTTACTATGCCATTA
424	CCATAAATAATCATCCTCCTAAAACTAGTTGCAGAATAAACCCTCCGAT
382	ACTAGTTTTAGGAGGATGATTATTTATGG
129	TTGAAGCTGATAGGGGAGCCTTAGT
131	ACTAAGGCTCCCCTATCAGCTTCAA

Table 3. Oligonucleotides used in this study. (cont.)

Oligonucleotide	Sequence
E49	TGCAGTTGACAAATTGCAGTAGG
E22	CCTACTGCAATTTGTCAACTGCAGGTATCGATAAGCTTGATATCG
E23	GCTCTAGAACTAGTGGATCCCC
E24	GGGGATCCACTAGTTCTAGAGCGGGGATATTATGGTATGAATTTTTC
E51	GAGGATCCAGAGGAAAGAATAACGCAAATTACAAATTCCCGGTAACCA TTCC

DNA manipulations

Routine DNA manipulations were performed using standard procedures unless otherwise indicated. Oligonucleotides were synthesized by StabVida (Caparica, Portugal). FastDigest restriction enzymes, Phusion DNA polymerase, Rapid DNA ligation kit (Thermo Scientific) and KAPA High Fidelity DNA polymerase (Roche) were used according to the manufacturer's instructions. Plasmids were purified using a Macherey Nagel plasmid purification kit according to the manufacturer's protocol. To extract plasmids from *S. cerevisiae*, an established protocol was modified as follows. After being grown in 15 ml of SD medium for 48 hours, yeasts were collected (5000 g, 1 min), resuspended in 520 µl of Yeast Lysis Solution (500 µl of Lyticase Buffer: 0.1 M Na_2EDTA (pH 7.5) (AppliChem), 1M sorbitol (Sigma-Aldrich); 20 µl of Lyticase Solution: 10 mM sodium phosphate (Na_2HPO_4, pH 7.5) (Merk), 1.2 M sorbitol, 500 U Lyticase from *Arthrobacter luteus* (Sigma-Aldrich)) and incubated at 37 °C for 1.5 h. After Lyticase treatment, protoplasts were collected (5000 g, 2 min) and from this step onward samples were treated according to the manufacturer's protocol.

Plasmids were transformed in *Escherichia coli* by electroporation (1 mm cuvette; 200Ω, 25µF, 1250V; Gene Pulser X-Cell electroporator). *Staphylococcus aureus* competent cells were generated as previously described in (Lee, 1995). Plasmids were transformed in *Staphylococcus aureus* by electroporation (1mm cuvette; 100Ω, 25µF, 1250V; Gene Pulser X-Cell electroporator). To transform *S. cerevisiae*, a 20 ml overnight culture grown in 2x YPD, 30 ˚C and 200 rpm was diluted 1.5:100 in fresh medium and incubated under shaking conditions until OD_{595nm} 1.0. 3ml of the culture were collected, washed twice with 1 ml of 0.1 M Lithium acetate (LiAc) (pH 7.5) and used for transformation. The aforementioned pellets were resuspended in the transformation mixture (containing 260 µl of 50% (w/v) polyethylene glycol 4000 (PEG; Merck), 36 µl of 1.0 M LiAc (Sigma-Aldrich), 50 µl of 2 mg ml^{-1} single-stranded carrier DNA (Sigma-Aldrich) and 14 µl of the DNA to be transformed) and incubated at 42 ˚C for 45 minutes under shaking conditions. After the incubation period, cells were collected (13000 g, 30 sec), washed twice with 1 ml of water and resuspended in 200 µl of water. Yeast suspension was plated in SD solid medium and incubated at 30 ˚C for 48-72 hours.

Construction of $pEMPTY_0$ derivatives

To ensure the absence of sgRNA off-target activity and to generate the templates for the PCRs needed in the yeast-mediated SaPI assembly, 4 plasmids based on a no-thermosensitive predecessor of pEMPTY, $pEMPTY_0$, were constructed. Primers 247, 294, E7 and E15, containing the strong constitutive SP01 promoter from *Bacillus subtilis* bacteriophage SP01 (Stewart *et al.*, 1998) and the gRNA sequence that allows

targeting either the highly conserved plasmid sequence described in Chapter II or the RsaE, RsaH and RsaI coding sequences, were used in combination with primer 245 to amplify the sequences responsible for the Cas9-directed activity. Plasmid pFREE-Amp (Lauritsen *et al.*, 2017) was used as template for the PCR amplification. Resulting fragments were cloned into the pJET1.2/blunt and then sub-cloned into $pEMPTY_0$ digested with PstI and SmaI enzymes leading to plasmids $pEMPTY_0$::sgRNA2, $pEMPTY_0$::$sgRNA_{rsaE}$, $pEMPTY_0$::$sgRNA_{rsaH}$ and $pEMPTY_0$::$sgRNA_{rsaI}$.

Removal of chromosomal genes

To generate deletional mutants, two fragments of at least 500 bp, which flanked the left and right sequences of the region targeted for deletion, were PCR amplified. As PCR template, chromosomal DNA from *S. aureus* RN4220 was used. To amplify *rsaE*, *rsaH* and *rsaI* flanking regions primers 330-332 and 334-336, E1-E2 and E3-E4, and E9-E10 and E11-E12 were respectively used. The overlap PCR of the aforementioned fragments was performed using primers 330-336 (*rsaE*), E1-E4 (*rsaH*) and E9-E12 (*rsaI*). Overlapped products were gel-purified and either cloned into pJET1.2/blunt or treated for directional cloning into pMAD_lic without restriction enzyme digestion or ligation reactions (Aslanidis and de Jong, 1990; Burgui *et al.*, 2018).

In the first strategy, pJET1.2/blunt:: *rsaH* and pJET1.2/blunt:: *rsaI* cloned fragments were digested with NcoI and BamHI or NcoI and EcoRI enzymes, respectivley, purified and ligated into the shuttle vector pMAD (Arnaud *et al.*, 2004),

leading to plasmids pMAD:: *rsaH* and pMAD:: *rsaI*. In the second approach, to produce specific plasmid-insert complementary overhangs, an ApaI linearized pMAD_lic plasmid and the amplified *rsaE*-related PCR fragment were treated with T4 DNA polymerase (Novagen) in the presence of dTTP and dATP (Novagen), respectively, for 30 min at 22°C. After the incubation period, the enzyme was inactivated. A mix of vector and insert was incubated for 5 min at 22°C and then, 6.25 mM EDTA was added and an additional incubation of 5 min at 22°C was applied. The annealed species were transformed into chemically competent *E. coli* NovaBlue GigaSingles™ cells from which the pMAD_lic::*rsaE* plasmid was purified.

Resulting plasmids were checked by PCR, purified from *E. coli* and transformed into *S. aureus* by electroporation. Homologous recombination experiments were performed as previously described in (Arnaud *et al.*, 2004). Erythromycin-sensitive white colonies, which did not further contain the pMAD plasmid, were tested by PCR using primers located outside the amplified-flanking regions (346-348 for *rsaE* mutants; E5-E6 for *rsaH* mutants; and E13-E14 for *rsaI* mutants). All constructed plasmids were confirmed by Sanger sequencing.

Plasmid construction in yeast and *S. aureus* Pathogenicity Islands rebooting

S. aureus Pathogenicity Islands (SaPIs) assembly in yeast was performed as described elsewhere (Ibarra-Chávez *et al.*, 2020). Briefly, KAPA High Fidelity DNA polymerase was used to amplify the fragments of the plasmid to be constructed. Overlapping PCR fragments (≥ 30 bp) were generated mirroring the structure of the integrated SaPIs in the chromosome.

The set of primers used for the amplification of the different fragments were: 404-410 (product obtained: linearized plasmid pAUR112; template: pAUR112), E50-E17 (product obtained: Fragment 1, partial SaPIbov2 sequence; template: genomic DNA RN4220 SaPIbov2 *bap*::tetM), E18-E19 (product obtained: Fragment 2, partial SaPIbov2 sequence; template: genomic DNA RN4220 SaPIbov2 *bap*::tetM), E20-452 (product obtained: Fragment 3, partial SaPIbov2 sequence; template: genomic DNA RN4220 SaPIbov2 *bap*::tetM), 422-424 (product obtained: Fragment 4.1, strong constitutive P_{blaZ} promoter; template: pCN40), 382-129 (product obtained: Fragment 4.2, 5' UTR and partial *cas9* sequence; template: $pEMPTY_0$), 131-E49 (product obtained: Fragment 5, partial *cas9* sequence and module containing the constitutive promoter SP01 promoter-sgRNA-tracrRNA; template: $pEMPTY_0$::sgRNA2/$pEMPTY_0$::$sgRNA_{rsaE}$/$pEMPTY_0$::$sgRNA_{rsaH}$/$pEMPTY_0$::$sgRNA_{rsaI}$), E22-E23 (product obtained: Fragment 6, *tetM* resistance cassette; template: pRN6680), and E24-E51 (product obtained: Fragment 7, partial SaPIbov2 sequence; template: genomic DNA RN4220 SaPIbov2 *bap*::tetM). Fragments 4.1 and 4.2 were fused using primers 422-129 generating Fragment 4. The first and last fragments included 500 bp outside the *attL* and *attR* site, respectively. For clarity, the whole amplificacion and assembly process is depicted in **Figure 1**.

PCR products were purified using the QIAquick PCR Purification Kit (Qiagen) and quantified (Eppendorf BioPhotometer model 6131). The amplified pAUR112 fragment was treated with DpnI. 250 ng of the amplified DpnI-treated pAUR112 vector and 500 ng of each PCR product suspended in a maximum volume of 14 µl were transformed into the yeast as described above. Fragments used for

transformation were not shorter than 1000 bp as several reports have highlighted poor cloning efficiency when assembling small DNA fragments (Watson and García-Nafría, 2019). Colonies obtained after transformation were checked by colony PCR, plasmid extraction was performed and the presence of the different cloned fragments was confirmed by PCR amplification.

S. aureus competent cells were transformed with >2 µg of the yeast-assembled plasmids (pAUR112 derivatives), incubated for 2-4 hours at 37°C and 200 rpm, plated in medium containing 3 µg ml^{-1} tetracycline and grown for 24-48 hours at 37°C. Tetracycline-resistant colonies obtained after the rebooting process were checked by colony PCR.

Marking and moving phage 80α Δ*terS*

Phage 80α Δ*terS* was marked with an erythromycin-resistance cassette by lateral transduction (Chen *et al.*, 2018) using a lysate from RN450 80α::*ermC* on a RN4220 80α Δ*terS* strain. Phage 80α Δ*terS*::*ermC* was mobilized by generalized transduction after trans-complementing the lysogenic strain with the gene encoding the terminase small-subunit (pCN51(Cm^R)::P_{cad}-$terS_{80\alpha}$-TT).

Phage and SaPI induction and titration

An *S. aureus* overnight culture was diluted (1:50) in fresh TSB medium and incubated at 37°C and 200 rpm until an OD_{595nm} of 0.2-0.3. The culture was treated with 2 µg ml^{-1} of mitomycin C and incubated at 32°C and 80 rpm for the next 3-4

hours and then left overnight at room temperature under static conditions. Phage/SaPI stocks were filtered (0.2 μm) and stocked at 4°C.

To obtain higher titers, remove the presence of mitomycin C and perform a buffer exchange to phage buffer, lysates were centrifuged using Amicon® centrifugal filters 10 k-10,000 NMWL (Merk).

Phages and SaPIs used in this study are marked with erythromycin and tetracycline resistance markers, respectively, that allow the selections of transductants in media containing the aforementioned drugs. To titrate both phages and SaPIs, an overnight culture of the *S. aureus* laboratory strain RN4220 was diluted (1:50) in fresh TSB medium and incubated at 37 °C and 200 rpm until an OD_{595nm} of 1.4. Serial dilutions of the lysate were made in phage buffer (1 mM NaCl; 0.05 M Tris pH 7.8; 1 mM $MgSO_4$; 4 mM $CaCl_2$) and added to the recipient bacteria in a proportion of 100 μl of lysate per ml of bacterial culture. The mixture was homogenized and incubated at 37°C for 20 minutes without shaking. 3 ml of TTA (TSB Top Agar: TSB + 0.75% (w/v) agar) at 55°C were added to the tube containing the lysate-cell combination and immediately poured over the surface of a plate containing the selective drug and 1.7 mM of sodium citrate. To illustrate the sequence-dependent activity of the sgRNAs, drops of 20 μl were plated. Once solidified, plates were incubated at 37°C for 24-48 hours.

Determination of antibiotic minimal inhibitory concentration

Minimal inhibitory concentrations (MICs) for the antibiotics ceftaroline, linezolid, vancomycin and daptomycin were established by E-test (Biomerieux) (CLSI. Performance standards for antimicrobial susceptibility testing. 28th ed. CLSI supplement M100, 2018).

Synergy assays

Overnight *S. aureus* cultures were washed twice with fresh TSB medium and the cellular density was adjusted to an OD_{595nm} of 0.1. 20 µl of the aforementioned bacterial suspension was mixed with 80 µl of fresh TSB medium and 100 µl of phage buffer containing 10^5 SaPI particles. Growth assays were carried out using 96 multi-well plates. The total volume of medium per well was 200 µl. Growth kinetics were obtained using a Synergy H1 Hybrid Multi-Mode Microplate Reader (Biotek). Growth data (OD_{595nm}) was collected every 15 minutes for up to 48 hours at 37 ˚C and 425 cpm. All the experiments were repeated at least three times. To supplement the culture with new SaPI particles every 8 hours, extra SaPI-dosages, concentrated 10 fold (10 µl of phage buffer containing 10^5 SaPI particles), were supplied.

When required, media was supplemented with ceftaroline, linezolid, vancomycin, daptomycin or chloramphenicol. Antibiotics were used at the minimal inhibitory concentration.

In-vivo rodent model for biofilm treatment on medical devices

A modified version of the murine model of catheter-associated biofilm formation described in (Cucarella *et al.*, 2001) was followed. Briefly, overnight cultures of *S. aureus* MW2 grown at 37 °C on TSA medium were resuspended in PBS to to an OD_{595nm} of 0.2 (10^8 CFUs ml^{-1}). Groups of five, 5 five weeks-old ICR female mice (EnVigo) were anaesthetized with isoflurane (B. Braun) and two 19 mm intravenous catheters (24G; B. Braun) were aseptically implanted into the interscapular space of each mouse. Dilutions of the bacterial suspension were made and 100 µl containing 10^4 CFUs were inoculated into the catheters. An initial sole dose of linezolid was subcutaneously administered at two different concentrations: 5 mg kg^{-1} and 10 mg kg^{-1}. 50 µl of phage buffer containing 10^5 SaPI particles were daily inoculated. A group of animals was daily treated with phage buffer (vehicle) and served as negative control. On day 5 post-infection, animals were anaesthetized using isoflurane and euthanatized by cervical dislocation. Catheters were aseptically removed, placed in a sterile microcentrifuge tube containing 1 ml of PBS and vortexed at high speed for 3 min. Serial dilutions of the bacterial mixture were plated on TSA and incubated at 37°C. The number of bacteria was determined by plate count.

Ethics statement

Animal procedures were reviewed and approved by "Comité de Ética para la Experimentación Animal (CEEA) de la Universidad de Navarra" (protocol 114-17). Described animal work was carried out at "Centro de Investigación Médica Aplicada" building (ES312010000132) under the principles and guidelines established in the

European Directive 2010/63/EU for the protection of animals used with experimental purposes.

Statistics

Statistical analyses were performed with the GraphPad Prism 5.01 program. A nonparametric Mann-Whitney *U* test was used to assess differences in the murine model of catheter-associated biofilm formation.

Results

Assembly of an engineered SaPI-CRISPR-Cas9 device

We designed and constructed a set of synthetic SaPIs carrying the CRISPR-Cas9 system (**Figure 1**). SaPIbov2 was used as scaffolding SaPI since it does not contain the capsid-morphogenesis *cpmAB* genes and therefore, only produces phage-sized capsids. The advantage of this is to provide enough space to efficiently package recombinant SaPIs up to 45kb (Damle *et al.*, 2012). Primers with homology overhangs of ≥30 bp were designed to amplify SaPIbov2 in four different PCR fragments and the CRISPR-Cas9-TetM in three different fragments (Table 3). The *5′* region of the first fragment of SaPI and the *3′* region of the last fragment of SaPI carried homology overhangs with the YAC (pAUR112) fragment containing the essential genes for selection and assembly in yeast. All the seven SaPIbov2-CRISPR-Cas9-TetM fragments were transformed into *S. cerevisiae* BJ5464 cells to assemble the synthetic SaPI genome ($SaPI_{CRISPR}$). Colonies of *S. cerevisiae* were restreaked and analyzed by colony PCR to confirm the presence of $SaPI_{CRISPR}$. After their assembly in the yeast, synthetic SaPIs were rebooted into a *S. aureus* RN4220 lacking the gRNAs target sequences and lysogenic for the phage 80α deficient in *terS*, which ensures that the lysate will only contain engineered SaPI particles. To inactivate *S. aureus* cells, three genes conserved at family, *rsaE*, or genus level, *rsaH* and *rsaI*, were selected as CRISPR-Cas9 targets (Table 4) (Geissmann et al., 2009). A fourth island containing a CRISPR-Cas9 system directed against a DNA region conserved in plasmids but rarely found in the bacterial chromosome was generated and used as a negative control.

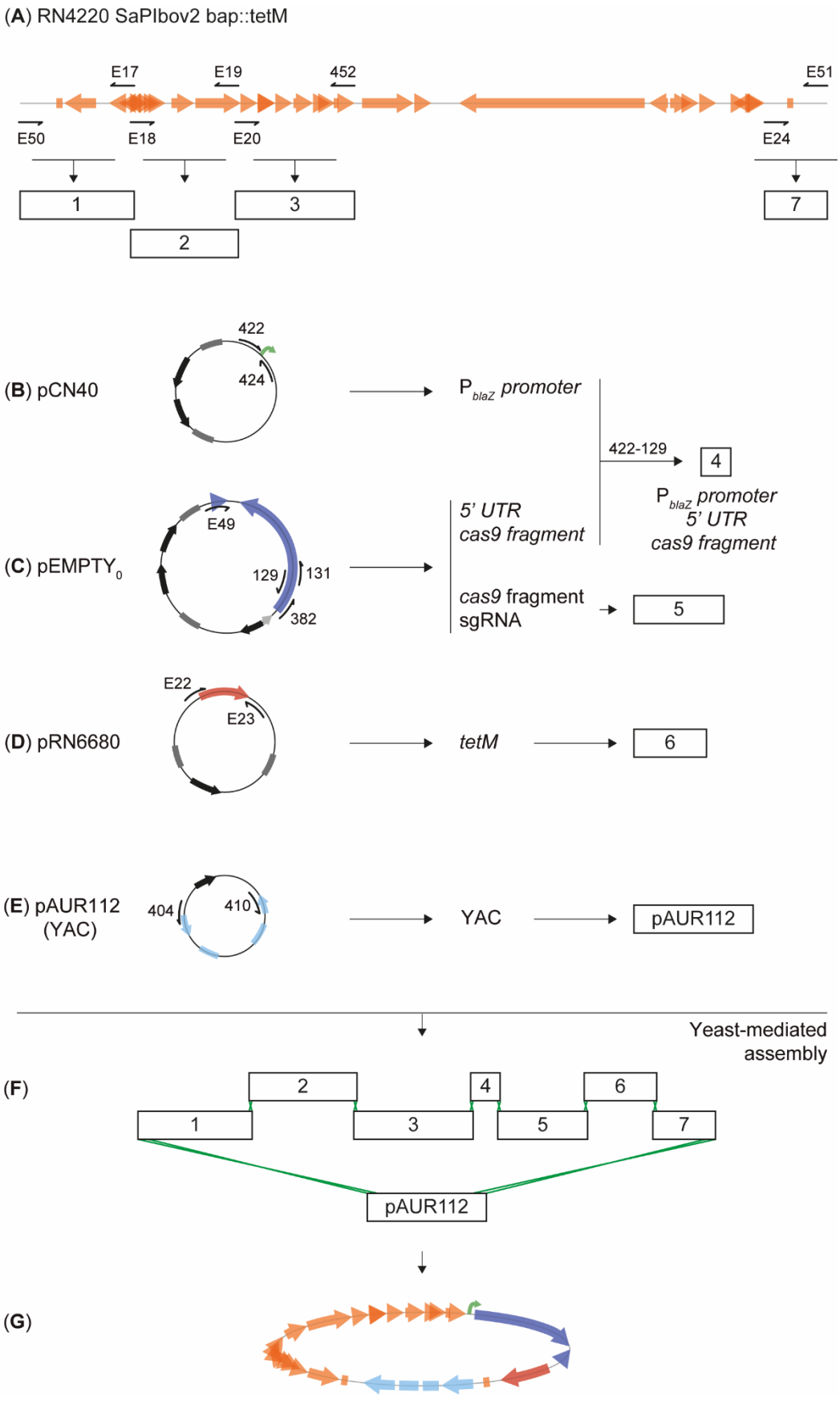

Figure 1. Schematic representation of yeast-mediated SaPI assembly. (A-E) DNA templates and primers used to generate the fragments needed for CRISPR-carrying SaPI construction. (A) From the SaPIbov2 genome, only those regions essential to the SaPI lifecycle (fragments 1, 2, 3 and 7) were amplified and used in the assembly process. Fragments 1 and 7 include around 500 bp homologous to the RN4220 genome (regions flanking the SaPI *att* sites). (B) The strong constitutive P_{blaZ} promoter, used to control *cas9* expression in the modified SaPIs, was amplified from plasmid pCN40. (C) Two overlapping fragments were PCR amplified from $pEMPTY_0$ to generate fragment 5. The first one contained the RBS of the superoxide dismutase (Malone *et al.*, 2009) and the initial sequence of the *cas9* gene, whereas the second included the rest of the *cas9* open reading frame, the λ t_0 transcriptional terminator (Scholtissek and Grosse, 1987) and the sgRNA module (SP01 promoter + gRNA + tracrRNA). (D) The tetracycline resistance cassette, *tetM*, needed to monitor SaPI presence once rebooted, was amplified from plasmid pRN6680. (E) The pAUR112 plasmid, used as a scaffold for the assembly and required for construct selection, replication and maintenance in the yeast, was PCR amplified and subsequently treated with the restriction enzyme DpnI (template removal).(F) Representation of the homology-based recombination process. (G) Graphical illustration of the resulting plasmid carrying the synthetic SaPI.

Table 4. gRNAs sequences

gRNA	Sequence
gRNA2	CAAGTTTTGGGATTGTTAAGGGTTCCG
rsaE	GGGAGAAATTTTTCACTTCAAACAAAG
rsaH	AGGTAAAAATTTGACTCCCTTTAGTAG
rsaI	TTATTACTTACTTTCCTTTCTATTTGT

Engineered SaPIs show antibacterial *in vitro* activity

To assess the efficiency of the engineered $SaPI_{CRISPR}$ elements, the islands containing the sgRNA that targets *rsaE*, *rsaH* or *rsaI* were transduced into *S. aureus* RN4220 and also into the triple mutant *S. aureus* RN4220 Δ*rsaE* Δ*rsaH* Δ*rsaI*. Very few transductants were obtained in the case of RN4220 wildtype strain transduced with any of the three synthetic islands, confirming that the engineered SaPIs were, somehow, affecting the transduction efficiency. In contrast, reduction in transduction rates was not observed when either *S. aureus* RN4220 Δ*rsaE* Δ*rsaH* Δ*rsaI* was used as a recipient strain or when a lysate containing the control island, $SaPI_{gRNA2}$, was used for transduction (**Figure 2**).

Next, to demonstrate the killing activity of $SaPI_{CRISPR}$, we infected the wildtype *S. aureus* RN4220 strain with the modified SaPIs, either alone or in combination (**Figure 3**) and growth over time was monitored using a Multiskan microplate spectrophotometer. All experiments were carried out with at least three biological replicates per condition. We observed a similar moderate killing activity when any of the three islands targeting *rsaE*, *rsaH* or *rsaI* genes were used, as compared to the control SaPI, $SaPI_{gRNA2}$. These results indicated that the CRISPR-Cas9 system present

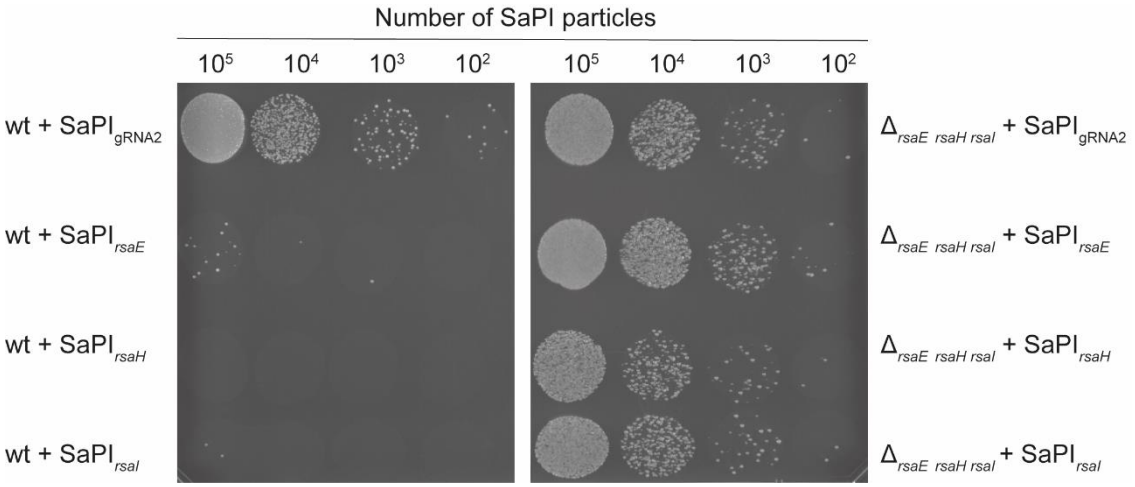

Figure 2. sgRNAs sequence specificity evaluation. (Left) *S. aureus* RN4220 wildtype strain and (right) a derivative mutant lacking the three small RNA coding genes *rsaE*, *rsaH* and *rsaI* were treated with serial dilutions of lysates containing either the control $SaPI_{gRNA2}$ (top) or SaPIs containing guide RNAs that target the small RNA coding genes *rsaE*, *rsaH* and *rsaI*. Transductants were visualized by plating on TSA medium containing tetracycline as selective agent.

in the modified SaPIs was able to detect the corresponding *rsaE, rsaH* and *rsaI* genes, cleave the double-stranded DNA, and trigger cell death. When *S. aureus* RN4220 was treated simultaneously with the three $SaPI_{CRISPR}$, no significant improvement with respect to single treatments was observed (**Figure 3**). Consequently, the island carrying the sgRNA against *rsaE* ($SaPI_{rsaE}$) was selected for further experiments.

The combination of engineered SaPIs and antibiotics has synergistic activity on *S. aureus*

A recent study demonstrated that combination of phages and antibiotics (daptomycin and vancomycin) were synergistic in order to reduce *S. aureus* viability (Kebriaei *et al.*, 2020). Thus, we hypothesized that a combination of our $SaPI_{CRISPR}$ particles with antibiotics might improve the killing capacity of the antibiotics alone. To prove our hypothesis, growth kinetics during 24 hours of *S. aureus* RN4220 cultures in the presence of combinations of four antibiotics (ceftaroline, linezolid, vancomycin and daptomycin) at the minimum inhibitory concentration with the engineered $SaPI_{rsaE}$ or the control $SaPI_{gRNA2}$ were assayed. As shown in **Figure 4**, when ceftaroline, linezolid and daptomycin were used in combination with $SaPI_{rsaE}$ to treat *S. aureus* RN4220, graph trends experienced a reduction in terms of total growth if compared with treatment with the same antibiotic combined with the control $SaPI_{gRNA2}$. For vancomycin, no positive outcome could be observed as treatment with the antibiotic alone was enough to completely restrict bacterial growth.

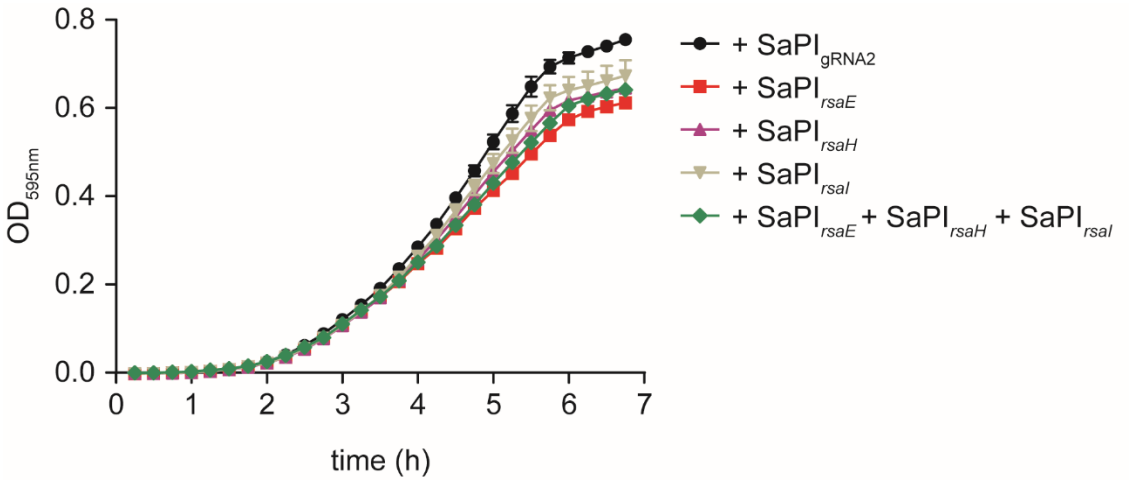

Figure 3. Antimicrobial activity of the synthetic SaPIs on an active dividing bacterial population. Data corresponding to growth dynamics were collected for RN4220 populations growing in TSB medium in the presence of the different SaPI$_{CRISPR}$ either alone or in combination. SaPI$_{gRNA2}$ was used as a control of no bactericidal effect. Three technical replicates were used for each of the tested SaPIs. Experiments were repeated at least three times.

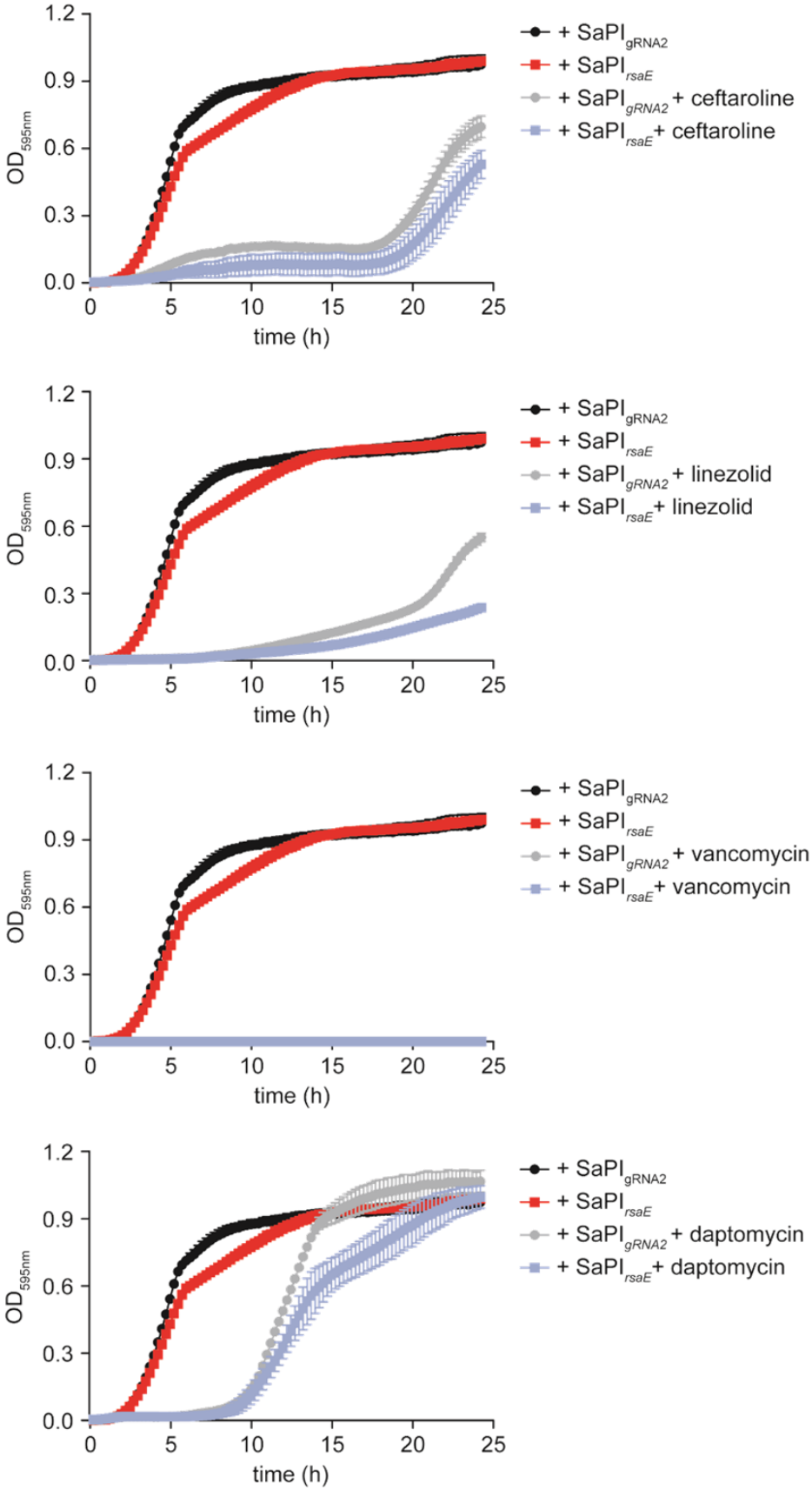

Figure 4. Assessing the synergistic effect of SaPI$_{CRISPR}$-antibiotic combinations. The coordinated SaPI-antibiotic effect was analyzed by the growth dynamics information obtained from cultures incubated in the presence of ceftaroline, linezolid, vancomycin or daptomycin with either the control SaPI$_{gRNA2}$ or SaPI$_{rsaE}$. Antibiotics were used at their minimal inhibitory concentration. For each of the tested conditions, 3 technical replicates were performed. Experiments were repeated at least three times.

Compared to phages, SaPIs are not able to replicate autonomously upon infection of a new host and consequently, in the assay, the number of SaPI$_{CRISPR}$ elements that can mediate cell death is limited. Because those bacteria that escape the initial SaPI$_{CRISPR}$ killing can replicate during the experiment, we repeated the dual SaPI-antibiotic treatment adding a dose of SaPI$_{rsaE}$ particles every eight hours until 32 hours post initial treatment (**Figure 5**). In this experiment, we used the antibiotic linezolid as a proof of principle. The results revealed that exposure of bacteria to linezolid and repeated doses of the SaPI$_{rsaE}$ particles caused a significant reduction in bacterial growth compared with the outcome obtained with the antibiotic and a single SaPI$_{rsaE}$ dose (**Figure 5**).

From this *in-vitro* approach, we can conclude that combinations of commonly used antibiotics for the clinical treatment of *S. aureus* with SaPI$_{CRISPR}$ particles have a synergistic bactericidal activity on *S. aureus* and that the effect can be potentiated if repeated applications of SaPI$_{CRISPR}$ are used.

Evaluation of an antibiotic and SaPI$_{CRISPR}$ combined treatment in a murine model of catheter-associated biofilm formation

To investigate the potential of SaPI$_{CRISPR}$ as an adjuntive therapy, we next used a murine model that assesses the capacity of *S. aureus* to colonize and form a biofilm on subcutaneous catheters. For that, two intravenous catheters were aseptically implanted into the subcutaneous interscapular of each mouse and inoculated with 10^4 CFUs of *S. aureus* MW2 strain. A combination of 5mg kg^{-1} or 10 mg kg^{-1} of

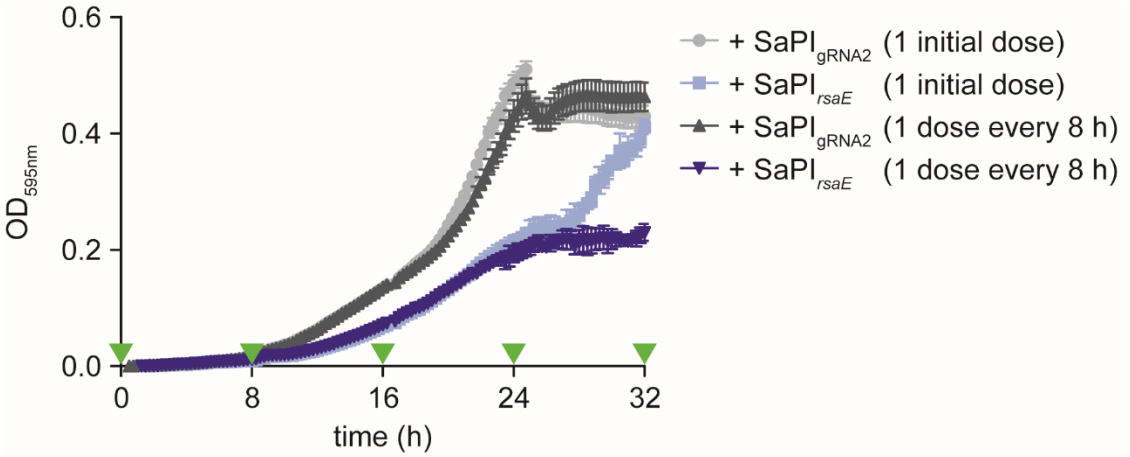

Figure 5. Periodic pulses of SaPI$_{CRISPR}$ particles improve treatment output when combined with antibiotics. RN4220 cultures treated with a sole dose of linezolid at the minimal inhibitory concentration were periodically supplemented with SaPIs carrying either the control sgRNA2 or the lethal cargo sgRNA$_{rsaE}$. The time when SaPIs were regularly administered is shown as green triangles on the x axis of the graph. Replicates where a sole SaPI dose was initially administered were carried out in parallel. 3 technical replicates were used for each of the tested conditions. Experiments were repeated at least three times.

linezolid and SaPI*rsaE* was immediately applied after implantation and then, SaPI*rsaE* treatment was repeated every 24 hours up to five days post infection. As a control of no combination therapy, the same linezolid concentrations together with $SaPI_{gRNA2}$ were used. Also, a group of animals was not treated with linezolid and only received pulsed doses of phage buffer in order to retreive data on catheter colonization ability without treatment. Assessment of the capacity of MW2 strain to colonize the implant was performed by counting viable bacteria on each catheter removed upon animal euthanasia, 24 hours after the last treatment. As shown in **figure 6**, when animals were treated with either 5 mg kg^{-1} or 10 mg kg^{-1} of linezolid and the control $SaPI_{gRNA2}$, colonization levels were only slightly reduced when compared with no treatment. Combination of linezolid with repeated doses of SaPI*rsaE* did not significantly improved killing efficacy, though a slight positive tendency was observed when 10 mg kg^{-1} of linezolid was used in the combination therapy.

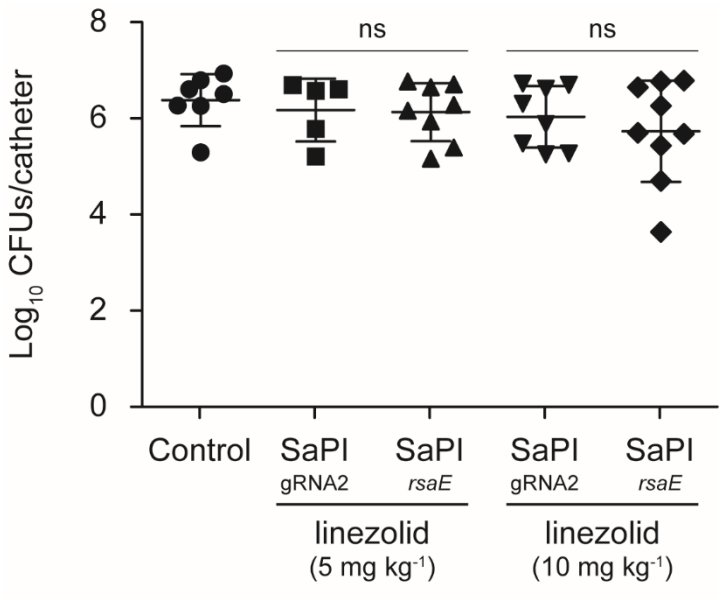

Figure 6. Efficacy of combined therapy with linezolid and SaPI$_{rsaE}$ to avoid catheter colonization by *S. aureus*. Number of viable bacteria obtained from removed catheters upon treatment of mice with two doses of linezolid either alone or in combination with pulsed doses of SaPI$_{rsaE}$ or the control SaPI$_{gRNA2}$. A group of mice that received no treatment was used as a control of MW2 strain capacity to colonize implanted catheters. Although a total of ten catheters were used for each treatment condition, a variable number of catheters were recovered from each group due to natural catheter expulsion during the course of the experiment. The plots display values obtained from individual catheters and the mean is represented by horizontal bars. Statistical significance was determined with a Mann-Whitney *U* test. ns; no significatnt difference.

Discussion

Staphylococcus aureus is an extraordinarily adaptable pathogen with a proven ability to develop antibiotic resistance (Chambers and DeLeo, 2009). Use of modified pathogenicity islands as an alternative method to antimicrobial use for the treatment of staphylococcal infections has already been proposed (Ram *et al.*, 2018). The main difference between these already described modified islands (Ram *et al.*, 2018) and the ones reported in this work lies in the gRNAs coverage that, in our case, allows to go beyond the species level. This may prove useful in the case of infections where not only *S. aureus* but other staphylococci are involved. Future work should be done on this aspect to evaluate the range of species covered by SaPIbov2 and, if needed, generate new chimeric SaPIs containing lethal CRISPR-sgRNA cassette(s).

Our results show that a modest but significant effect was observed *in-vitro* when an active-dividing bacterial population was treated with the synthetic islands. Note that no improvement followed the combined action of the three identical SaPIs differing exclusively in the gRNA and, therefore, in their chromosomal target sequence, with respect to the use of a single $SaPI_{CRISPR}$. This suggests either that one $SaPI_{CRISPR}$ is sufficient to kill the bacteria, or that the infectivity ratio was below 1 because either some SaPIs particles have been damaged during growth or they harbour mutations in then CRISPR-Cas9 module. We had technical difficulties to obtain higher titers of the SaPI, and consequently, we could not use infection ratios higher than 10. In this conditions, it is likely that not all bacteria have received a SaPI particle. In fact, in (Ram *et al.*, 2018), authors presented a dose-response curve where a correlation between surviving cells and particle dose was shown. Intriguingly, they

were able to obtain higher SaPI titers, suggesting that it is technically possible to obtain higher particle-to-bacteria ratio. Other reasons that may explain these differences could refer to the efficiency of each particular sgRNA, the island integration rate or the levels of Cas9/sgRNA produced. As regards integration rate, our preliminary data indicate that the island has to integrate into the bacterial chromosome for the system to work (data not shown).

Here, we proposed the use of modified pathogenicity islands as an adjunt therapy to the use of antibiotics. Importantly, when SaPI$_{rsaE}$ was used in combination with commonly used antibiotics for the treatment of methicillin-resistant *S. aureus* infections (ceftaroline, linezolid and daptomycin), a significant synergistic effect on bacterial growth was observed that was augmented when sequential doses of SaPI$_{rsaE}$ were administered. To validate the use of this combined therapy *in-vivo*, we chose a model that analyses the capacity of *S. aureus* to colonize subcutaneous catheters implanted in mice. This model was selected because *S. aureus* biofilm formation capacity plays a key role in the patho-physiology of chronic staphylococcal infections that are cahracterized by their recalcitrance to antibiotic clearance (Otto, M., 2018). In contrast to what was observed *in-vitro*, the SaPI$_{rsaE}$ and linezolid combination used in this work did not resulted in an improved outcome when compared with treatment with the antibiotic alone. These results are still very preliminary and thus, future work could be focused on aspects such as increasing the dose of linezolid and administration regimes (Andes *et al.*, 2002; Kaur *et al.*, 2016; Li *et al.*, 2018) and/or increasing the amount of SaPI$_{rsaE}$ particles administered to mice.

Phage-antibiotic combinations have already shown promise for the treatment of *S. aureus* related infections and for killing staphylococcal cells inside biofilms (Doub, J.B., *et al*., 2020; Kolenda, C., *et al*., 2020; Kebriaei, R. *et al*., 2020; Gutiérrez, D. *et al*., 2015). Taking into consideration the advantages that the use of engineered SaPIs provide over phages, such as the absence of interference mechanisms between SaPIs that allows the repeated use of the same SaPI treatment and also, avoidance of gene mobilization between the population that may lead to improved pathogenicity or antimicrobial resistance (Penadés and Christie, 2015), synthetic SaPIs represent a promising strategy to complement antibiotic treatment which, although conceptually implemented here in *S. aureus*, could theoretically be extrapolated to other organisms recalcitrant to conventional antibiotic treatment, e.g. ESKAPE pathogens (Rice, 2008; Navidinia, 2016; Mulani *et al.*, 2019). The only limitation would be the availability of well-characterized islands susceptible to be engineered with the CRISPR-Cas9 module.

References

Andes, D., Van Ogtrop, M.L., Peng, J., and Craig, W.A. (2002) In vivo pharmacodynamics of a new oxazolidinone (linezolid). *Antimicrob Agents Chemother* **46**: 3484–3489.

Arnaud, M., Chastanet, A., and Débarbouillé, M. (2004) New vector for efficient allelic replacement in naturally nontransformable, low-GC-content, Gram-positive bacteria. *Appl Environ Microbiol* **70**: 6887–91.

Aslanidis, C. and de Jong, P.J. (1990) Ligation-independent cloning of PCR products (LIC-PCR). *Nucleic Acids Res* **18**: 6069–6074.

Bondy-Denomy, J., Qian, J., Westra, E.R., Buckling, A., Guttman, D.S., Davidson, A.R., and Maxwell, K.L. (2016) Prophages mediate defense against phage infection through diverse mechanisms. *ISME J* **10**: 2854–2866.

Burgui, S., Gil, C., Solano, C., Lasa, I., and Valle, J. (2018) A systematic evaluation of the two-component systems network reveals that ArlRS is a key regulator of catheter colonization by *Staphylococcus aureus*. *Front Microbiol* **9**: 342.

Carpena, N., Manning, K.A., Dokland, T., Marina, A., and Penadés, J.R. (2016) Convergent evolution of pathogenicity islands in helper *cos* phage interference. *Philos Trans R Soc B Biol Sci* **371**: 20150505.

Chambers, H.F. and DeLeo, F.R. (2009) Waves of resistance: *Staphylococcus aureus* in the antibiotic era. *Nat Rev Microbiol* **7**: 629–641.

Charpentier, E., Anton, Ana I, Barry, P., Alfonso, B., Fang, Y., and Novick, R.P. (2004) Novel cassette-based shuttle vector system for Gram-positive bacteria. *Appl Environ Microbiol* **70**: 6076–85.

Chen, J., Quiles-Puchalt, N., Chiang, Y.N., Bacigalupe, R., Fillol-Salom, A., Chee, M.S.J., *et al*. (2018) Genome hypermobility by lateral transduction. *Science* **362**: 207–212.

CLSI. Performance standards for antimicrobial susceptibility testing. 28th ed. CLSI supplement M100 (2018) Wayne, PA.

Cucarella, C., Solano, C., Valle, J., Amorena, B., Lasa, Í., and Penadés, J.R. (2001) Bap, a *Staphylococcus aureus* surface protein involved in biofilm formation. *J*

Bacteriol **183**: 2888–2896.

Damle, P.K., Wall, E.A., Spilman, M.S., Dearborn, A.D., Ram, G., Novick, R.P., *et al*. (2012) The roles of SaPI1 proteins gp7 (CpmA) and gp6 (CpmB) in capsid size determination and helper phage interference. *Virology* **432**: 277–282.

Doub, J.B., Ng, V.Y., Johnson, A.J., Slomka, M., Fackler, J., Horne, B., *et al*. (2020) Salvage bacteriophage therapy for a chronic MRSA prosthetic joint infection. *Antibiotics* **9**.

Gallagher, J., Olson, E.S., and Stanley, D.C. (1993) Microbial desulfurization of dibenzothiophene: a sulfur-specific pathway. *FEMS Microbiol Lett* **107**: 31–35.

Gutiérrez, D., Vandenheuvel, D., Martínez, B., Rodríguez, A., Lavigne, R., and García, P. (2015) Two phages, phiIPLA-RODI and phiIPLA-C1C, lyse mono-and dual-species staphylococcal biofilms. *Appl Environ Microbiol* **81**: 3336–3348.

Harada, L.K., Silva, E.C., Campos, W.F., Del Fiol, F.S., Vila, M., Dąbrowska, K., et al. (2018) Biotechnological applications of bacteriophages: state of the art. *Microbiol Res* **212–213**: 38–58.

Ibarra-Chávez, R., Haag, A.F., Dorado-Morales, P., Lasa, I., and Penadés, J.R. (2020) Rebooting synthetic phage-inducible chromosomal islands: one method to forge them all. *BioDesign Res* **2020**: 5783064.

Kaur, S., Harjai, K., and Chhibber, S. (2016) *In vivo* assessment of phage and linezolid based implant coatings for treatment of methicillin resistant *S. aureus* (MRSA) mediated orthopaedic device related infections. *PLoS One* **11**:.

Kebriaei, R., Lev, K., Morrisette, T., Stamper, K.C., Abdul-Mutakabbir, J.C., Lehman, S.M., *et al*. (2020) Bacteriophage-antibiotic combination strategy: an alternative against methicillin-resistant phenotypes of *Staphylococcus aureus*. *Antimicrob Agents Chemother* **64**:.

Kilbane, J.J. and Jackowski, K. (1992) Biodesulfurization of water-soluble coal-derived material by *Rhodococcus rhodochrous* IGTS8. *Biotechnol Bioeng* **40**: 1107–1114.

Kolenda, C., Josse, J., Medina, M., Fevre, C., Lustig, S., Ferry, T., and Laurent, F. (2020) Evaluation of the activity of a combination of three bacteriophages alone or in association with antibiotics on *Staphylococcus aureus* embedded in biofilm

or internalized in osteoblasts. *Antimicrob Agents Chemother* **64**.

Lauritsen, I., Porse, A., Sommer, M.O.A., and Nørholm, M.H.H. (2017) A versatile one-step CRISPR-Cas9 based approach to plasmid-curing. *Microb Cell Fact* **16**: 135.

Levy, S.B. and Bonnie, M. (2004) Antibacterial resistance worldwide: causes, challenges and responses. *Nat Med* **10**: S122–S129.

Li, B., Ni, S., Chen, F., Mao, F., Wei, H., Liu, Y., *et al*. (2018) Discovery of potent benzocycloalkane derived diapophytoene desaturase inhibitors with an enhanced safety profile for the treatment of MRSA, VISA, and LRSA infections. *ACS Infect Dis* **4**: 208–217.

Malone, C.L., Boles, B.R., Lauderdale, K.J., Thoendel, M., Kavanaugh, J.S., and Horswill, A.R. (2009) Fluorescent reporters for *Staphylococcus aureus*. *J Microbiol Methods* **77**: 251.

Manning, K.A., Quiles-Puchalt, N., Penadés, J.R., and Dokland, T. (2018) A novel ejection protein from bacteriophage 80α that promotes lytic growth. *Virology* **525**: 237–247.

Mir-Sanchis, I., Martínez-Rubio, R., Martí, M., Chen, J., Lasa, Í., Novick, R.P., *et al*. (2012) Control of *Staphylococcus aureus* pathogenicity island excision. *Mol Microbiol* **85**: 833–845.

Monk, I.R., Tree, J.J., Howden, B.P., Stinear, T.P., and Foster, T.J. (2015) Complete bypass of restriction systems for major *Staphylococcus aureus* lineages. *mBio* **6**: 1–12.

Mulani, M.S., Kamble, E.E., Kumkar, S.N., Tawre, M.S., and Pardesi, K.R. (2019) Emerging strategies to combat ESKAPE pathogens in the era of antimicrobial resistance: a review. *Front Microbiol* **10**: 539.

Navidinia, M. (2016) The clinical importance of emerging ESKAPE pathogens in nosocomial infections . *J Paramed Sci* **7**: 43–57.

Novick, R.P., Christie, G.E., and Penadés, J.R. (2010) The phage-related chromosomal islands of Gram-positive bacteria. *Nat Rev Microbiol* **8**: 541–551.

Otto, M. (2018) Staphylococcal biofilms. *Microbiol Spectr* **6:** 4.

Penadés, J.R., Chen, J., Quiles-Puchalt, N., Carpena, N., and Novick, R.P. (2015) Bacteriophage-mediated spread of bacterial virulence genes. *Curr Opin Microbiol* **23**: 171–178.

Penadés, J.R. and Christie, G.E. (2015) The phage-inducible chromosomal islands: a family of highly evolved molecular parasites. *Annu Rev Virol* **2**: 181–201.

Peng, H.L., Novick, R.P., Kreiswirth, B., Kornblum, J., and Schlievert, P. (1988) Cloning, characterization, and sequencing of an accessory gene regulator (*agr*) in *Staphylococcus aureus*. *J Bacteriol* **170**: 4365–72.

Del Pozo, J.L., Alonso, M., Arciola, C.R., Gonzalez, R., Leiva, J., Lasa, I., and Penades, J. (2007) Biotechnological war against biofilms. Could phages mean the end of device-related infections? *Int J Artif Organs* **30**: 805–812.

Quiles-Puchalt, N., Carpena, N., Alonso, J.C., Novick, R.P., Marina, A., and Penadés, J.R. (2014) Staphylococcal pathogenicity island DNA packaging system involving *cos*-site packaging and phage-encoded HNH endonucleases. *Proc Natl Acad Sci USA* **111**: 6016–6021.

Ram, G., Chen, J., Kumar, K., Ross, H.F., Ubeda, C., Damle, P.K., et al. (2012) Staphylococcal pathogenicity island interference with helper phage reproduction is a paradigm of molecular parasitism. *Proc Natl Acad Sci USA* **109**: 16300–16305.

Ram, G., Ross, H.F., Novick, R.P., Rodriguez-Pagan, I., and Jiang, D. (2018) Conversion of staphylococcal pathogenicity islands to CRISPR-carrying antibacterial agents that cure infections in mice. *Nat Biotechnol* **36**: 971.

Rice, L.B. (2008) Federal funding for the study of antimicrobial resistance in nosocomial pathogens: no ESKAPE. *J Infect Dis* **197**: 1079–1081.

Rohwer, F. and Segall, A.M. (2015) In retrospect: a century of phage lessons. *Nature* **528**: 46–48.

Scholtissek, S. and Grosse, F. (1987) A cloning cartridge of λ t0 terminator. *Nucleic Acids Res* **15**: 3185.

Stewart, C.R., Gaslightwala, I., Hinata, K., Krolikowski, K.A., Needleman, D.S., Peng, A.S.-Y., et al. (1998) Genes and regulatory sites of the "host-takeover module" in the terminal redundancy of *Bacillus subtilis* bacteriophage SPO1.

Virology **246**: 329–340.

Sulakvelidze, A. (2005) Phage therapy: an attractive option for dealing with antibiotic-resistant bacterial infections. *Drug Discov Today* **10**: 807–809.

Tacconelli, E., Carrara, E., Savoldi, A., Harbarth, S., Mendelson, M., Monnet, D.L., *et al*. (2018) Discovery, research, and development of new antibiotics: the WHO priority list of antibiotic-resistant bacteria and tuberculosis. *Lancet Infect Dis* **18**: 318–327.

Tallent, S.M., Langston, T.B., Moran, R.G., and Christie, G.E. (2007) Transducing particles of *Staphylococcus aureus* pathogenicity island SaPI1 are comprised of helper phage-encoded proteins. *J Bacteriol* **189**: 7520–7524.

Tormo, M.Á., Ferrer, M.D., Maiques, E., Úbeda, C., Selva, L., Lasa, Í., *et al*. (2008) *Staphylococcus aureus* pathogenicity island DNA is packaged in particles composed of phage proteins. *J Bacteriol* **190**: 2434–2440.

Úbeda, C., Barry, P., Penadés, J.R., and Novick, R.P. (2007) A pathogenicity island replicon in *Staphylococcus aureus* replicates as an unstable plasmid. *Proc Natl Acad Sci USA* **104**: 14182–8.

Úbeda, C., Maiques, E., Tormo, M., Campoy, S., Lasa, Í., Barbé, J., *et al*. (2007) SaPI operon I is required for SaPI packaging and is controlled by LexA. *Mol Microbiol* **65**: 41–50.

Úbeda, C., Olivarez, N.P., Barry, P., Wang, H., Kong, X., Matthews, A., *et al*. (2009) Specificity of staphylococcal phage and SaPI DNA packaging as revealed by integrase and terminase mutations. *Mol Microbiol* **72**: 98–108.

Úbeda, C., Tormo, M.Á., Cucarella, C., Trotonda, P., Foster, T.J., Lasa, Í., and Penadés, J.R. (2003) Sip, an integrase protein with excision, circularization and integration activities, defines a new family of mobile *Staphylococcus aureus* pathogenicity islands. *Mol Microbiol* **49**: 193–210.

Watson, J.F. and García-Nafría, J. (2019) *In vivo* DNA assembly using common laboratory bacteria: a re-emerging tool to simplify molecular cloning. *J Biol Chem* **294**: 15271–15281.

FUTURE PROSPECTS

Biofilms are the main bacterial lifestyle in nature, clinical and industrial settings. Basically, biofilms are communities of bacteria embedded in a self-produced matrix of extracellular polymeric substances. Bacteria, when structured as biofilms, exhibit a substantially different behaviour from that of their free-living counterparts. The complex spatial organization, the nature of the matrix in which bacteria are encased, the increased genetic exchange, the secreted enzymes, the retention of water, nutrients and lysed cell contents, and the enhanced cell-to-cell communication caused by the close proximity between bacterial cells, create optimal conditions for cooperation and make of the biofilm a highly metabolic active entity (Lear, 2016). Living inside biofilms has also been described to offer bacteria protection against predation, a higher tolerance to certain antimicrobial agents and adaptation to severe environments (Flemming *et al.*, 2016). Based on these features, biofilms are especially suitable for the treatment of recalcitrant compounds and the development of novel biology-based production processes.

Staphylococcus aureus, a pathogenic bacterial species, whose strong biofilm formation capacity is one of its principal virulence factors, displays a wide variety of mechanisms for biofilm development (Moormeier and Bayles, 2017). In **Chapter I**, three of these strategies were considered in order to promote biofilm formation of *Rhodococcus erythropolis*, a bacterial species with significant biodegradation abilities. The evaluated approaches were: (i) the heterologous production of the universal exopolysaccharide PIA/PNAG through the expression of the *S. aureus ica* operon, (ii) the exogenous addition of the recombinant B region of the *S. aureus* Bap protein, and (iii) the increase in cytoplasmic c-di-GMP levels by means of overexpressing the *adrA*

gene from *Salmonella enterica* serovar Enteritidis, encoding the highly active diguanylate cyclase AdrA. In this regard, we previously tested c-di-GMP production and biofilm formation of *R. erythropolis* overexpressing GdpS, the only protein harbouring a conserved GGDEF domain in *S. aureus*. However, *gdpS* expression caused neither an increase in c-di-GMP nor a change in the biofilm formation capacity of *Rhodococcus*, so this approach was discarded. These results are in agreement with previous studies that failed to prove the diguanylate activity of GdpS (Holland *et al.*, 2008; Shang *et al.*, 2009; Fischer *et al.*, 2014; Chen *et al.*, 2015; Zhu *et al.*, 2017) and thus, they support the hypothesis that the GdpS protein might be the remnant of a c-di-GMP signalling system that is now absent in *S. aureus*.

The results obtained in **Chapter I** show that, from the three methodologies explored, only the rise in c-di-GMP levels caused a macroscopic change in the *R. erythropolis* phenotype in terms of aggregation and biofilm development. This indicates that not all the biofilm formation strategies can be universally extrapolated among bacterial taxa and that depending on the genetic context, and usually on certain environmental cues, the final output may totally differ.

Interestingly, an increase in c-di-GMP levels in the cytoplasm of *R. erythropolis* led to an improvement in dibenzothiophene desulfurization capacity through mechanisms that we still do not know but that are most probably related to biofilm formation. To elucidate whether the enhancement in metabolic activity is related to the formation of a bacterial community and not to other c-di-GMP targets or side-effects, the biofilm formation process might be induced independently of c-di-GMP. To do so, the genetic determinants involved in the synthesis of the *Rhodococcus*

biofilm matrix should be identified and activated. Then, the metabolic activity of this biofilm might be tested and compared to that of its planktonic and AdrA-mediated biofilm equivalents. As regards the reasons why the rate of biodesulfurization increases when *Rhodococcus* grows in the physical form of a biofilm, and considering the hydrophobic nature of dibenzothiophene, it can be speculated that a molecule with biosurfactant properties might be taking part of the *Rhodococcus* biofilm matrix, which would enhance bioavailability and hence, degradation of dibenzothiophene.

Although in our study we used DBT biodegradation by *R. erythropolis* as a proof of concept, we believe that promoting biofilm formation through an increase in c-di-GMP levels will probably have the same enhancing effects in other biosynthetic or degradation pathways. Plenty of metabolic routes of great interest in the biotechnological field have been described in different *Rhodococcus* species (Martínková *et al.*, 2009; Busch *et al.*, 2019; Zampolli *et al.*, 2019), and any of them, as long as the metabolites involved can be easily monitored, might be used to prove this hypothesis.

Last, elevated c-di-GMP levels not only increased the biodesulfurization capability of *Rhodococcus* but also promoted biofilm formation on different surfaces (silicone and polystyrene) under continuous flow conditions, which opens new and attractive possibilities when alternatives for future industrial scaling processes are considered (e.g. the use of fluidized bed reactors for biodegradation processes).

Plasmids are major drivers of horizontal gene transfer. In *S. aureus*, plasmids play a role in the dissemination of antibiotic resistance genes and virulence factors, such as toxins and biofilm formation genetic determinants (Novick, 1989; Feßler *et al.*,

2017; Haaber *et al.*, 2017). Although plasmids have been extensively studied, little is known about the mechanisms underlying their maintenance in the long term in the absence of selection for plasmid-encoded traits, as according to mathematical prediction models, plasmids should be lost over time (Carroll and Wong, 2018). In Gram-negative bacteria, effort has been undertaken to unveil the molecular basis behind this paradox, however little or no information can be found about the mechanisms governing this phenomenon in *S. aureus*. To study the biology of plasmids, tools that enable an easy manipulation of these elements are required. However, traditional techniques for plasmid removal are time-consuming and, in most cases, mutagenic (Trevors, 1986).

Considered these precedents, in **Chapter II**, we designed and constructed a CRISPR-based vector that allows plasmid removal from *S. aureus* in a simple and straightforward fashion. We then evaluated its performance using an array of laboratory and clinical isolates obtaining curing efficiencies ranging from 96 to 100%.

To investigate the adaptations experienced by *S. aureus* following plasmid acquisition, one of the cured clinical isolates, MW2 ΔpMW2, was selected and used as a recipient of four plasmids including its own (pMW2, pUR2940, pN315 and pLAC-p03). The cost associated to those plasmids was estimated monitoring bacterial growth and attending at each clone performance. Data analysis revealed a clear decrease in the area under the growth curve and a delay in the lag phase of those clones carrying plasmid pUR2940 whereas minor or no differences were observed for

the rest of them. This cost that was compensated after 35 days of continued growth under no selection regimes.

It cannot be concluded, however, that there is no cost associated to the three remaining plasmids but instead that, if there is any, it is not reflected in the parameters we selected. Although we think that the experimental workflow described in **Chapter II** constitutes an ideal framework to study plasmids and their impact on *S. aureus* biology, the presented approach is far for complete as there may be subtle outcomes unmeasurable by our methods, and it would be convenient to complement the data obtained using transcriptomic approaches prior and immediately after transformation and at the end of the evolution process.

pUR2940, a multidrug-resistance plasmid, proved to be unstable and costly, even in the strain from which it was originally isolated, *S. aureus* C2940. The source of this cost seems to be associated to a plasmid region where an elevated number of antibiotic resistance genes are translocated between IS replicons. ISs are prone to mediate rearrangements that will result, in the absence of selective pressure, in the loss of the ARG cluster and, consequently, in smaller stable uncostly plasmids. Several plasmids of *S. aureus*, such as pKKS25, pKKS2187, pUR1902 or pUR2941 to mention a few, contain IS replicons (Kadlec and Schwarz, 2009, 2010; Gómez-Sanz *et al.*, 2013). It would be important to expand our approach to strains containing this type of plasmids to confirm that fitness cost in the absence of selective pressure is reduced by IS-mediated rearrangements.

All of this considered, it is logical to hypothesize that upon arrival to a new unadapted host and under no selection regimes, plasmids carrying several ARGs

would negatively affect the global fitness of the bacteria and therefore, the chances of plasmid-bearing clones succeeding in the population would be scarce. But again, models that mimic the *S. aureus* natural niches are needed to confirm this hypothesis.

Staphylococcus aureus has become a worldwide health issue due to the rapid emergence of strains recalcitrant to antibiotic treatment. Alternative available options are limited and, consequently, finding new effective antimicrobials has become a priority.

In a pioneering study, engineered *Staphylococcus aureus* pathogenicity islands (SaPIs) were proposed as therapeutic agents against staphylococci by the laboratory of R. Novick (Ram *et al.*, 2018). In **Chapter III**, we went a step further and combined clinically relevant antibiotics and modified SaPI-elements for the treatment of *S. aureus* infections. The results obtained, although promising (synergistic effects were observed for the combination of linezolid and daptomycin with SaPI particles), are preliminary. In fact, to develop an optimal system, other conformations, such as the construction of an island containing three sgRNAs modules in its genome or the use of different SaPIs varying in their scaffolding genome but carrying the same sgRNA, should be considered and evaluated.

A problem that can be encountered with this approach is that some bacteria might scape the action of the modified islands due to mutations in the CRISPR system. This issue can be solved by adding an extra gene coding for a toxin in the engineered SaPI genome. The toxin candidates should prove functional in *Staphylococcus* and, if possible, should be obtained from distant taxa to avoid putative crossed protection due to some non-canonical antitoxin partners. Another aspect that

needs to be considered is the mechanism of action of the effector protein(s). If the toxin causes the lysis of the bacteria, it might provoke the release of endotoxins which could be associated with the risk of excessive inflammation, leading to a cytokine storm or systemic inflammatory response syndrome.

Another issue that needs further investigation is the role of the immune response against the SaPI vector and also the immunotoxicity of the SaPI. The patient's immune response against viral vectors has been implicated in the failure of virus-mediated gene therapy. Thus, a thorough examination of the effects of the innate and adaptive immune responses on SaPI will be necessary to evaluate the overall safety of this type of treatment.

References

Busch, H., Hagedoorn, P.L., and Hanefeld, U. (2019) *Rhodococcus* as a versatile biocatalyst in organic synthesis. *Int J Mol Sci* **20**.

Carroll, A.C. and Wong, A. (2018) Plasmid persistence: costs, benefits, and the plasmid paradox. *Can J Microbiol* **64**: 293–304.

Chen, C., Zhang, X., Shang, F., Sun, H., Sun, B., and Xuea, T. (2015) The *Staphylococcus aureus* protein-coding gene *gdpS* modulates *sarS* expression via mRNA-mRNA interaction. *Infect Immun* **83**: 3302–3310.

Feßler, A.T., Zhao, Q., Schoenfelder, S., Kadlec, K., Brenner Michael, G., Wang, Y., *et al*. (2017) Complete sequence of a plasmid from a bovine methicillin-resistant *Staphylococcus aureus* harbouring a novel *ica*-like gene cluster in addition to antimicrobial and heavy metal resistance genes. *Vet Microbiol* **200**: 95–100.

Fischer, A., Kambara, K., Meyer, H., Stenz, L., Bonetti, E.J., Girard, M., *et al*. (2014) GdpS contributes to *Staphylococcus aureus* biofilm formation by regulation of eDNA release. *Int J Med Microbiol* **304**: 284–299.

Flemming, H.C., Wingender, J., Szewzyk, U., Steinberg, P., Rice, S.A., and Kjelleberg, S. (2016) Biofilms: an emergent form of bacterial life. *Nat Rev Microbiol* **14**: 563–575.

Gómez-Sanz, E., Kadlec, K., Feßler, A.T., Zarazaga, M., Torres, C., and Schwarz, S. (2013) Novel *erm*(*T*)-carrying multiresistance plasmids from porcine and human isolates of methicillin-resistant *Staphylococcus aureus* ST398 that also harbor cadmium and copper resistance determinants. *Antimicrob Agents Chemother* **57**: 3275–3282.

Haaber, J., Penadés, J.R., and Ingmer, H. (2017) Transfer of antibiotic resistance in *Staphylococcus aureus*. *Trends Microbiol* **25**: 893–905.

Holland, L.M., O'Donnell, S.T., Ryjenkov, D.A., Gomelsky, L., Slater, S.R., Fey, P.D., *et al*. (2008) A staphylococcal GGDEF domain protein regulates biofilm formation independently of cyclic dimeric GMP. *J Bacteriol* **190**: 5178–5189.

Kadlec, K. and Schwarz, S. (2009) Identification of a novel trimethoprim resistance gene, *dfrK*, in a methicillin-resistant *Staphylococcus aureus* ST398 strain and its

physical linkage to the tetracycline resistance gene *tet*(*L*). *Antimicrob Agents Chemother* **53**: 776–778.

Kadlec, K. and Schwarz, S. (2010) Identification of a plasmid-borne resistance gene cluster comprising the resistance genes *erm*(*T*), *dfrK*, and *tet*(*L*) in a porcine methicillin-resistant *Staphylococcus aureus* ST398 strain. *Antimicrob Agents Chemother* **54**: 915–918.

Lear, G. ed. (2016) Biofilms in bioremediation. Current research and emerging technologies, Caister Academic Press.

Martínková, L., Uhnáková, B., Pátek, M., Nešvera, J., and Křen, V. (2009) Biodegradation potential of the genus *Rhodococcus*. *Environ Int* **35**: 162–177.

Moormeier, D.E. and Bayles, K.W. (2017) *Staphylococcus aureus* biofilm: a complex developmental organism. *Mol Microbiol* **104**: 365–376.

Novick, R.P. (1989) Staphylococcal plasmids and their replication. *Annu Rev Microbiol* **43**: 537–563.

Ram, G., Ross, H.F., Novick, R.P., Rodriguez-Pagan, I., and Jiang, D. (2018) Conversion of staphylococcal pathogenicity islands to CRISPR-carrying antibacterial agents that cure infections in mice. *Nat Biotechnol* **36**: 971.

Shang, F., Xue, T., Sun, H., Xing, L., Zhang, S., Yang, Z., *et al*. (2009) The *Staphylococcus* aureus GGDEF domain-containing protein, GdpS, influences protein A gene expression in a cyclic diguanylic acid-independent manner. *Infect Immun* **77**: 2849–2856.

Trevors, J.T. (1986) Plasmid curing in bacteria. *FEMS Microbiol Lett* **32**: 149–157.

Zampolli, J., Zeaiter, Z., Di Canito, A., and Di Gennaro, P. (2019) Genome analysis and -omics approaches provide new insights into the biodegradation potential of *Rhodococcus*. *Appl Microbiol Biotechnol* **103**: 1069–1080.

Zhu, T., Zhao, Y., Wu, Y., and Qu, D. (2017) The *Staphylococcus epidermidis gdpS* regulates biofilm formation independently of its protein-coding function. *Microb Pathog* **105**: 264–271.

CONCLUSIONS

1. The heterologous expression of the highly active diguanylate cyclase AdrA from *Salmonella enterica* Ser. Enteritidis and the subsequent increment in the intracellular levels of c-di-GMP induces biofilm development in *Rhodococcus erythropolis*. In contrast, the exogenous addition of the recombinant B region of the Bap protein or the heterologous production of the exopolysaccharide PIA/PNAG from *Staphylococcus aureus* in *Rhodococcus erythropolis* does not translate in a phenotypic change either in terms of aggregation or biofilm formation.

2. An increase in c-di-GMP levels leads to high dibenzothiophene biodegradation yields and enhances the adhesion capacity of *Rhodococcus erythropolis* to different surfaces, such as silicone and polystyrene, under flow conditions. These improved features open the possibility of using *R. erythropolis* biofilm cells in the development of fluidized bed reactors in industrial biodegradation processes.

3. We have constructed a new CRISPR-based tool that enables plasmid removal from clinical *Staphylococcus aureus* isolates. This tool has allowed us to evaluate the fitness cost and adaptation to plasmid carriage in *Staphylococcus aureus* in the absence of selection for plasmid encoded traits. Our results highlight the importance of plasmid rearrangement mediated by insertion sequences and the subsequent loss from the plasmid of antimicrobial resistance genes in plasmid maintenance. They also indicate that a reduction in the use of antibiotics for the treatment of *Staphylococcus*

aureus related infections may help in the selection of clones that are no longer resistant to antimicrobials.

4. We have constructed *Staphylococcus aureus* modified pathogenicity islands carrying a CRISPR-Cas9 system targeting conserved sequences of the staphylococcal chromosome. The combined use of these modified pathogenicity islands with antibiotics showed a synergistic bactericidal effect on *Staphylococcus aureus* and represents a promising strategy for the treatment of recalcitrant staphylococcal infections.

Diseño portada: Unidad de Comunicación y Diseño, Navarrabiomed 2020